

Mechanistic Insight into Phosphoregulation of the Lipin Family

James Maitland Eaton

Baltimore, Maryland

MS, Biological and Physical Science, University of Virginia, 2011

BA, Chemistry, Kenyon College, 2009

A Dissertation Presented to the Graduate Faculty  
of the University of Virginia in Candidacy for the Degree of  
Doctor of Philosophy

Department of Pharmacology

University of Virginia

August 2014

## ABSTRACT

Quietly emerging as essential regulators of lipid metabolism, the lipin protein family consisting of lipin 1, 2 and 3 are phosphatidic acid phosphatases that catalyze the penultimate step in triacylglycerol (TAG) biosynthesis, the conversion of phosphatidic acid to diacylglycerol.<sup>1</sup> These soluble enzymes reversibly associate with the endoplasmic reticulum membrane, a distinction from the rest of TAG biosynthetic enzymes, which allow for dual function; lipin 1 also translocates into the nucleus to alter gene expression, thereby potentially linking lipid metabolism to gene expression. The importance of the lipin family in lipid metabolism is exemplified by mutant phenotypes. Loss of lipin 1 results in lipodystrophy and rhabdomyolysis in mouse and man, respectively, while loss of lipin 2 in humans results in Majeed's syndrome.

In adipocytes, lipin 1 is downstream of the insulin/PI3K/mTOR signaling pathway, and is highly phosphorylated in response to insulin stimulation, which correlates with cytosolic location. The work herein has built upon the prior literature by examining how phosphorylation can alter lipin 1 localization. We have provided evidence that the lipins bind PA by the electrostatic hydrogen-bond switch mechanism through a PA binding domain consisting of nine basic amino acids and that this process is inhibited in a phosphorylation dependent manner, in the case of lipin 1, and independent, in the case of lipin 2. We have made the observation that lipin 1 forms high molecular weight complexes upon membrane binding, which have implications for lipin structure-function. In addition we demonstrate the rhabdomyolysis associated mutations in lipin 1 lead to defective PAP activity, providing a role for its phosphatase activity in the pathogenesis of this acute syndrome.

## ACKNOWLEDGEMENT

First and foremost I would like to thank my mentor, Thurl E. Harris. Because of the combination of his good nature and scientific acumen, I was able to have a successful graduate student career. With a background in chemistry, I had a very superficial understanding of anything biology. Knowing this, he still gave me an opportunity; quite a brave decision.

I would like to thank my thesis committee. Your insight was especially helpful considering the limited number of times we met. I would specifically like to thank Dr. Carl Creutz for being a great scientist mentor and valuable resource.

I would like to thank the members of the Harris lab for being a fun group of lab mates and great collaborators. Specifically, thank you to Garrett for quantifying phosphate hydrolysis by lambda phosphatase, Sankeerth for measuring lipin 2 membrane binding, Kelley for the immunofluorescence and Salome for the adipocyte radiolabelling experiments. Additionally, thank you to Samantha for keeping the lab running. Outside of Harris lab, I would like to thank Rob Lawrence for his analysis of lipin 2 phosphorylation by mass spectrometry.

Additionally, I would like to thank the Pharmacology Department. Paula Barrett and Jolene Kidd were instrumental to my success.

Last but not least, I would like to thank my family and friends for their support throughout this process.

**TABLE OF CONTENTS**

<b>ABSTRACT</b> .....	2
<b>ACKNOWLEDGEMENT</b> .....	3
<b>TABLE OF CONTENTS</b> .....	4
<b>APPENDIX OF FIGURES</b> .....	8
<b>APPENDIX OF TABLES</b> .....	10
<b>APPENDIX OF ACRONYMS</b> .....	11
<b>CHAPTER 1: GENERAL INTRODUCTION</b> .....	12
<b>CHAPTER 2: EXPERIMENTAL METHODS</b>	
<b>MATERIALS</b> .....	34
<b>RECOMBINANT EXPRESSION PLASMID FOR LIPIN 1</b> .....	34
<b>PLASMIDS AND ADENOVIRUS CONSTRUCTS FOR LIPIN 2</b> .....	34
<b>PURIFICATION OF RECOMBINANT LIPIN 1</b> .....	35
<b>EXPRESSION AND PURIFICATION OF LIPIN 2</b> .....	36
<b>QUANTITATION OF PHOSPHATE REMOVAL BY LAMBDA PHOSPHATASE</b> ....	36
<b>PREPARATION OF [<sup>32</sup>P]PA</b> .....	37
<b>PREPARATION OF TRITON X-100:PA-MIXED MICELLES</b> .....	37

MEASUREMENTS OF PAP ACTIVITIES.....	37
MEASUREMENT OF LIPIN 1 MEMBRANE BINDING.....	39
MEASUREMENT OF LIPIN 2 MEMBRANE BINDING.....	39
RADIOLABELING OF LIPIN 2 IN 3T3-L1 ADIPOCYTES.....	40
MASS SPECTROMETRY.....	40
IMMUNOFLUORESCENCE.....	41
SUBCELLULAR FRACTIONATIONS.....	42
PREPARATION OF LIPIN SAMPLES FOR DRY IMAGING IN AIR.....	42
PREPARATION OF LIPIN ON SUPPORTED LIPID BILAYERS FOR IMAGING IN BUFFER.....	42
ATOMIC FORCE MICROSCOPY.....	43

**CHAPTER 3: PHOSPHORYLATION AND CHARGE ON THE PHOSPHATIDIC ACID  
HEAD GROUP CONTROL LIPIN 1 MEMBRANE BINDING AND PHOSPHATASE  
ACTIVITY**

ABSTRACT.....	45
INTRODUCTION.....	46
RESULTS.....	48
DISCUSSION.....	58

**CHAPTER 4: LIPIN 2 BINDS PHOSPHATIDIC ACID BY THE ELECTROSTATIC  
HYDROGEN BOND SWITCH INDEPENDENT OF PHOSPHORYLATION**

ABSTRACT.....	84
INTRODUCTION.....	85
RESULTS.....	87
DISCUSSION.....	94

**CHAPTER 5: ASSEMBLY OF HIGH MOLECULAR WEIGHT COMPLEXES OF LIPIN  
ON A SUPPORTED LIPID BILAYER OBSERVED BY ATOMIC FORCE  
MICROSCOPY**

ABSTRACT.....	118
INTRODUCTION.....	120
RESULTS.....	121
DISCUSSION.....	124

**CHAPTER 6: RHABDOMYOLYSIS ASSOCIATED MUTATIONS IN HUMAN LIPIN 1  
LEAD TO DEFECTIVE PHOSPHATIDIC ACID PHOSPHATASE ACTIVITY**

ABSTRACT.....	142
INTRODUCTION.....	143
RESULTS.....	144

DISCUSSION.....	145
<b>CHAPTER 7: CONCLUSIONS AND FUTURE DIRECTIONS</b>	
SUMMARY AND CONCLUSIONS.....	150
FUTURE DIRECTIONS.....	152
<b>CHAPTER 8: PUBLICATIONS RESULTING FROM THIS WORK.....</b>	
REFERENCES.....	156

## APPENDIX OF FIGURES

### CHAPTER 1

<b><u>Figure 1.1</u></b> Intermediate lipid species in TAG synthesis.....	28
<b><u>Figure 1.2</u></b> Primary structure of lipin 1.....	30
<b><u>Figure 1.3</u></b> Intracellular trafficking of lipin.....	32

### CHAPTER 3

<b><u>Figure 3.1</u></b> Phosphorylation status of lipin 1 does not change PAP activity using the conventional Triton X-100 mixed micelle assay.....	64
<b><u>Figure 3.2</u></b> PAP activity of phosphorylated and dephosphorylated lipin 1 in liposomes.....	66
<b><u>Figure 3.3</u></b> Effect of PC or PE on lipin 1 physical association with liposomes.....	69
<b><u>Figure 3.4</u></b> Effect of amphiphilic amines on lipin 1 association with membranes and PAP activity.....	71
<b><u>Figure 3.5</u></b> Effect of pH on lipin 1 PAP activity.....	73
<b><u>Figure 3.6</u></b> Effect of mTOR inhibition and S/T mutation to A on lipin 1 PAP activity.....	77
<b><u>Figure 3.7</u></b> Role of the polybasic domain (PBD) in lipin 1 PAP activity.....	79
<b><u>Figure 3.8</u></b> Model representation of lipin 1 binding to PA.....	82

### CHAPTER 4

<b><u>Figure 4.1</u></b> Purification and initial characterization of lipin 2.....	99
<b><u>Figure 4.2</u></b> Effects of PA charge on lipin 2 PA phosphatase activity.....	101
<b><u>Figure 4.3</u></b> Effects of PA charge on lipin 2 membrane binding.....	104
<b><u>Figure 4.4</u></b> Mass spectrometric analysis of lipin 2 phosphorylation.....	106
<b><u>Figure 4.5</u></b> Lambda phosphatase treatment of lipin 2.....	108
<b><u>Figure 4.6</u></b> Effect of lipin 2 phosphorylation on PA phosphatase activity.....	110
<b><u>Figure 4.7</u></b> Phosphorylation of lipin 1 and 2 in 3T3-L1 adipocytes.....	112
<b><u>Figure 4.8</u></b> Lipin 2 subcellular localization in 3T3-L1 adipocytes.....	114

<b><u>Figure 4.9</u></b> Model of lipin 1 vs lipin 2 enzymatic activity.....	116
--	-----

## CHAPTER 5

<b><u>Figure 5.1</u></b> Lipin imaged in air on mica.....	128
---	-----

<b><u>Figure 5.2</u></b> Histograms of the molecular volumes of lipin particles calculated as described in Materials and Methods.....	130
---	-----

<b><u>Figure 5.3</u></b> Lipin imaged in buffer on a supported lipid bilayer and on mica.....	132
---	-----

<b><u>Figure 5.4</u></b> After extended incubation in buffer, lipin adheres strongly enough to the mica to be visualized.....	134
---	-----

<b><u>Figure 5.5</u></b> Higher-magnification view of lipin bound to the supported lipid bilayer seen in Figure 3.....	136
--	-----

<b><u>Figure 5.6</u></b> Large lipin particles leave behind “footprints” when they are displaced by the AFM probe.....	138
--	-----

## CHAPTER 6

<b><u>Figure 6.1</u></b> Lipin 1 mutations associated with rhabdomyolysis.....	147
--	-----

<b><u>Figure 6.2</u></b> Lipin 1 proteins with disease-associated mutations lack PAP activity.....	149
--	-----

## APPENDIX OF TABLES

### CHAPTER 3

<b><u>Table 3.1</u></b> Kinetic data for lipin 1b +/- $\lambda$ phosphatase using liposomes composed of 10 mol% PA and 90 mol% (PC + PE), with PE mol% indicated.....	68
<b><u>Table 3.2</u></b> Kinetic data for lipin 1b +/- $\lambda$ phosphatase using TX:PA micelles at varying pH.....	75
<b><u>Table 3.3</u></b> Kinetic data for lipin 1b +/- $\lambda$ phosphatase using TX:PA micelles at pH 8 with respect to the surface concentration of PA.....	76
<b><u>Table 3.4</u></b> Kinetic data for the PBD mutant of lipin 1b +/- $\lambda$ phosphatase using liposomes composed of 10 mol% PA and 90 mol% (PC + PE) with PE mol% indicated.....	81

### CHAPTER 4

<b><u>Table 4.1</u></b> Steady-state kinetic data for lipin 2 using liposomes composed of 10 mol % PA and 90 mol% (PE + PC) with PE mol % indicated.....	103
--	-----

### CHAPTER 5

<b><u>Table 5.1</u></b> Dimensions (nanometers) of lipin particles and their respective footprints on the supported bilayer.....	140
<b><u>Table 5.2</u></b> Average dimensions of lipin particles and comparison with hypothetical volumes based on molecular weight.....	141

**APPENDIX OF ACRONYMS**

DMEM	Dulbecco's Modified Eagle's Medium
DTT	Dithiothreitol
mTOR	Mechanistic target of rapamycin
PAP	Phosphatidic acid phosphatase
PBD	Polybasic Domain
WT	Wild type
DAG	Diacylglycerol
TAG	Triacylglycerol
PE	Phosphatidylethanolamine
Tx	Triton X-100
DMSO	Dimethyl sulfoxide
ER	Endoplasmic reticulum
FBS	Fetal bovine serum
LC-MS/MS	Liquid chromatography coupled to tandem mass spectrometry
LHR	Low Homology Region
PDI	Protein disulfide isomerase
PC	1,2 dioleoyl- <i>sn</i> -glycero-3-phosphocholine
PE	1,2-dioleoyl- <i>sn</i> -glycero-3-phosphoethanolamine
PGC-1 $\alpha$	Peroxisome proliferator-activated receptor gamma, coactivator 1 alpha
SREBP	Sterol Regulatory Element-Binding Proteins
TCA	Trichloroacetic acid
PS	L- $\alpha$ -phosphatidylserine from porcine brain

## CHAPTER 1

### GENERAL INTRODUCTION

#### *Phospholipid and Triacylglycerol Synthesis*

Upon insulin stimulation in adipocytes, triglycerides are synthesized at the ER membrane and subsequently stored in the neutral core of lipid droplets.<sup>2</sup> In order to use fatty acids for future sources of lipid synthesis and energy expenditure through beta-oxidation, fatty acids must be inertly stored to circumvent the detergent like chemical properties they possess.

Esterification of fatty acids into neutral triglycerides requires five enzymatic steps (**Figure 1.1**). Fatty acids are converted to coenzyme A esters, followed by two acylation additions to glycerol-3-phosphate at the *sn*-1 and *sn*-2 positions producing phosphatidic acid (PA) by LPAAT and AGPAT, respectively. PA is then dephosphorylated producing diacylglycerol which contains a free hydroxyl at the *sn*-3 position. Fatty acid esterification of the *sn*-3 position by the DGATs completes the biosynthesis of triacylglycerol. The lipin family of phosphatidic acid phosphatases (PAP) consisting of lipin 1, 2 and 3 are responsible for conversion of the intermediate phosphatidic acid to diacylglycerol, the penultimate step in triacylglycerol biosynthesis. Dephosphorylation of PA occurs when lipin translocates between the cytosol and ER membrane and binds PA for subsequent phosphate hydrolysis in contrast to the LPAATs, AGPATs and DGATs which are integral membrane proteins. This unique feature among the rest of the TAG biosynthetic enzymes affords the lipins with a unique regulatory aspect for TAG biosynthesis, the control of its cellular location.

PAP activity is important not only for DAG and TAG synthesis but it can affect the synthesis of other phospholipids. By nature of two separate lipid synthesis branch points initiating from the lipin substrate and product, lipin catalytic activity can influence the levels of PA and DAG at the ER membrane, both of which are substrates for distinct lipid synthesis pathways. Phosphatidylinositol (PI), phosphatidylglycerol (PG), and cardiolipin (CL) are synthesized from PA whereas the most ER membrane abundant lipids phosphatidylcholine (PC), phosphatidylethanolamine (PE) and phosphatidylserine (PS) are derived from DAG. Therefore, through mass action lipin catalytic activity can influence the directionality within the glycerolipid synthesis pathway and as a result so too can stimuli controlling lipin translocation from the cytosol to ER membrane.

### *Lipin History*

In the 1950's Kennedy and colleagues hypothesized that the dephosphorylation of phosphatidic acid could link two known lipid synthesis pathways. This hypothesis was driven by two separate experimental results. First, they had observed that it was possible to generate phosphatidic acid from glycerol using liver homogenates. This finding, in addition to their prior experimental results, suggested that DAG could be used as a substrate for the synthesis of PC and TAG. By demonstrating that PA could be used to produce PC *in vitro* they validated their hypothesis and chemically defined the lipid species in what was termed the Kennedy Pathway for PC synthesis.<sup>3</sup> While this described the lipid intermediates that are enzymatically processed to convert fatty acids and glycerol to PC and TAG for phospholipid synthesis and energy storage, little was known about the enzymes associated with each biochemical lipid modification.

In the Kennedy Pathway, the dephosphorylation of phosphatidic acid is an essential step which leaves a free hydroxyl group at the *sn*-3 position of the glycerol backbone for fatty acid esterification resulting in TAG formation. In the 1960's it was found that  $Mg^{2+}$  was required for dephosphorylation of PA; suggesting that the PAP active site binds PA in part through coordination with a divalent cation. In addition an unexpected experimental finding showed that PAP was more readily isolated from the soluble portions of cell homogenates, implying that PAP was a soluble enzyme that could reversibly associate with membranes for catalytic processing of its insoluble substrate.<sup>4</sup> In the 1980's these results were further validated; PAP activity in rat liver extracts was found to translocate *in vitro* between a soluble cytosolic location and internal membranes in a dynamic fashion influenced by the presence of fatty acids.<sup>5</sup> However, the molecular identity of PAP remained elusive and efforts to purify the enzyme to homogeneity were unsuccessful due to its labile nature.

Identification of the lipin gene became possible when a spontaneous mutation arose in mice in the Jackson labs which exhibited features of human lipodystrophy. These mice, termed fatty liver dystrophy, *fld*, mice are phenotypically characterized by hyperlipidemia, impaired adipocyte differentiation, impaired glucose tolerance and slow growth. In 2001, using a positional cloning strategy, Reue and coworkers identified the genetic rearrangements responsible for the *fld* phenotype and named the novel protein of 891 amino acid lipin.<sup>6</sup> Further analysis revealed two other lipin related genes in mice and also the presence of three lipin genes in humans, the first indication of a lipin protein family in both humans and mice. Shortly thereafter, Todd Huffman from the Lawrence lab at University of Virginia discovered a protein with an electrophoretic mobility between 120 and 140 kD that was highly phosphorylated in response to insulin in adipocytes.<sup>7</sup> Further investigation revealed the unknown protein to be lipin

1 and was hence characterized as downstream target in the insulin/PI3K/mTOR signaling pathway. More specifically, the phosphorylation of serine 106 was shown to be rapamycin sensitive, thereby establishing a possible link between nutrient state and adipocyte development through kinase activity of mTORC1 and phosphorylation of lipin 1.<sup>7</sup>

The Lawrence lab, whose primary research interest was mTOR signaling, began to further investigate the function of the lipin protein in adipocytes. While studies were ongoing, Carmen and colleagues retrieved nearly purified Pah1p, the yeast PAP enzyme, from a freezer and identified it as an ortholog of the mammalian lipin gene by capitalizing on improvements in protein mass spectrometric analysis.<sup>8</sup> Almost 50 years after the Kennedy pathway was defined the protein responsible for the dephosphorylation of PA was identified.

Shortly thereafter, Harris et al. determined that multisite phosphorylation and subcellular localization of lipin 1 are controlled by insulin signaling through mTORC1 kinase activity.<sup>9</sup> Insulin stimulated phosphorylation of lipin 1 promoted a cytosolic location, while dephosphorylated lipin 1 was observed to associate with membranes, thereby correlating phosphorylation status with cellular location. This translocation was ablated through inhibition of mTORC1 by rapamycin, implicating mTORC1 dependent phosphorylation with control of lipin 1 cytosol to ER membrane translocation. Considering that insulin stimulation in adipocytes increases TAG synthesis and given the lipin's requirement in the TAG biosynthetic pathway, the finding that insulin stimulation promotes lipin cytosolic localization was paradoxical.

### ***Lipin Physiology***

## Lipin 1

The gene encoding lipin 1 was identified when a spontaneous mutation arose in mice from the Jackson labs resulting in the fatty liver dystrophy, *fld*, mice.<sup>10</sup> Reue and coworkers were the first to identify and clone the lipin gene and subsequently identified two other lipin isoforms. The *fld* mice display a neonatal fatty liver, which resolves around two weeks of age, followed by peripheral neuropathy resulting from demyelination of peripheral nerves developing in adulthood.<sup>11,12</sup> The *fld* mice are further characterized by impaired adipocyte differentiation and virtually a total absence of TAG in what little white adipose tissue they do possess, along with glucose intolerance and insulin resistance.<sup>6,11</sup> Because lipin 1 is the predominant isoform in adipose, muscle and other tissues, its absence results in tissue specific accumulation of lipid intermediates. PA accumulation in lipin 1 null adipose tissue and Schwann cells leads to inhibition of differentiation pathways through increased MAPK signaling causing the lipodystrophy and peripheral neuropathy associated with the *fld* mice.<sup>13,14</sup> The lipin 1 null phenotype exemplifies the important contributions lipin 1 has to adipose tissue which underscores its role in lipid homeostasis.

In contrast to mice, loss of lipin 1 in humans does not copy the lipodystrophic lipin 1 null murine phenotype, and is associated with childhood rhabdomyolysis.<sup>15</sup> Rhabdomyolysis is an acute syndrome resulting from skeletal muscle injury of either a physical or hereditary variety which leads to the release of muscle proteins into the bloodstream.<sup>16</sup> For instance, elevated levels of myoglobin in the blood are a result of muscle fiber breakdown. The increased serum levels of myoglobin lead to acute tubular necrosis through generation and accumulation of reactive oxygen species due imbalanced iron homeostasis. As a result glomerular filtration rate is perturbed thereby inhibiting normal excretory functions of the kidney. Clinical features may

include weakness, pigmenturia, renal failure, cardiomyopathy, or encephalopathy. If untreated or unrecognized rhabdomyolysis can result in death from renal or cardiac dysfunction.<sup>16</sup>

Associated with rhabdomyolysis, there are nineteen distinct mutations in the human lipin 1 gene, most of which are frame shift mutations or missense mutations that result in loss of expression, truncation and/or loss of catalytic activity.<sup>17</sup> Recurrent rhabdomyolysis episodes associated with lipin deficiency are caused by febrile illness, exercise and fasting.<sup>18</sup>

Recent work has identified a point of convergence between lipin 1 deficiency in skeletal muscle and the use of cholesterol lowering statins. As a side effect of the treatment with the statins, myopathies have also been reported from individuals carrying heterozygous missense mutations in their lipin 1 gene.<sup>19</sup> Reue et al. has established a mechanistic link between muscle specific lipin 1 deficiency and myopathies by defining a role for lipin 1 PAP activity in autophagy, specifically through the maturation of autolysosomes.<sup>20</sup>

In skeletal muscle, lipin 1 deficiency and statin treatment separately result in elevated PA and decreased DAG levels, through unknown mechanisms, and this effect is compounded when both are present. As a result of reduced DAG levels the Protein Kinase D (PKD) – Vps34 phosphatidylinositol 3-kinase pathway is not properly activated thereby inhibiting proper autophagy clearance.<sup>20</sup> These defects likely contribute to the mechanism of rhabdomyolysis caused in lipin 1 null muscle tissue. Patients with recurrent rhabdomyolysis often exhibit normal muscle function between episodes, suggesting that mitochondrial function is sufficient to meet normal energy demands while episodes are typically associated with intense exercise or fasting, both of which initiate autophagy. It was determined that a fifty percent reduction in lipin 1 protein expression in mouse, similar to humans with a heterozygous missense mutation, promotes muscle damage in a statin dependent manner.<sup>20</sup>

Currently there is no answer for the phenotypic discrepancies between man and mouse with regard to loss of lipin 1. Whether other human lipin isoforms can compensate for loss of lipin 1 to prevent a lipodystrophic phenotype that is associated with mice or other compensatory developmental mechanisms are responsible for the different phenotypes remains a question. Furthermore it is possible that the predominant PAP isoforms show different patterns of tissue expression when man and mouse are compared to each other.

### Lipin 2

Lipin 2 expression is most prominent in the liver but has also been observed in adipose, macrophages, and the cerebellum, where its function in these cell types is best understood to contribute to lipid homeostasis<sup>21</sup>. More specifically, in the liver lipin 2 expression is induced by fasting, diet-induced-obesity, and ER stress<sup>22</sup>. Among the lipin family there are tissues in which expression of more than one lipin isoform occur, suggesting distinct and overlapping functions. For example, in 3T3-L1 adipocytes lipin 2 expression decreases during adipogenesis while lipin 1 expression increases, suggesting distinct functionalities of the two enzymes<sup>23</sup>.

Because lipin 1, the founding member of the lipin family, has received the majority of research efforts it has been studied in isolation while only recently have efforts been made to elucidate the functional consequences of multiple lipin isoform tissue expression. Lipin 1 and lipin 2 have been functionally linked in the murine liver where loss of lipin 1 results in a compensatory increase in lipin 2 expression such that PAP activity measured in lysates is restored to wild type levels. This compensation highlights a complicating issue when studying lipin function. This suggests that in tissues where multiple isoforms are expressed the different isoforms can work together to contribute to total cellular PAP activity.

In the mouse, whole body knock out of lipin 2 does not appear to result in any abnormal phenotype.<sup>24</sup> However, after five to six months in age lipin 2 knockout mice display ataxia and tremor resulting in impaired balance, which is reminiscent of cerebellar disease in humans. Further confirmation of a lipin 2 dependent phenotype is the accumulation of PA levels in the cerebellum.<sup>24</sup> Whether additional phenotypes are caused by loss of lipin 2 cannot be definitively ruled out at the present time because the possibility remains that these mice were not given the appropriate challenge.

In humans, mutations in the gene encoding lipin 2 result in Majeed's syndrome.<sup>25</sup> This genetic disorder is defined by chronic recurrent multifocal osteomyelitis and congenital dyserythropoietic anemia beginning in childhood, as well as a transient inflammatory dermatosis with a neutrophilic skin infiltration.<sup>25,26</sup> Three mutations in the lipin 2 gene are associated with Majeed's syndrome including frame shift, nonsense and splice site mutations. All mutations result in truncated catalytically inactive protein suggesting that loss of lipin 2 PAP activity is a defining feature of the disease. Majeed's syndrome has not been very well studied because this rare disease that has only been identified in three families.<sup>25</sup>

Again, phenotypic discrepancies exist between man and mouse with regard to loss of lipin 2 suggesting that the lipin family compensates differently when expression and function of one isoform is compromised.

### Lipin 3

Lipin 1 and lipin 2 together have received the vast majority of investigation in the lipin field while lipin 3 has remained understudied. Preliminary reports suggest that lipin 3 is an important piece of the overall puzzle that is the lipin family contribution to lipid homeostasis and control of cellular PAP activity in mouse adipose. Studies using lipin 3 whole body knockout

mice do not reveal any overt phenotypic abnormalities.<sup>27</sup> However, PAP activity from lipin 3KO adipocytes has approximately 15% of the wild type PAP activity, suggesting that lipin 1 and 3 act in concert to regulate PAP activity in adipocytes.<sup>27</sup> Considering that humans null for lipin 1 do not have any noticeable lipodystrophy these results suggest that a compensatory mechanism increases adipose PAP activity, possibly through lipin 3 function.

### *Lipin Protein Structure*

The lipin family is defined by several conserved regions, the most prominent of which is the catalytic active site residues, DxDxT, located within the conserved CLIP (Carboxyterminal Lipin domain). (**Figure 1.2**) In addition to the CLIP, the NLIP (Aminoterminal Lipin domain) region shares sequence similarity across the lipin family. Found within the NLIP is serine 106, the best validated mTORC1 dependent phosphorylation site. Moving towards the carboxy terminus from the NLIP by approximately 50 amino acids lies a stretch of nine lysines and arginines residues within the proteins of the lipin family, with each members sequence being unique. This region, the Polybasic domain, PBD, was first implicated in the literature as a nuclear localization sequence;<sup>28</sup> however, the PBD has been demonstrated to bind PA and whose regulation is largely controlled by phosphorylation, specifically mTOR dependent phosphorylation.<sup>29</sup> It is not known whether the PBD functions distinctly as a nuclear localization signal and a PA binding protein, or whether these events are coupled. Continuing on in the primary structure of lipin towards the carboxy terminus is the Serine Rich Domain, SRD. This region is highly phosphorylated and mediates the interaction between hyper-phosphorylated

lipin 1 and 14-3-3.<sup>30</sup> In the Haloacid Dehalogenase (HAD) domain, a transcription factor binding motif is found, LxxIL. In addition known phosphorylation sites are marked.

The lipin protein family is a member of the Haloacid Dehalogenase superfamily which includes dehalogenases, phosphoesterases, ATPases, phosphonatasases and sugar phosphomutases. Many members of the HAD superfamily have a solved crystal structure and have been demonstrated to form oligomers.<sup>31</sup> While structure-function analysis of lipin proteins is hindered by a lack of structural data other methods have provided insights into molecular architecture of this protein family.

In solution, Lipin 1 has been shown to form homo and hetero-oligomers with itself and lipin 2 and 3.<sup>32</sup> Using co-immunoprecipitation experiments, intramolecular FRET and various cell culture techniques the lipin family proteins were demonstrated to form stable homo and hetero oligomers. Oligomers formed in a “head-to-head” and “tail-to-tail” configuration, meaning that the NLIP from one lipin monomer would presumably interact with an NLIP from another lipin monomer and likewise for the CLIP. While the functional implications of these findings have not been fully explored, in light of the fact that lower organisms only have one lipin isoform, the formation of hetero-oligomers raises questions about potentially altered functionality. Because  $V_{max}$  for lipin 1 is several fold higher than that of lipin 2, questions arise about the functionality of a hetero-oligomer composed of lipin 1 and 2. Would the  $V_{max}$  of the oligomer reflect both components? Likewise would lipin 2 be trafficked into the nucleus and interact with known transcription factors that lipin 1 has been reported to interact with such as PPAR $\alpha$  and NFATc4.<sup>33,34</sup> Hetero-oligomer formation should be considered for future investigations into the functional consequences of the distinct and overlapping tissue expression of the lipin family.

### *Phosphorylation of Lipin*

The lipins are highly phosphorylated with over 25 sites identified in the founding member, lipin 1<sup>9,35</sup>. Although hormonal signaling can promote or inhibit lipin 1 phosphorylation, which appears to direct the localization of lipin within the cell to separate cellular compartments, the mechanisms by which phosphorylation controls lipin 1 translocation are not clear. Due to the obvious constraints of cytosolic lipin on PAP activity, intracellular localization has long been thought to be the determining factor controlling lipin PAP activity.<sup>9</sup> Consequently, stimuli influencing lipin propensity to bind the ER membrane were believed to be the regulatory mechanisms influencing total cellular PAP activity. With the exception of the highly phosphorylated lipin 1, there is little evidence for post-translational regulation of the other TAG biosynthetic enzymes,<sup>36</sup> suggestive that regulation of lipin intracellular localization can significantly affect both the rate of TAG biosynthesis and production of other phospholipids.

Previous studies have demonstrated a correlation between lipin 1 phosphorylation status and location. In 3T3-L1 adipocytes, insulin stimulation activates kinase activity of mTORC1 and results in increased lipin 1 phosphorylation coinciding with cytosolic localization. (**Figure 1.3**) Through the action of the integral membrane phosphatase, Dullard, and other unidentified phosphatases dephosphorylation promotes lipin 1 accumulation at internal membranes.<sup>9</sup> Inhibition of the mTOR complexes using the ATP binding site competitive inhibitor, Torin 1, causes lipin to translocate from the cytosol to the ER membrane. While an interaction between hyper-phosphorylated lipin and 14-3-3 proteins has been previously demonstrated, this protein-protein interaction does not account for cytosolic localization as a consequence of mTORC1

kinase activation. Lipin phosphorylation sites within the SRD are responsible for the phosphorylation dependent interaction with 14-3-3, whereas characterized mTORC1 dependant phosphosites, S106 and S472, lie outside of this region.<sup>35</sup> Alternatively, mTORC1 dependent phosphorylation of lipin 1 could be exerting its cytosolic localizing effect through a decrease in affinity for lipin 1 with PA and membranes. While the role of phosphorylation on the intracellular localization would be predicted to alter lipin 1 PAP activity, there is little direct evidence supporting such a regulation of function. Highly phosphorylated lipin 1 from 3T3-L1 adipocytes showed no difference in PAP activity compared to the same lipin 1 dephosphorylated with recombinant protein phosphatase 1c when measured using Triton X-100:PA mixed micelles as a substrate<sup>9</sup>. Furthermore, despite dramatically altering lipin 1 phosphorylation, hormonal signaling was also without effect on total lipin 1 phosphatase activity. In contrast, using similar assay conditions it has been reported that blocking cells in mitosis inhibits lipin 1 PAP activity<sup>23b</sup>. However, the lipin 1 examined under these conditions, either in lysates or immobilized as immune complexes on beads, was impure and prevented a detailed kinetic analysis. Three human lipin 1 alternatively spliced isoforms have been characterized biochemically and show considerable differences in enzymatic activity, however, specific roles for each have not been defined<sup>37</sup>. At this time there have been no detailed studies of the effects of phosphorylation on mammalian lipin 1 that has been purified to homogeneity. Thus, a mechanism for how insulin stimulated phosphorylation controls lipin 1 localization was not defined.

In contrast, much more is known about how phosphorylation regulates Pah1p, the yeast homolog of lipin 1. Several studies have reported the different kinases and phosphatases that control the phosphorylation status of Pah1p<sup>38</sup>. Out of 16 Ser/Thr sites within yeast Pah1p to be

identified, mutation of seven to Ala has been shown to be sufficient to affect Pah1p enzymatic activity and association with membranes<sup>38f</sup>. Although there are structural similarities between mammalian lipin proteins and yeast Pah1p, the phosphorylation sites and their respective kinases are not highly conserved. Cdc28p, PKA and Pho80p-Pho85p can phosphorylate Pah1p, and phosphorylation by PKA and Pho80p-Pho85p inhibits Pah1p activity when measured *in vitro* with Triton X-100:PA mixed micelles.<sup>38a-d</sup> The phosphatase responsible for dephosphorylating Pah1p is the Nem1p/Spo7p complex<sup>39</sup>. The Nem1p/Spo7p complex is an integral membrane phosphatase in which Nem1p acts as the catalytic component and Spo7p as a regulatory subunit. Loss of either Nem1p or Spo7p leads to accumulation of hyper-phosphorylated Pah1p that compromises its function. The mammalian orthologs of Nem1p and Spo7p have been identified. Dullard, also known as CTDNEP1, is orthologous to the Nem1p phosphatase, and NEP1-R1 is the mammalian version of the Spo7p regulatory partner. Evidence exists that Dullard, or CTDNEP1, can de-phosphorylate lipin 1 *in vitro* and *in vivo*<sup>40</sup>.

***PA ionization and the electrostatic hydrogen bond switch mechanism  
of PA binding proteins***

The lipin family has a high degree of specificity for phosphatidic acid<sup>8, 37, 41</sup>, which is structurally unique possessing a phosphomonoester polar head group. Among the phospholipids only LPA has a similar polar headgroup structure. What separates this structural motif from the rest of the phosphodiester based phospholipid headgroups is an additional dissociable proton. More importantly, the second dissociable proton has a pKa within the physiological pH range.

Thus, at internal membranes PA can carry either a mono or di-anionic charge depending on the local pH. Since PA is readily ionizable at physiological pH, its phosphate group is available for hydrogen bonding, specifically the oxygen atoms function as hydrogen bond acceptors. At the ER membrane the most abundant hydrogen bond donor is the primary amine in the PE head group. When in proximity to PA, this primary amine can form a hydrogen bond with the oxygen from the phosphate headgroup of PA, thereby promoting the dissociation of the second proton and a resultant di-anionic charge is formed.

This dynamic aspect of PA biochemistry was determined experimentally by investigating the chemical environment around the phosphorus atom in the PA phosphate headgroup when contained within mixed membranes using magic angle spinning  $^{31}\text{P}$  NMR.<sup>42</sup> The peak corresponding to the phosphate from the PA headgroup was shifted down field when the membrane composition included PE while the phosphorous atom in PA remained shielded and its corresponding peak remained up field when contained in PC, which has a quaternary amine incapable of hydrogen bonding, membranes. A dose dependent downfield shift in the  $^{31}\text{P}$ -PA peak in response to increasing molar percentages of PE in the bilayer was further proof of the ability of primary amines to promote the formation of di-anionic PA. More specifically, at physiological pH when PE is present,  $\text{pK}_{\text{a}2}$  of PA changes from  $\sim 7.9$  to  $\sim 6.9$ . Thus, PA ionization is dependent on pH and the composition of the local membrane environment.<sup>43,42</sup>

While other proteins which bind anionic lipids, such as the phosphatidylinositol phosphate species, have evolved specific recognition domains likely due to the steric accessibility of these particular head groups,<sup>44</sup> there are currently no known conserved PA binding motifs. However, all identified PA binding proteins contain positively charged amino acids, such as lysine or arginine, that are responsible for binding to PA<sup>45</sup>. One mechanistic

hypothesis proposed by Kooijman et al. suggested that these basic residues, which contain primary amines, compete with the primary amines from PE to preferentially bind PA in its deprotonated di-anionic state, effectively making PA a preferred docking site for positively charged protein membrane binding domains. This is referred to as the electrostatic hydrogen bond switch mechanism of PA binding proteins.<sup>46</sup> Therefore, both intracellular pH and the composition of different intracellular membranes can affect the charge of PA found in those membranes, and potentially, the ability of PA to recruit PA-binding proteins. This mechanism may extend to other proteins which bind phosphomonoester containing lipids, as the ionization properties and modulators thereof for the phosphomonoester containing sphingolipid ceramide-1-phosphate have been demonstrated to be similar to those of PA.<sup>47</sup>

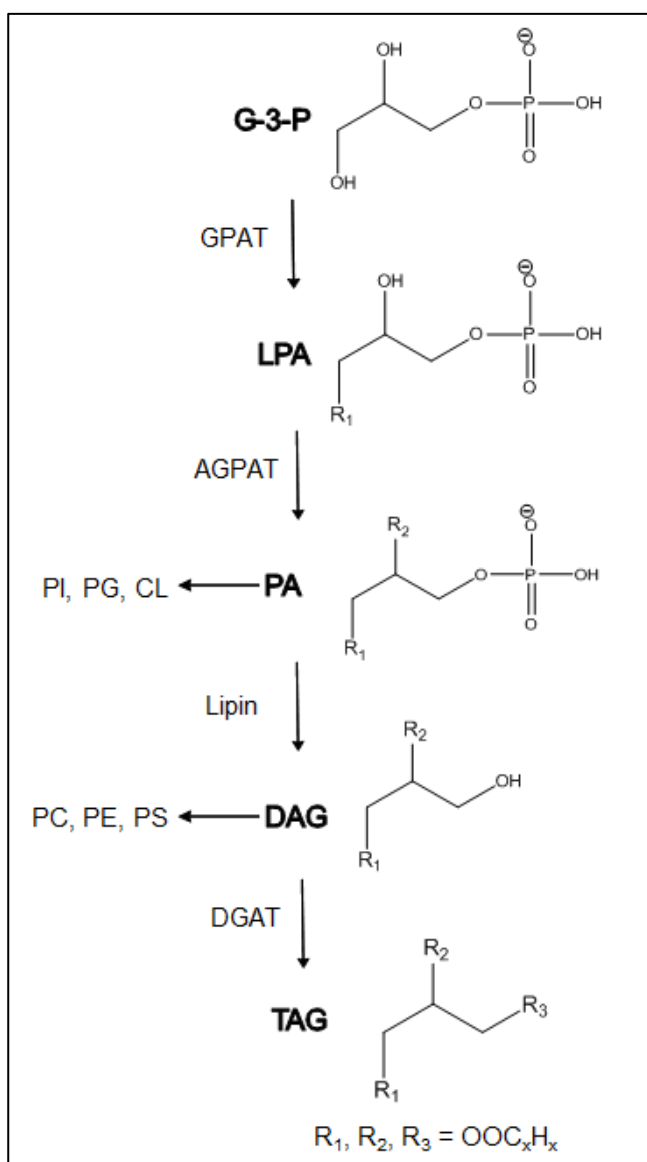
### *Surface Dilution Kinetics*

The ability of a soluble enzyme to act on a lipid substrate is constrained by two factors; movement of the enzyme through three dimensions to bind to a membranous surface, and movement across the surface to bind to the substrate and catalyze the reaction. A kinetic model that accounts for these types of reactions has been described (reviewed in<sup>48</sup>). This means that the action of soluble enzymes acting on an insoluble lipid at a membrane interface can be broken down into two steps.

The first step, defined as the ‘bulk step’, is the enzyme binding to a membranous surface, either non-specifically (surface binding model) or specifically (phospholipid binding model). The second step, or ‘surface step’, measures the combination of the enzyme binding the substrate

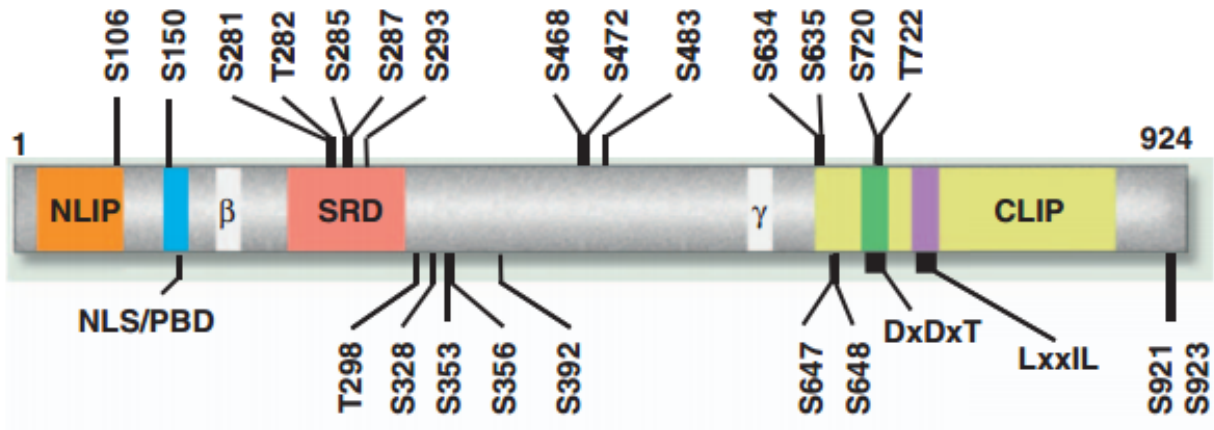
and subsequent catalysis. Thus, to examine how the enzyme binds to a membrane surface, in the bulk step the total concentration of substrate is varied. On the other hand, to examine the kinetics of the surface step, or how the membrane bound enzyme catalyzes the conversion of successive substrate molecules to product, the concentration of substrate within the membranous surface is varied while keeping the molar concentration constant. Examining the activity of the enzyme under these two conditions allows determination of the kinetic rates of each enzymatic step simply as a function of molar or surface concentration of substrate.

Figure 1.1 Intermediate lipid species in PC and TAG synthesis.



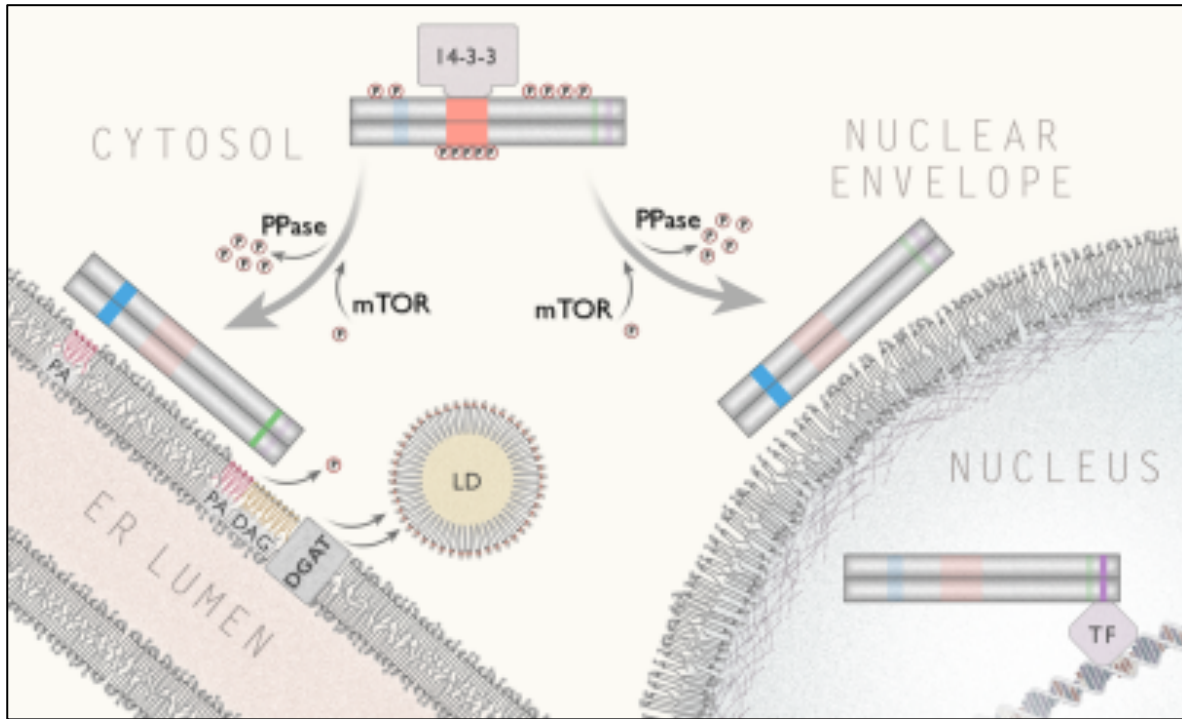
**Figure 1.1 Intermediate lipid species in PC and TAG synthesis.** Glycerol-3-phosphate is acylated by glycerol-phosphate acyltransferase to form lysophosphatidic acid. Acylglycerol-phosphate acyltransferase converts LPA to PA. PA is used as a substrate for the synthesis of PI, PG, and CL. The lipin family converts PA to DAG. Diacylglycerol is used as a substrate for PC, PE and PS synthesis. TAG formation is complete when Diacylglycerol acyltransferase esterifies a third fatty acid to the glycerol backbone.

Figure 1.2 Primary structure of lipin 1.



**Figure 1.2 Primary structure of lipin 1.** Phosphorylation sites are shown in relation to lipin domains. NLIP and CLIP are conserved NH<sub>2</sub>- and COOH- lipin homology domains.  $\beta$  and  $\gamma$  represent alternatively spliced exons, DxDxT is the Haloacid Dehalogenase catalytic motif. The Serine Rich Domain, SRD, mediates interactions with 14-3-3. The Polybasic Domain mediates PA binding. LxxIL is transcriptional coactivator binding motif.

Figure 1.3 Intracellular trafficking of lipin.



**Figure 1.3. Intracellular trafficking of lipin.** At center hyperphosphorylation of the SRD of lipin 1 leads to association with 14-3-3 proteins and cytosolic retention. mTOR dependent phosphorylation of lipin 1 has been determined to promote cytosolic localization while unknown phosphatases promote lipin 1 membrane association.

## CHAPTER 2

### EXPERIMENTAL METHODS

#### Materials

1,2- dioleoyl-*sn*-glycerol, 1,2-dioleoyl-*sn*-glycero-3-phosphate, 1,2-dioleoyl-*sn*-glycero-3-phosphocholine, and 1,2-dioleoyl-*sn*-glycero-3-phosphoethanolamine were from Avanti Polar Lipids. Triton X-100, anti-FLAG M2 affinity gel, diacylglycerol kinase, dodecylamine, dodecyltrimethylammonium chloride, chlorpromazine, epinephrine, and most commonly used chemicals were from Sigma Aldrich.

#### Recombinant expression plasmid for Lipin 1

The FLAG-tagged lipin 1b expression vector (pRK5-FLAG-lipin 1b) has been previously described<sup>35</sup>. The FLAG-tagged PBD mutant was generated from this construct by PCR mutagenesis and designated pRK5-FLAG-lipin 1b-PBD. All amino acid numbering conforms to phosphatidic acid phosphatase LPIN1 isoform b [*Mus musculus*], Accession # NP\_056578.

#### Plasmids and adenovirus constructs for Lipin 2

The *Mus musculus* Lpin2 cDNA from a triple-HA tagged expression vector that was previously described was removed with EcoRV and inserted into pCMV-Tag2C (Stratagene) to produce pCMV-TAG2C-Lipin 2<sup>22a</sup>. This tagged lipin 2 was then subcloned into the pAdTRACK-CMV shuttle vector<sup>49</sup> and then into the pAdEASY system for adenovirus generation. High-titer adenovirus was purified by CsCl-banding as described<sup>49</sup>. The lipin 2 antibody has been previously described<sup>22a</sup>. To generate Venus (yellow fluorescent protein)-tagged lipin 2 the triple HA-tagged Lipin2 was inserted downstream of FLAG-tagged Venus in pcDNA3. To generate

the Venus-tagged lipin 1 the FLAG-tagged Venus sequence was subcloned immediately upstream of lipin 1b in pcDNA3.

#### Purification of Recombinant Lipin 1

HEK293T cells were cultured in 15 cm plates in DMEM containing 5% fetal calf serum and Penicillin/Streptomycin (Gibco). Cells were transiently transfected with 30 µg of plasmid/15 cm plate using Lipofectamine 2000 at a 2:1 ratio of DNA:Lipofectamine. Eighteen-24 plates were used for each purification of lipin 1. Transfected HEK293T cells were harvested by centrifugation at 16,000 x g for 10 min, washed with ice cold phosphate-buffered saline (PBS), and either used directly or frozen at -80°C. For radiolabeling experiments, 48 h after transfection the HEK293T cells were switched from culture medium to low phosphate buffer (145 mM NaCl, 5.4 mM KCl, 1.4 mM CaCl<sub>2</sub>, 1.4 mM MgSO<sub>4</sub>, 25 mM NaHCO<sub>3</sub>, 5 mM glucose, 5 mg/ml BSA, 0.2 mM sodium phosphate, and 10 mM HEPES, pH 7.4) containing 10% serum and were radiolabeled with 0.02 µCi/ml [<sup>32</sup>P]ATP for two h before protein isolation. Cells were lysed in buffer A (150 mM NaCl, 20 mM HEPES, pH 7.2, 0.1% Brij 35) and the lysates cleared by centrifugation at 16,000 g for 10 min, and the supernatant was incubated with anti-FLAG beads for 2-4 h at 4°C. Beads were isolated by centrifugation at 2,000 x g and the supernatant was removed. After washing, the slurry was incubated for 30 min at 30°C in phosphatase buffer (100 mM NaCl, 1 mM MnCl<sub>2</sub>, 2 mM DTT, 50 mM HEPES, pH 7) with or without 2,000 units of Lambda Protein Phosphatase (NEB) and subjected to gentle agitation. The slurry was packed onto a screening column, washed with buffer A and lipin 1 was eluted by 5 successive additions of an equal volume of 0.5 mg/mL FLAG peptide (Lifetein) in 150 mM NaCl, 20 mM HEPES, pH 7.2. Elution fractions containing lipin 1 were pooled and dialyzed three times against 150 mM

NaCl, 20 mM Hepes, pH 7.2 and 1% glycerol. Purified lipin 1 was quantitated using UV absorbance and comparison of bands of lipin 1 and bovine serum albumin standards on Coomassie Blue-stained SDS-PAGE gels.

### Expression and Purification of Lipin 2

Lipin 2 with a FLAG tag was expressed in HeLa cells using 72 h adenoviral infection with MOI ~10. Cells were harvested by centrifugation at 800 x g for 10 min, washed with ice cold phosphate-buffered saline (PBS), and either used directly or frozen at -80°C. All subsequent steps were carried out on ice or at 4° C unless otherwise noted. Cells were lysed in buffer A (500 mM NaCl, 0.1% Brij 35, and 20 mM Hepes, pH 7.2) and the supernatant was incubated with anti-FLAG beads for 2-4 h. Beads were isolated by centrifugation at 600 x g and the supernatant was removed. After washing, the slurry was incubated for 30 minutes at 30° C in 50 mM Hepes, 100 mM NaCl, 1 mM MnCl<sub>2</sub>, 2 mM DTT with or without 2000 units of Lambda Protein Phosphatase (NEB) and subjected to gentle agitation. The slurry was packed onto a screening column, washed with five column volumes of buffer A, followed by five column volumes of buffer B (150 mM NaCl, 0.1% Brij 35, and 20 mM Hepes, pH 7.2) and lipin 2 was eluted by five successive additions of an equal volume of 0.5 mg/mL FLAG peptide in buffer B. Elution fractions containing lipin were pooled and dialyzed three times against 1 L of 150 mM NaCl, 10% glycerol, and 20 mM Hepes, pH 7.2. Purified lipin was quantitated using UV absorbance and comparison of bands of lipin and bovine serum albumin standards on Coomassie Blue-stained SDS-PAGE gels.

### Quantitation of phosphate removal by Lambda phosphatase

HeLa cells were infected with adenovirus expressing FLAG-tagged lipin 2 for 72 h then were switched from culture medium to low phosphate buffer (145 mM NaCl, 5.4 mM KCl, 1.4 mM CaCl<sub>2</sub>, 1.4 mM MgSO<sub>4</sub>, 25 mM NaHCO<sub>3</sub>, 5 mM glucose, 0.2 mM sodium phosphate, and 10 mM HEPES, pH 7.4) containing 10% serum, and were radiolabeled with 0.02 mCi/ml [<sup>32</sup>P]ATP for 2 h before protein isolation. Lipin 2 was isolated as described above and treated with Lambda phosphatase for the indicated amount of time at 30°C subject to gentle agitation. Lipin 2 was electrophoresed on an 8.75% acrylamide gel, transferred to PVDF membrane and quantitation of phosphate removal was determined by autoradiography.

#### Preparation of [<sup>32</sup>P]PA

[<sup>32</sup>P]Phosphatidic acid was purified by thin layer chromatography after using [ $\gamma$ -<sup>32</sup>P] ATP and *E. coli* diacylglycerol kinase to phosphorylate 1,2- dioleoyl-*sn*-glycerol<sup>50</sup>.

#### Preparation of Triton X-100:PA-mixed Micelles

PA was transferred to a glass tube and solvent was eliminated *in vacuo* for 1h. Triton X-100 (TX) was added to produce the appropriate concentration of TX:PA micelles. The mol % of lipid in a Triton X-100/lipid-mixed micelle was calculated using the formula, mol% = 100 x [lipid (M)] / ([lipid (M)] + [Triton X-100 (M)]).

#### Measurements of PAP Activities

PAP activity was determined by using a modification of Han and Carman<sup>50</sup> to measure [<sup>32</sup>P] phosphate release from [<sup>32</sup>P]PA. Briefly, purified lipin 1 was added to reaction mixtures (100 $\mu$ l) containing Triton X-100:lipid-mixed micelles or liposomes, 10 mM  $\beta$ -mercaptoethanol, [<sup>32</sup>P]PA

(10,000 cpm/nmol), 0.5 mM MgCl<sub>2</sub>, and 50 mM Tris-HCl, pH 7.5 or 8.0 where indicated. For assays performed at pH 7.0, 50 mM Tris-maleate was used instead. After 20 min at 30°C, reactions were terminated by adding 0.5 ml of 0.1 N HCl in methanol. [<sup>32</sup>P] phosphate was extracted by vigorous mixing after adding 1 ml of chloroform and 1 ml of 1 M MgCl<sub>2</sub>. The [<sup>32</sup>P] phosphate in 0.5 ml of the aqueous phase was determined by scintillation counting. A unit of PAP activity (U) is defined as the amount required to convert one μmol of PA to diacylglycerol/min. All enzyme activity assays were performed in triplicate and error is shown as +/- standard deviation. The kinetic data was analyzed using GraphPad Prism 5 using Michaelis-Menten, or Allosteric Sigmoidal equations where appropriate.  $k_{cat}$  was calculated according to the equation  $k_{cat} = V_{max}/E_t$ , where  $E_t$ =enzyme catalytic site concentration. Each assay was confirmed with an independent enzyme purification preparation.

#### Preparation of liposomes

Unilamellar phospholipid vesicles were prepared by the lipid extrusion method of MacDonald et al.<sup>51</sup>. Briefly, the indicated concentrations of lipids and amphiphilic amines were dried *in vacuo* overnight to form a thin film which was suspended in buffer B consisting of 20 mM Tris-HCl, 1 mM EDTA, and pH 7.2 unless otherwise indicated. The lipid suspensions were extruded 11 times using a mini-extruder (Avanti) through a 100 nm diameter polycarbonate filter after five freeze/thaw cycles. Liposome production and diameter was verified using a Dynamic Light Scattering instrument from DynaPro. Liposomes were used immediately after generation. For PAP assays utilizing liposomes, [<sup>32</sup>P]PA (10,000 cpm/nmol) was added to the lipids before drying to a film. The subsequent steps for liposome production were performed in a ½” acrylic ultra-clear glove box to minimize exposure.

### Measurement of Lipin 1 Membrane Binding

Binding of lipin 1 to large unilamellar vesicles was measured following a slightly modified version of Höfer et al.<sup>52</sup>. Briefly, lipin 1 was incubated for 20 min at 30°C with liposomes containing the indicated phospholipid concentrations and then an equal volume of 80% (w/v) sucrose in buffer B was added. This mixture was placed in 5 x 41 mm Beckman tubes and was carefully overlaid with 150 µl of 20% (w/v) sucrose in buffer B, and 50 µl of buffer B without sucrose and centrifuged in a SW 55Ti swinging bucket rotor containing nylon inserts at 240,000 x g for one h. The top 50 µl fraction was collected with a Hamilton syringe and analyzed by SDS-PAGE. All binding assays were performed at least three times. The average relative binding compared to PC:PA (20 mol%) liposomes is shown, +/- standard deviation. Student's *t* test was used to determine statistical significance.

### Measurement of Lipin 2 Membrane Binding

Binding of lipin to large unilamellar vesicles was measured following a slightly modified version of Höfer et al.<sup>52</sup>. Briefly, Venus tagged lipin 2 was incubated for 20 minutes at 30° C with liposomes containing the indicated phospholipid concentrations and 0.1 mol% pyrene-PC and then an equal volume of 80% (w/v) sucrose in Buffer B was added. This mixture was placed in 5 x 41 mm Beckman tubes and was carefully overlaid with 150 µl of 20% (w/v), and then 50 µl of 0% (w/v) sucrose in Buffer B and centrifuged in a SW 55Ti swinging bucket rotor containing nylon inserts at 240,000 x g for one h. The top 50 µl fraction was collected with a Hamilton syringe and pyrene and Venus absorption was measured to determine the percent liposome recovery after flotation in addition to the fraction of lipin 2 bound to the liposomes. All binding assays were performed at least three times. The average relative binding compared to PC:PA (20

mol%) liposomes is shown, +/- standard deviation. Student's *t* test was used to determine statistical significance.

#### Radiolabeling of lipin 2 in 3T3-L1 adipocytes

Day 6-8 3T3-L1 adipocytes were infected with adenovirus expressing FLAG-tagged lipin 2. Two days after infection, the cells were incubated for a total of 120 minutes in low phosphate buffer plus 0.1% BSA and supplemented with 0.5 mCi/ml [<sup>32</sup>P] orthophosphate. During this time, the cells were incubated as follows: no additions, 10 mU/ml of insulin for the last 15 minutes only, and 250 nM of Torin1 for last 30 minutes followed by 10 mU/ml of insulin for the last 15 minutes. The cells were lysed in buffer A and the lysates were cleared by centrifugation at 16,000 x g for 10 minutes. The supernatant was incubated with anti-FLAG beads for 2 hours at 4° C. Beads were isolated by centrifugation at 2000 x g for 10 sec and the supernatant was removed. The beads were washed three times with buffer B. Samples were subjected to SDS-PAGE and incorporation of <sup>32</sup>P was visualized using a phosphor imager.

#### Mass Spectrometry

Phosphatase treated and natively phosphorylated lipin 2 were TCA precipitated, suspended in 50 mM ammonium bicarbonate pH 7.7, reduced with 5 mM dithiothreitol, alkylated with 15 mM iodoacetamide, and digested overnight with trypsin. LC-MS/MS analysis was conducted in triplicate on a hybrid ion trap-Orbitrap mass spectrometer to identify phosphorylation sites and to approximate site stoichiometry based on the phosphatase-treated sample. The remaining tryptic peptides were further purified using metal affinity chromatography to enrich phosphopeptides prior to LC-MS/MS<sup>53</sup>. Acquired spectra were searched using Sequest against a concatenated

forward and reverse version of the uniprot mouse protein sequence database (v11.29.2012) allowing for phosphorylation of serine, threonine, and tyrosine (+79.96633 Da). An in-house implementation of the "Ascore" algorithm was used to correctly localize phosphorylation sites<sup>54</sup>. Approximate phosphorylation site stoichiometry was calculated at the peptide level. The increased relative abundance of an unmodified peptide after phosphatase treatment is a proxy for phosphorylation site stoichiometry. We defined 'high' stoichiometry as >67%, 'medium' as 33-66%, and 'low' as <33% of peptides phosphorylated.

### Immunofluorescence

Day 5 post-differentiation 3T3-L1 adipocytes were plated onto poly-L-lysine coated coverslips in 6-well plates and incubated in DMEM with 10% FBS. Day 8 mature adipocytes were treated overnight (16 hr) with either 250 nM Torin1 or vehicle (0.025% DMSO). After treatment, cells on coverslips were washed three times with ice cold PBS, fixed with 4% paraformaldehyde for 20 min at room temperature, washed three times with PBS, and then permeabilized with 0.25% (v/v) Triton X-100 with 10% normal goat serum in PBS for 10 min and washed an additional three times with PBS. Cells were incubated in blocking buffer containing 10% normal goat serum and 0.1% Triton X-100 in PBS, for 1 hr followed by primary antibody incubation for 1 hour at 37°C incubation with PDI primary at room temperature, when present, and 2 hours at room temperature with lipin1/2 primary. Primary antibodies were diluted in 5% normal goat serum and 0.1% Triton X-100 in PBS (1:200 CT-lipin 1, 1:75 lipin 2, 1:200 PDI). Cells were washed 3 times with PBS and incubated with secondary antibody dilution (1:200 Alexa Fluor 555 Goat Anti-Rabbit, 1:400 Alexa Fluor 488 Goat Anti-Mouse) containing 8 ng/μl BODIPY 493/503, when present, in 5% normal goat serum and 0.1% Triton X-100 in PBS for 1 hr at room temperature in the dark. Coverslips were washed four times with PBS and then mounted onto

glass slides using Vectashield containing DAPI. Slides were imaged using a Zeiss LSM 510 microscope equipped with a 100x oil immersion plan-apochromatic lens. The images represent a z-stack projection of 7-10 confocal sections from basal to apical cell side.

### Subcellular Fractionations

3T3-L1 adipocytes were fractionated by slight modification of the method previously described<sup>9</sup>. For each treatment, two 6 cm-diameter plates of cells were homogenized in 0.5 ml of TES buffer (0.25 M sucrose, 1 mM EDTA, and 10 mM Tris-HCl, pH 7.4). The homogenates were centrifuged at 16,000 x g for 20 min and the resulting supernatants were centrifuged at 175,000 x g for 1 h. The high speed supernatants containing soluble proteins were collected, and the high speed pellets containing microsomes were suspended in 0.5 ml of TES buffer.

### Preparation of lipin samples for dry imaging in air

100  $\mu$ l of a 0.57  $\mu$ g/ml solution of lipin in 150 mM NaCl, 50 mM HEPES-NaOH (pH7.4), 1 mM EGTA was applied to a 13 mm freshly cleaved mica disk glued to a 15 mm steel support disk. After 5 min the lipin solution was washed off with several mL of deionized water and the mica surface dried under a stream of argon before the disk was mounted in the AFM.

### Preparation of lipin on supported lipid bilayers for imaging in buffer

Supported bilayers were prepared by the vesicle fusion technique.<sup>55,56,57</sup> 1,2-Dioleoyl-*sn*-glycero-3-phosphatidylcholine (PC), porcine brain l- $\alpha$ -phosphatidylserine (PS), and ovine cholesterol obtained from Avanti Polar Lipids as chloroform stocks were mixed in a ratio 2:1:1

by weight. The chloroform was evaporated under a stream of argon, and the lipids were rehydrated in deionized water to give a total lipid concentration of 2 mg/mL. The lipid mixture was vortexed to produce large multilamellar vesicles, from which small unilamellar vesicles were prepared by sonication with a probe sonicator for 1 min. For the formation of supported lipid bilayers, 50  $\mu$ L of the vesicle suspension was mixed with 950  $\mu$ L of 150 mM NaCl, 50 mM HEPES-NaOH (pH7.4), 2 mM CaCl<sub>2</sub> and 100  $\mu$ L of this suspension was then applied to a freshly cleaved mica disk. After 2 min the mica was washed with several mL of the same buffer to remove unbound vesicles. Lipin was then applied to the bilayer in 100  $\mu$ L of the same buffer at a concentration of 0.57  $\mu$ g/ml. After 5 min the lipin concentration was reduced by a brief wash with 2 mL of buffer and the sample was then imaged in the AFM under buffer. This final wash was necessary to reduce the free lipin concentration sufficiently that it did not adhere to the probe and interfere with imaging.

#### Atomic force microscopy

Samples were examined with a Veeco Multimode 8 atomic force microscope. Dry samples in air were imaged in Peak-Force tapping mode<sup>58</sup> using SCANASYST-AIR probes (Veeco) with a spring constant of 0.4 N/m. Samples under fluid were imaged in tapping mode<sup>9</sup> with Micromasch NSC19ALBS probes with a spring constant of 0.6 N/m. Samples were examined at 29 to 30 degrees C, the ambient temperature of the microscope head during operation. Images were acquired at a scan rate of 2 Hz with a resolution of 512 lines X 512 pixels per line. Image forces were kept to the minimum values compatible with stable imaging by maximizing the amplitude set point in standard tapping mode and minimizing the peak force set point in Peak-Force tapping mode (typically less than 0.1V). For images acquired in tapping mode both the

height image, to give topographic information, and the amplitude error image, to give better edge definition, are shown.

Particle heights and diameters at half-height were determined from the average of measurements of two cross sections at approximately right angles to one another. Following the procedure of Schneider and colleagues<sup>59</sup>, molecular volumes were calculated by modeling the particles as spherical caps and using the formula

$$V_m = (h/6) (3r^2 + h^2)$$

where  $h$  = the height of the particle and  $r$  = the radius of the particle at half height. The diameter and radius were taken at half height since previous empirical studies suggest this tends to compensate for the increase in apparent diameter due to the finite size of the probe when measuring the volumes of isolated proteins.<sup>59</sup> Statistics on particle measurements are given as means +/- sample standard deviations.

## CHAPTER 3

### PHOSPHORYLATION AND CHARGE ON THE PHOSPHATIDIC ACID HEAD GROUP CONTROL LIPIN 1 MEMBRANE BINDING AND PHOSPHATASE ACTIVITY

#### ABSTRACT

The lipin gene family encodes a class of Mg(2+)-dependent phosphatidic acid phosphatases involved in the de novo synthesis of phospholipids and triglycerides. Unlike other enzymes in the Kennedy pathway, lipins are not integral membrane proteins, and they need to translocate from the cytosol to intracellular membranes to participate in glycerolipid synthesis. The movement of lipin 1 within the cell is closely associated with its phosphorylation status. Although cellular analyses have demonstrated that highly phosphorylated lipin 1 is enriched in the cytosol and dephosphorylated lipin 1 is found on membranes, the effects of phosphorylation on lipin 1 activity and binding to membranes has not been recapitulated *in vitro*. Herein we describe a new biochemical assay for lipin 1 using mixtures of phosphatidic acid (PA) and phosphatidylethanolamine that reflects its physiological activity and membrane interaction. This depends on our observation that lipin 1 binding to PA in membranes is highly responsive to the electrostatic charge of PA. The studies presented here demonstrate that phosphorylation regulates the ability of the polybasic domain of lipin 1 to recognize di-anionic PA and identify mTOR as a crucial upstream signaling component regulating lipin 1 phosphorylation. These results demonstrate how phosphorylation of lipin 1 together with pH and membrane phospholipid composition play important roles in the membrane association of lipin 1 and thus the regulation of its enzymatic activity.

## INTRODUCTION

Lipin proteins are a class of mammalian  $Mg^{2+}$ -dependent phosphatidic acid phosphatases that have dual functions in lipid synthesis and transcriptional regulation. Lipin family members catalyze the dephosphorylation of phosphatidic acid (PA) to diacylglycerol (DAG) in the de novo pathway of neutral and phospholipid synthesis. There are three lipin family members, Lipin 1-3, and all contain a carboxy-terminal region (CLIP) with a haloacid dehalogenase –like (HAD) domain as the catalytic core and an amino terminal domain (NLIP) of unknown function<sup>6, 8</sup>. There is also evidence that the lipins play a role in directly regulating gene transcription in the nucleus<sup>1</sup>. Lipin 1 is capable of regulating cellular lipid status at multiple levels by controlling lipid synthesis directly through its PAP activity, and indirectly through modulating the activity of transcription factors important for lipid biosynthesis and breakdown.

Our previous work demonstrated phosphorylation of lipin 1 through the mTOR signaling pathway decreased the association of lipin 1 with membranes. While developing an *in vitro* assay to measure how phosphorylation might affect lipin 1 enzymatic activity, we found that lipin 1 association with membranes occurs more readily with deprotonated, di-anionic PA. This demonstrates that lipin 1 enzymatic activity and binding can be affected by membrane composition and pH. In addition, we find that phosphorylation impairs lipin 1 association with PA by inhibiting the action of the PA-binding region located in the polybasic domain. This suggests that lipin 1 binds to PA via the electrostatic/hydrogen bond switching mechanism<sup>60</sup>. Thus, the ionization status of PA plays a key role in lipin 1 PAP activity and is the mechanism by which phosphorylation regulates binding of the polybasic domain to PA. These results provide new mechanistic insights explaining how mTOR-induced phosphorylation controls the

physiological expression of lipin 1 and also provide a new *in vitro* assay that reflects this regulation.

## RESULTS

### *Phosphorylation of lipin 1 does not affect enzymatic activity under standard conditions-*

We sought to develop an *in vitro* assay that accurately reflects how phosphorylation is thought to affect lipin 1 PAP activity within cells. We transfected HEK293T cells with FLAG-tagged lipin 1b (termed lipin 1 in the remainder of the manuscript). Two days later we purified highly phosphorylated lipin 1 using FLAG affinity chromatography. While still bound to affinity beads, the samples were split into parallel reactions and treated with or without Lambda ( $\lambda$ ) phosphatase to dephosphorylate lipin 1. Treatment with phosphatase increased the mobility of the dephosphorylated form from ~140 kDa to ~120 kDa (**Figure 3.1A**). Note that 120 kDa is still a rather aberrant mobility for a protein with a predicted molecular weight of ~95 kDa. In order to more precisely define the extent of phosphate removal by lambda phosphatase, in a parallel series of experiments we isolated FLAG-lipin 1 from cells radiolabeled with  $^{32}\text{P}$ . **Figure 3.1B** shows that lambda phosphatase treatment removed >95% of the phosphate from lipin 1. Under certain conditions lipin 1 has also been reported to be sumoylated<sup>61</sup>. However, we found no evidence for lipin 1 sumoylation in HEK293T cells under these conditions by western blot.

Phosphorylated ( $-\lambda$ ) and dephosphorylated ( $+\lambda$ ) lipin 1 was then eluted with FLAG peptide and dialyzed. PAP activity was measured in TX:PA mixed micelles (9.1 mol%) according to previous protocols<sup>9, 50</sup>. Under these conditions there is no apparent difference in the rate of product formation between the phosphorylated and de-phosphorylated forms (**Figure 3.1C**). Note that this is in stark contrast to the reports for the lipin 1 ortholog from yeast, where phosphorylation of Pah1p decreases PAP activity<sup>38a, 38d, 38e</sup>. Consistent with previous findings using immune complex-bound lipin 1, **Figure 3.1C** suggests that the purification state of lipin 1

is not the critical factor in determining whether phosphorylation will affect enzymatic activity *in vitro*.

We reasoned that perhaps the lack of effect of phosphorylation on lipin 1 enzymatic activity was due to the use of Triton X-100 mixed micelles for substrate presentation. We hypothesized that perhaps when PA in micelles was presented to lipin 1 it might mask the effect of phosphorylation on enzymatic activity. Although TX-100 mixed micelles provide a convenient assay system for determining the kinetics of PA phosphatase activity, the micelles may not accurately reflect the presentation of PA on the surface of internal membranes. For example, the relatively small size of the micelles implies that they have an extreme surface curvature. Alternatively, the phospholipids that make up internal membranes may themselves influence the interaction of lipin 1 with membranes and hence, unmask the effects of lipin 1 phosphorylation on the dephosphorylation of PA within these membranes. For example, mixtures of PC with PA were previously shown to provide favorable substrates for measuring the PAP reaction of the lipins versus that of the lipid phosphate phosphatases<sup>62</sup>. To more closely approximate a membrane surface, we generated 100 nm liposomes composed of PC and PA. Liposome sizes were verified by dynamic light scattering (not shown). We measured the enzymatic activities of phosphorylated and dephosphorylated lipin using increasing concentrations of liposomes (**Figure 3.1D**), with PA at a final surface concentration of 10 mol%, as has been previously described for yeast Pah1p<sup>38c</sup>. As reported for yeast Pah1p, lipin 1 showed activity against PA in PC:PA liposomes. Under these conditions both phosphorylated and dephosphorylated lipin 1 again showed similar activity when measured as a function of PA concentration.

*Phosphatidylethanolamine increases activity and the binding of lipin 1 to PA-containing liposomes*- Intracellular membranes contain other phospholipids besides PC and PA, with the next most abundant being PE and phosphatidylserine (PS). To more accurately represent a model membrane we prepared 100 nm PC liposomes containing PA at 10 mol% and PE at an increasing molar ratio. The inclusion of increasing concentrations of PE in the liposomes uncovered rather dramatic differences in the enzymatic activity of lipin 1 that was dependent on its phosphorylation state (**Figure 3.2A-D**). In the presence of PE the  $k_{cat}$  of dephosphorylated lipin 1 was significantly greater than that of phosphorylated lipin 1 (**Table 3.1**). Note that while phosphorylated and dephosphorylated lipin 1 both show an increase in  $k_{cat}$  with PC:PE:PA liposomes compared to PC:PA liposomes, at equal mol% PE and PC the overall increase for dephosphorylated lipin 1 was 8-fold compared to a <2-fold increase with phosphorylated lipin 1 (45 mol% PE, **Table 3.1**). This suggests that PE enhances lipin 1 catalytic efficiency preferentially for dephosphorylated lipin 1. To visualize the effect of PE on lipin 1 PAP activity the turnover number was graphed as a function of the mol% PE (**Figure 3.2E**). Dephosphorylated, but not phosphorylated, lipin 1 displayed a sigmoidal curve suggesting a cooperative effect of the PE concentration on lipin 1 PAP activity. In addition, an examination of the kinetic data from Table 1 indicates that increasing PE concentrations decrease the apparent  $K_m$  of dephosphorylated lipin 1, but not phosphorylated lipin 1 (**Table 3.1**). This suggests that PE enhances the affinity of lipin for substrate, but only for dephosphorylated lipin 1.

The enhanced lipin 1 activity in the presence of PE could be due to either an increase in the binding affinity of lipin 1 for PA, an increase in the active site efficiency, or both. However, *in vivo* studies have demonstrated that phosphorylation can affect the association of lipin 1 with intracellular membranes, suggesting that phosphorylation is more likely to affect lipin 1

membrane interaction. To examine this question *in vitro*, we investigated how the presence of PE affects lipin 1 binding to PA-containing liposomes. A well characterized fluorescence spectrometric method has been developed for examining yeast Pah1p association with liposomes<sup>38c</sup>. Despite repeated attempts we were unsuccessful in adapting this method for mammalian lipin 1, most likely due to the high number of tryptophan residues compared to yeast Pah1p (12 versus only 5 in Pah1p). Therefore we employed a liposome binding assay that uses liposome flotation through a density gradient to examine lipin 1 association with membranes. PC liposomes of 100 nm in diameter were prepared by extrusion and contained either no PA or 20 mol% PA. The concentration of PA was increased to 20 mol% to enhance the level of lipin 1 association with the liposomes. PC:PE:PA liposomes were similarly generated by using increasing concentrations of PE at the expense of PC, while maintaining PA at 20 mol%. Two hundred ng of purified lipin 1 was first incubated with the liposomes to allow binding, and the bound and free lipin 1 was separated by flotation centrifugation through a step gradient. In the absence of PA only a modest amount of lipin 1 binding to liposomes was observed (**Figure 3.3 A and B**). In PC:PA liposomes, the amount of lipin 1 recovered increased steadily through replacement of the PC with PE. Under all conditions phosphorylated lipin 1 showed greatly reduced binding levels, but a similar dependence on PE. Since liposomes were prepared in the presence of EDTA and no  $Mg^{2+}$  was added to the binding reaction, it does not appear that lipin 1 enzymatic activity is required for liposome association. In addition, the PAP activity of dephosphorylated lipin 1 shows a substantial decline in the apparent  $K_m$  with increasing mol% of PE when measured with PC:PE:PA liposomes (**Table 3.1**). Finally, we should point out that although some of the concentrations of PA and PE used in the measurements of lipin 1 PAP activity and binding to membranes are higher than normally seen in cells, we do this in order to maximize activity and

binding in an *in vitro* assay system. Thus, PE increases lipin 1 membrane association in the presence of PA, and therefore lipin 1 PAP activity, with a relative preference for dephosphorylated lipin 1.

*Di-anionic PA; pH and amphiphilic amines-* We next investigated why PE both enhanced overall PAP activity and illuminated differences in phosphorylated versus dephosphorylated lipin 1. Phosphatidic acid is unique among the glycerolipids in that it has the smallest headgroup, giving it a cone shape. Furthermore, as a phosphomonoester, the second pK<sub>a</sub> of PA falls within the intracellular physiologic pH range. Biophysical studies of PA in model membranes showed that PE is capable of forming a hydrogen bond with an oxygen of the phosphate group and causing deprotonation of PA<sup>42</sup>. This effectively reduces the second pK<sub>a</sub> from 7.9 to 6.9, thus deprotonating PA to a -2 charge more readily at physiological pH. Some PA binding proteins prefer to associate with di-anionic PA, suggesting that the enhanced activity and membrane association we observed could be due to the effects of PE on the charge of PA<sup>46</sup>. Like PA, PE is a cone-shaped phospholipid. However, our finding that the inclusion of PE in liposomes increases lipin 1 PAP activity could be due to either steric effects on access to PA, effects of PE on PA charge, or both. To identify the determinant(s) for PE on lipin 1 enzymatic activity, we examined lipin 1 binding and activity in the presence of a membrane-incorporated primary amine other than PE. Dodecylamine and dodecyltrimethylammonium mimic the amines of PE and PC respectively, but they are amphiphilic amines. It has been previously demonstrated that dodecylamine, but not dodecyltrimethylammonium, can deprotonate PA at pH 7.0<sup>46</sup>. Therefore we generated PC:PA liposomes and PC:PA liposomes containing an increasing amount of dodecylamine or dodecyltrimethylammonium substituted for PC and determined the degree of lipin 1 binding by liposome flotation. As shown in **Figure 3.4A**, increasing concentrations of

dodecylamine increased the association of lipin 1 with liposomes. Dodecyltrimethylammonium, as a quaternary amine incapable of hydrogen bonding with PA, was without effect. For reasons that are not completely clear, both amines completely inhibited lipin 1 enzymatic activity (not shown).

Chlorpromazine is another amphiphilic amine that has been previously used in PAP enzymatic assays<sup>63</sup>. We generated liposomes composed of a 1:1 ratio of PA to chlorpromazine at 10 mol% in PC and measured lipin 1 PAP activity using an increasing concentration of substrate. As demonstrated in **Figure 3.4B**, the addition of chlorpromazine to PAP assays at pH 7.5 uncovers the difference between phosphorylated and dephosphorylated lipin 1, similar to the addition of PE to the micelles. There was a reduction in PAP activity of about five fold when compared to PA:PC liposomes alone, possibly reflecting a competition for binding to PA<sup>63</sup>. We next measured whether chlorpromazine enhanced the binding of lipin 1 to liposomes (**Figure 3.4C**). Similar to PE and dodecylamine, the addition of chlorpromazine to PC:PA liposomes substantially increased lipin 1 binding.

To more firmly substantiate the hypothesis that lipin 1 prefers di-anionic PA, we measured the enzymatic activity of lipin 1 in TX:PA micelles that maintain a constant molar ratio of TX to PA at 9.1 mol% at pH 7.0, 7.5, and 8. Compared to pH 7.0 (**Figure 3.5A**), at pH 7.5 (**Figure 3.5B**) there was an increase in overall activity with no difference between phosphorylated and dephosphorylated lipin 1 in either case. This is consistent with previous findings that human lipin 1 has a pH optimum at pH 7.5<sup>37</sup>. Increasing the pH to 8, which is above the second pKa of PA, would cause >80% of the PA to be deprotonated. **Figure 3.5C** shows that increasing the pH to 8 resulted in phosphorylated lipin 1 having a significant decrease in activity when compared to dephosphorylated lipin 1. Thus, three different model systems that

manipulate the relative  $pK_a$  of PA in membranes or micelles gave similar results to enzymatic and binding activity by uncovering a difference in phosphorylated and dephosphorylated lipin 1.

We examined lipin 1 activity as a function of the surface concentration of PA (mol%), while keeping the total PA concentration constant at saturating levels (1 mM PA). Under these conditions rather than exhibiting Michaelis-Menten kinetics, lipin 1 functions according to an allosteric sigmoidal model with positive cooperative kinetics. **Figure 3.5D** demonstrates that phosphorylated lipin 1 has a significant decrease in  $V_{max}$  compared to dephosphorylated lipin 1. Calculation of the apparent  $K_m$  values according to the formula  $K_{prime} = K_m^h$  gives values of 6.4 mol% for dephosphorylated lipin 1 and 7.4 mol% for phosphorylated lipin 1. This gives  $k_{cat}$  values of  $37.7 \text{ s}^{-1}$  for phosphorylated lipin 1 and  $84.9 \text{ s}^{-1}$  for dephosphorylated lipin 1. Phosphorylated lipin 1 also shows a 50% increase in the Hill number compared to dephosphorylated lipin 1 (**Table 3.2**).

Finally, to ensure that the observed changes in lipin 1 PAP activity were caused by changes in PA association, we measured the ability of lipin 1 to bind to PC:PA liposomes at pH 7.2 and 8.0. At pH 7.2, the majority (>80%) of the PA will be mono-anionic, while at pH 8.0 most of the PA will be di-anionic. As seen in **Figure 3.5E** the binding to PC:PA liposomes is greatly increased for dephosphorylated lipin 1 at pH 8.0 when compared to pH 7.2. Phosphorylated lipin 1 binding is also increased at pH 8.0, but not nearly to the extent of dephosphorylated lipin 1.

*Inhibition of mTOR increases lipin 1 PAP activity.* Since phosphorylation of lipin 1 inhibits physiological activity by decreasing membrane association, we were interested in examining which phosphorylated residues were responsible. We identified that mouse lipin 1 has

at least 19 and as many as 23 phosphorylation sites<sup>9</sup>. Instead of primarily a cytosolic localization as observed with wild type lipin 1, mutation of 21 of these S/T residues to A promoted localization to the ER/nucleus suggesting an increase in membrane association<sup>35</sup>. To examine whether the identified S/T residues are the relevant phosphorylated sites that control membrane association, we purified wild type lipin 1 (WT) and the 21xA lipin 1 mutant (21xA) and examined enzymatic activity as a function of PA concentration (**Figure 3.6A**). Only the wild type lipin 1 was subjected to dephosphorylation with  $\lambda$  phosphatase. **Figure 3.6A** demonstrates that mutating the 21 S/T residues to A generates a lipin 1 protein that has similar activity as a lipin 1 protein that has had all phosphates removed by  $\lambda$ -phosphatase *in vitro*. This demonstrates that all of the S/T sites that can be phosphorylated and significantly affect activity are contained within the 21 sites mutated in the 21xA mutant.

Of the identified phosphorylated sites in lipin 1, only two have been demonstrated to be downstream of mTOR activation. However, inhibition of mTOR causes a dramatic change in the intracellular localization of lipin 1, suggesting that mTOR activity is sufficient to regulate lipin 1 association with membranes. Therefore, not all of the phosphorylated sites identified play a significant role in the control of lipin 1 association with membranes. To more specifically address the dependence of mTOR-mediated phosphorylation of lipin 1 on the control of membrane association, we treated cells for 16 h with 250 nM torin1 and purified lipin 1 from control and treated cells (**Figure 3.6B**). The mobility of lipin 1B from cells treated with torin1 was only modestly increased when compared to control cells, suggesting that the phosphorylation sites reliant on mTOR activity are only partially responsible for the phosphorylation-induced mobility changes. This is consistent with previous observations on lipin 1 mobility using rapamycin to inhibit mTORC1 activity in 3T3-L1 adipocytes<sup>9</sup>. Despite the

small change in electrophoretic mobility (inset), there was a significant increase in the PAP activity of lipin 1 (WT+Torin) from torin1-treated cells when compared to highly phosphorylated lipin 1 obtained from cells with active mTOR (WT- $\lambda$ ) (**Figure 3.6B**). Lipin 1 that was devoid of all phosphorylated sites (WT+ $\lambda$ ) had a similar  $k_{\text{cat}}$  ( $74.9 \text{ s}^{-1}$ ) to the lipin 1 lacking the mTOR-directed phosphorylation sites ( $58.8 \text{ s}^{-1}$ ). Both were more than two-fold higher than phosphorylated lipin 1 ( $27.8 \text{ s}^{-1}$ ). Thus, the majority of the effects of phosphorylation on lipin 1 PAP activity require mTOR kinase activity, suggesting that other kinase(s) have a less significant contribution in this respect.

*The polybasic domain is required for lipin 1 phosphorylation to affect activity.* In 2007 Kooijman et al. described an electrostatic/hydrogen-bond switch as a mechanism for PA-binding proteins. This theory posits that basic residues within PA-binding proteins, particularly lysine residues, are capable of forming hydrogen bonds causing deprotonation of PA and enhanced membrane association. Lipin 1 has a highly basic stretch with 9 lysine and arginine residues in a row at amino acids 153-161. This domain is required for interaction with PA, but curiously, had no effect on lipin 1 enzymatic activity<sup>28</sup>. To determine whether this region is involved in sensing di-anionic PA in the membrane, we mutated all nine basic residues to alanine and examined the effect on lipin 1 activity. PAP activity of the lipin 1-PBD mutant was assayed using liposomes at 10 mol% PA and 90 mol% (PC+PE), with PE at 0 and 30 mol%. **Figure 3.7A** and **B** have the respective wild type lipin 1 curves from **Figure 3.1D** and **3.2B** inserted as insets for comparison. Mutation of the PBD site greatly increases the apparent  $K_m$  when compared to wild-type lipin 1, and largely prevents the decrease in  $K_m$  and increase in turnover that occurs upon replacing 30 mol% of the PC in the liposomes with PE (**Table 3.3**). More importantly, mutation of the PBD sites completely eliminates the effect of phosphorylation on

lipin 1 PAP activity, suggesting that the function of phosphorylation is to prevent the PBD from interacting with PA. Since PA would be mostly di-anionic in the PC:PE:PA liposomes, this suggests that the PBD is required for recognition of the electrostatic charge of PA.

Mutation of the PBD in lipin 1 eliminates the decrease in the apparent  $K_m$  with PE, consistent with the involvement of the PBD in substrate binding. Dephosphorylated wild type lipin 1 shows a decrease in  $K_m$  with increasing PE concentrations (**Table 3.1**). However, phosphorylation of the PBD mutant had little effect on activity (**Table 3.3**), suggesting that phosphorylation affects binding to substrate via the PBD. To confirm that the PBD mutation specifically eliminates the effects of phosphorylation on lipin 1 binding, we tested the ability of phosphorylated and dephosphorylated PBD mutant to bind to membranes by liposome floatation. Because the PBD mutant is largely defective in PA binding it was necessary to use 1  $\mu\text{g}$  of protein for each binding reaction. **Figure 3.7C** shows that without the PA-binding PBD, the electrostatic charge of PA no longer influences the association of lipin 1 and phosphorylated lipin 1 can associate as readily as dephosphorylated lipin 1. This shows that in addition to PA binding through the PBD, a binding event that is regulated by phosphorylation, lipin 1 can associate with membranes independently of PA in a manner that is not regulated through phosphorylation.

## DISCUSSION

Lipin 1 phosphorylation has been proposed to play an important role in its function. When measured by biochemical fractionation of cells, hyperphosphorylated lipin 1 is found in the cytosol of 3T3-L1 adipocytes, while hypophosphorylated lipin 1 is localized to microsomal membranes. Overexpression of wild type lipin 1 shows cytosolic localization by immunofluorescence microscopy, while the 21xA mutant localizes to the ER/nucleus. Microscopic analysis of endogenous lipin 1 in 3T3-L1 adipocytes shows lipin 1 spread across the cytosol and localized to discrete punctuate spots, while treatment with torin1 causes a dramatic relocation to the ER/nucleus. These changes in localization were found to play a crucial role in the regulation of the transcriptional activity of SREB1c<sup>35</sup>. In addition, lipin 1 phosphorylation is thought to play a critical role in its enzymatic function, although evidence for this has been lacking until now. The studies presented here demonstrate that phosphorylation regulates the ability of the polybasic domain of lipin 1 to recognize di-anionic PA. We show that mTOR activity is required for phosphorylation of lipin 1 to negatively regulate lipin 1 PAP activity. In addition, while uncovering how phosphorylation regulates lipin 1 PAP activity we have made the novel identification of effectors that act in conjunction with phosphorylation to control the PAP activity of lipin 1.

This study demonstrates that lipin 1 binding to its substrate is dependent on the electrostatic charge of PA. The electrostatic/hydrogen bond switch model proposes that PA binding proteins preferentially associate with di-anionic PA (**Figure 3.8**). The ability of lipin 1 to associate with liposomes is dependent on both pH and the presence of hydrogen bond donor molecules in the liposomes such as PE or amphiphilic amines. This suggests that lipin 1 moves from three dimensions to the two-dimensional membrane surface via preferential interaction with

di-anionic PA, presumably by electrostatic attraction. Furthermore, once bound, we propose that the PBD of lipin 1 functions as an anchor to bind lipin 1 to the two-dimensional membrane surface by the hydrogen bond between the primary amine of PE to PA 'switching' to the primary amine of lysine within the PBD of lipin 1. The generation of a strong interaction between the PBD and PA would allow the catalytic site of lipin 1 to dephosphorylate multiple molecules of PA without lipin 1 releasing from the membrane surface. We suggest that this explains, at least in part, the functional cooperativity that is shown during surface step reaction kinetics. Lipin 1 can form homotetramers, or heterotetramers with other lipin proteins. Although it remains to be determined whether the PBD-mediated association with PA must occur within the same lipin 1 molecule that contains the active site for functional cooperativity, previous reports have suggested that the catalytic sites within lipin 1 homo-tetramers function independently<sup>32</sup>. Although mTOR has been demonstrated by immunofluorescence staining to control lipin 1 movement to membranes within cells, we have now shown that mTOR-directed phosphorylation regulates lipin 1 enzymatic function. Because mutation of the PBD eliminates the effects of phosphorylation on activity, we propose that mTOR-mediated phosphorylation prevents lipin 1 from recognizing PA containing two negative charges in membranes (**Figure 3.8**). The requirement for the PBD for membrane interaction provides a rationale that explains why lipin 1 interacts with PA. Other negatively charged lipids such as unsaturated fatty acids and acyl-CoA esters have also been shown to promote PAP accumulation on membranes<sup>64</sup>. Conversely, neutralizing this negative charge with an amphiphilic amine displaces PAP activity from endoplasmic reticulum membranes in cell-free systems<sup>64b</sup> and in hepatocytes<sup>65</sup>. Future experiments will be necessary to determine whether these effects on PAP localization occur via interactions with the lipin 1 PBD.

There could be two separate membrane binding regions within the lipin family of proteins. The single *Saccharomyces cerevisiae* homolog of the lipin family contains an amino-terminal amphipathic helix that interacts with membranes and is inhibited by phosphorylation<sup>38e</sup>. Mutation of the amphipathic helix decreases membrane recruitment, renders the mutant Pah1p protein resistant to phosphorylation-mediated inhibition of membrane binding, and functionally eliminates the ability of Pah1p to participate in lipid synthesis. Mammalian lipin 1 and 2 contain predicted amphipathic helices at their amino-terminus but whether the helix is required for membrane association has not been determined. In contrast, while all mammalian lipins contain a nine amino acid PBD, in *Saccharomyces cerevisiae* there is no such conserved stretch, although there is a KKKEK region in a similar position (amino acids 171-176). However, the *Saccharomyces pombe* homolog contains no more than two consecutive basic amino acids. The *Arabidopsis thaliana* homologs also lack a PBD and yet functions similarly to yeast Pah1p<sup>66</sup>. Evolutionarily, the nine amino acid PBD found in mammals did not occur until urochordata (*Ciona intestinalis*), and is largely conserved in all descendant species. It should be pointed out that most PA-binding proteins do not have such a large stretch of basic residues and frequently require only one or two basic residues for PA binding. It is interesting that the mammalian lipins have evolved such a strategy. Lipin 1 can still associate with liposomes in the absence of PA (**Figure 3.3A & B**) and the absence of the PBD (**Figure 3.7C**), albeit at greatly reduced efficiency. And increasing molar concentrations of PA:PC liposomes still increase Pah1p association even when the amphipathic helix was mutated such as to completely abolish membrane recruitment<sup>38e</sup>. Thus, both yeast and mammalian lipins may employ separable mechanisms for membrane binding. We suspect that the PBD is specific for PA association whereas the amphipathic helix is more likely involved in general membrane binding and/or

catalysis. However, future studies into the mechanism of lipin 1 membrane binding using combinations of the PBD/amphipathic helix will be necessary to fully identify the domains required for membrane binding, activity, and regulation by phosphorylation.

Lipin 1 is clearly required for phospholipid and neutral lipid synthesis. Insulin stimulation promotes triacylglycerol synthesis in adipose tissue<sup>67</sup>. It may seem paradoxical that insulin stimulation increases lipin 1 phosphorylation and decreases its interaction with membranes and thus its enzymatic activity<sup>9</sup>. However, a second major driving force for this reaction is increased fatty acid availability. This provides a feed-forward stimulus through the accumulation of fatty acids and PA in membranes that promotes the translocation of lipins to the endoplasmic reticulum and enables cells to match their rates of triacylglycerol synthesis to the fatty acid supply. This occurs during  $\beta$ -adrenergic stimulation of adipocytes which promotes lipolysis, increases fatty acid accumulation, and increases lipin 1 membrane association, resulting in increased fatty acid esterification<sup>9,68</sup>. This translocation would be favored by low insulin stimulated phosphorylation of lipin 1.

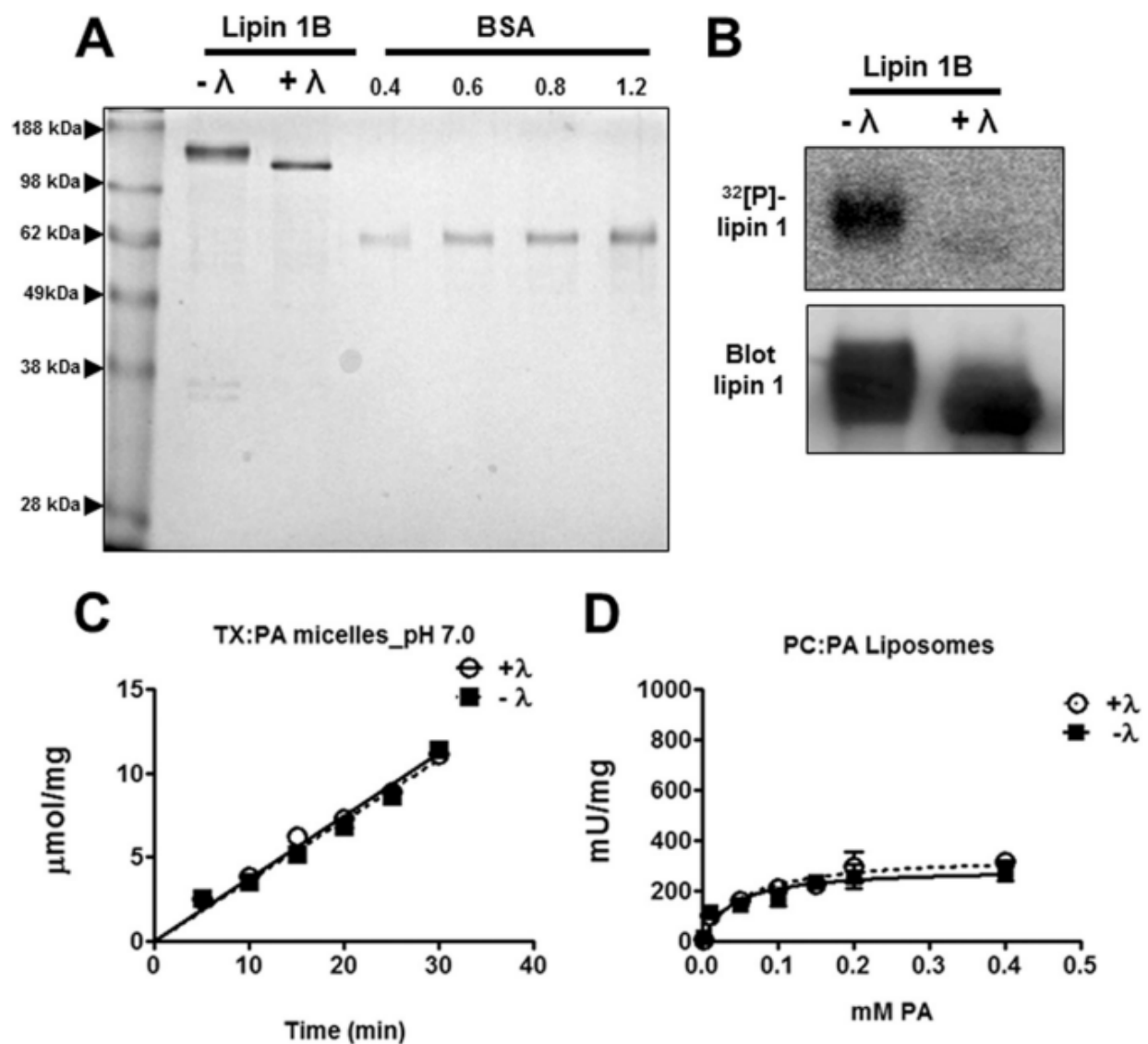
It is also possible that alterations in intracellular pH, combined with the effect of pH on the ability of lipin 1 to bind to PA, could contribute to the observations *in vivo*. To use adipocytes as an example, during insulin stimulation lipin 1 is highly phosphorylated. Presumably this will decrease lipin 1 affinity for PA. However, adipocytes also increase fatty acid esterification to PA during the influx of fatty acids from lipoprotein lipase postprandially. Therefore, the concentration of PA at the ER will increase, overcoming the inhibitory effect of phosphorylation. On the other hand, stimulation of adipocytes with a catecholamine, such as epinephrine, causes a profound induction of triacylglycerol lipolysis. The high levels of fatty acids flooding the cell decrease intracellular pH<sup>69</sup>. At the same time, insulin signaling pathways

are inhibited, particularly the mTORC1 pathway<sup>70</sup>. Thus, the reduction in pH decreases lipin 1 affinity for PA, yet at the same time lipin 1 phosphorylation is inhibited thereby increasing its affinity for PA. We postulate that lipin 1 phosphorylation is a necessary counterbalance to maintain PAP activity during changes in intracellular pH, alterations in PC:PE ratios, and possibly intracellular fatty acid accumulation. Maintaining a relatively similar degree of lipin 1 affinity for PA could be important because allowing lipin 1 to have a high affinity for PA at any pH could promote lipin 1-mediated hydrolysis of PA generated via insulin stimulation of PLD at the plasma membrane or other membrane surfaces outside of the ER. In addition, lipin 1 might show increasing phosphorylation because of the importance of preventing lipin 1 from binding to the inner leaflet of the plasma membrane, an important site for the PA's role in insulin-stimulated GLUT4 vesicle fusion<sup>71</sup>. Thus, as the intracellular pH changes, increasing or decreasing lipin 1 affinity for PA, phosphorylation is reciprocally regulated to maintain a relatively constant affinity for PA. We should point out that biochemical fractionation may not be an accurate measure of lipin 1 microsomal association, as changing the intracellular pH to the pH of the buffer during homogenization may artificially change lipin 1 association with membranes.

Determining that lipin 1 prefers to associate with membranes containing di-anionic PA has important implications in the control of intracellular PAP activity. Our studies show that intracellular pH will likely significantly affect lipin 1 enzymatic activity. Thus, lipin 1 may fall into a relatively novel class of proteins that function as pH sensors<sup>72</sup>. In this case, regulation of lipin 1 by pH could affect the production of phospholipids and triacylglycerols. Furthermore, changes in intracellular pH might also affect lipin 1 localization to the nucleus and thus regulate the ability of lipin 1 to function as a transcriptional co-activator or co-repressor. In addition, the

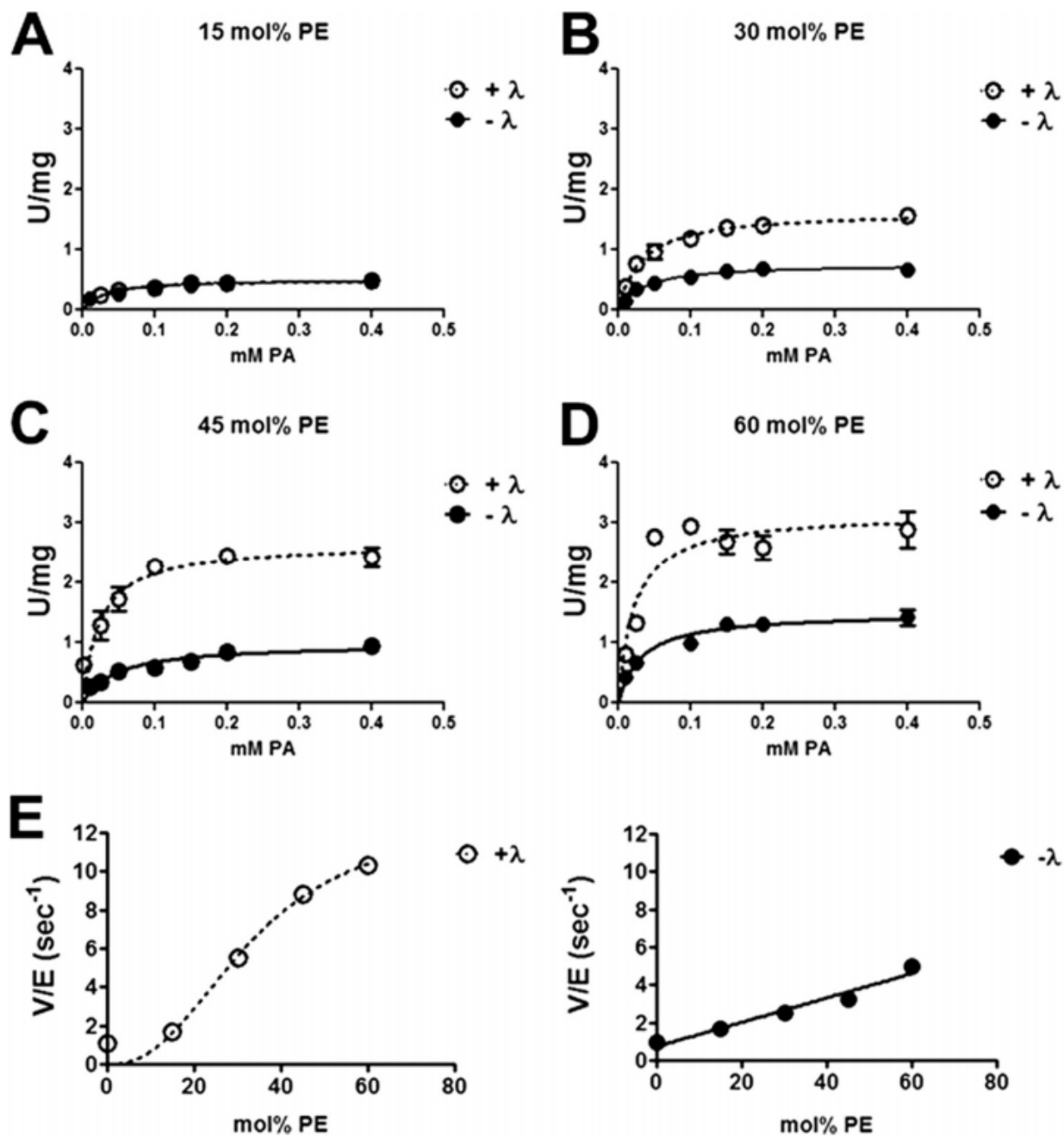
relative levels of PE to other phospholipids may be important in the control of lipin 1 localization; for example, conditions such as obesity can change the PC:PE ratio at the ER from 1.3 to 2.0<sup>73</sup>. Therefore changes in the PC:PE ratio, in conjunction with alterations in intracellular pH, could change the activity of lipin 1 at the ER or cause aberrant lipin 1 localization to other intracellular membranes. We conclude that the translocation of the cytosolic reservoir of lipin 1 to membranes enables lipin 1 to perform its various physiological functions and that this translocation is modulated by the phosphorylation of lipin 1, especially through mTOR.

Figure 3.1 Phosphorylation status of lipin 1 does not change PAP activity using the conventional Triton X-100 mixed micelle assay.



**Figure 3.1 Phosphorylation status of lipin 1 does not change PAP activity using the conventional Triton X-100 mixed micelle assay.** A, HEK293T cells were transfected with an expression vector for FLAG-tagged lipin 1b. Two days after transfection the cells were homogenized in buffer A and the lipin 1 contained in the extracts was bound to FLAG beads. After washing in buffer B, the beads were suspended in phosphatase buffer and treated with (+λ) or without (-λ) lambda phosphatase for 30 min. After further washing the lipin 1 was eluted with 0.5 mg/ml FLAG peptide and quickly dialyzed. A representative 8.75% acrylamide SDS-PAGE gel stained with Coomassie is shown. The μg of BSA are indicated. B, HEK293T cells were transfected as in A, and were radiolabeled with 0.02 μCi/ml [<sup>32</sup>P]ATP in low phosphate buffer containing 10% serum for two h before protein isolation. The radiolabeled lipin 1 contained within the protein extracts was immunoprecipitated with FLAG beads, washed, then treated or not with lambda phosphatase as in A. After phosphatase treatment lipin 1 was eluted by boiling in SDS load buffer, resolved by SDS-PAGE, and transferred to membrane. Radiolabeled lipin 1 was visualized by autoradiography and the membrane subjected to immunoblotting to detect total lipin 1. C, PAP enzymatic activity from 50 ng of phosphorylated (-λ) and dephosphorylated lipin 1 (+λ) was measured as a function of time in Tris-maleate buffer, pH 7.0, with 9.1 mol% PA in Triton X-100 micelles at a final concentration of 0.2 mM PA. D, Phosphorylated (-λ) and dephosphorylated (+λ) lipin 1 PAP activity measured as a function of PA concentration in 100 nm PC:PA liposomes at pH 7.5. The surface concentration of PA was 10 mol%.

Figure 3.2 PAP activity of phosphorylated and dephosphorylated lipin 1 in liposomes.



**Figure 3.2 PAP activity of phosphorylated and dephosphorylated lipin 1 in liposomes.** A, Phosphorylated (- $\lambda$ ) and dephosphorylated (+ $\lambda$ ) lipin 1 PAP activity measured as a function of the molar concentration of PA in 100 nm PC:PE:PA (75:15:10) mol% liposomes at pH 7.5. B, Lipin 1 PAP activity measured as in A, but with liposomes made with PC:PE:PA (60:30:10 mol%). C, Lipin 1 PAP activity measured as in A, but with liposomes made with PC:PE:PA (45:45:10 mol%). D, Lipin 1 PAP activity measured as in A, but with liposomes made with PC:PE:PA (30:60:10 mol%). E, Graph of  $k_{cat}$  values from Table 2 plotted as a function of the mol% PE for Dephosphorylated lipin 1 (left) and phosphorylated lipin 1 (right).

**Table 3.1**

Kinetic data for lipin 1b +/-  $\lambda$  phosphatase using liposomes composed of 10 mol% PA and 90 mol% (PC + PE), with PE mol% indicated.

<b><u>Lipin 1 +<math>\lambda</math></u></b>			
	<b><u><math>K_m^{\text{app}}</math> (<math>\mu\text{M}</math>)</u></b>	<b><u><math>k_{\text{cat}}</math> (<math>\text{sec}^{-1}</math>)</u></b>	<b><u><math>k_{\text{cat}}/K_m^{\text{app}}</math> (<math>\text{sec}^{-1} \mu\text{M}^{-1}</math>)</u></b>
<b>0% PE</b>	46 $\pm$ 19	1.07 $\pm$ 0.12	0.02
<b>15% PE</b>	29 $\pm$ 5	1.70 $\pm$ 0.10	0.06
<b>30% PE</b>	32 $\pm$ 3	5.50 $\pm$ 0.10	0.17
<b>45% PE</b>	23 $\pm$ 11	8.84 $\pm$ 0.90	0.38
<b>60% PE</b>	19 $\pm$ 11	10.33 $\pm$ 1.10	0.54
<b><u>Lipin 1 -<math>\lambda</math></u></b>			
	<b><u><math>K_m^{\text{app}}</math> (<math>\mu\text{M}</math>)</u></b>	<b><u><math>k_{\text{cat}}</math> (<math>\text{sec}^{-1}</math>)</u></b>	<b><u><math>k_{\text{cat}}/K_m^{\text{app}}</math> (<math>\text{sec}^{-1} \mu\text{M}^{-1}</math>)</u></b>
<b>0% PE</b>	39 $\pm$ 20	0.97 $\pm$ 0.12	0.03
<b>15% PE</b>	29 $\pm$ 11	1.68 $\pm$ 0.14	0.06
<b>30% PE</b>	33 $\pm$ 5	2.51 $\pm$ 0.10	0.08
<b>45% PE</b>	46 $\pm$ 12	3.28 $\pm$ 0.25	0.07
<b>60% PE</b>	32 $\pm$ 7	5.00 $\pm$ 0.30	0.16

Figure 3.3 Effect of PC or PE on lipin 1 physical association with liposomes.

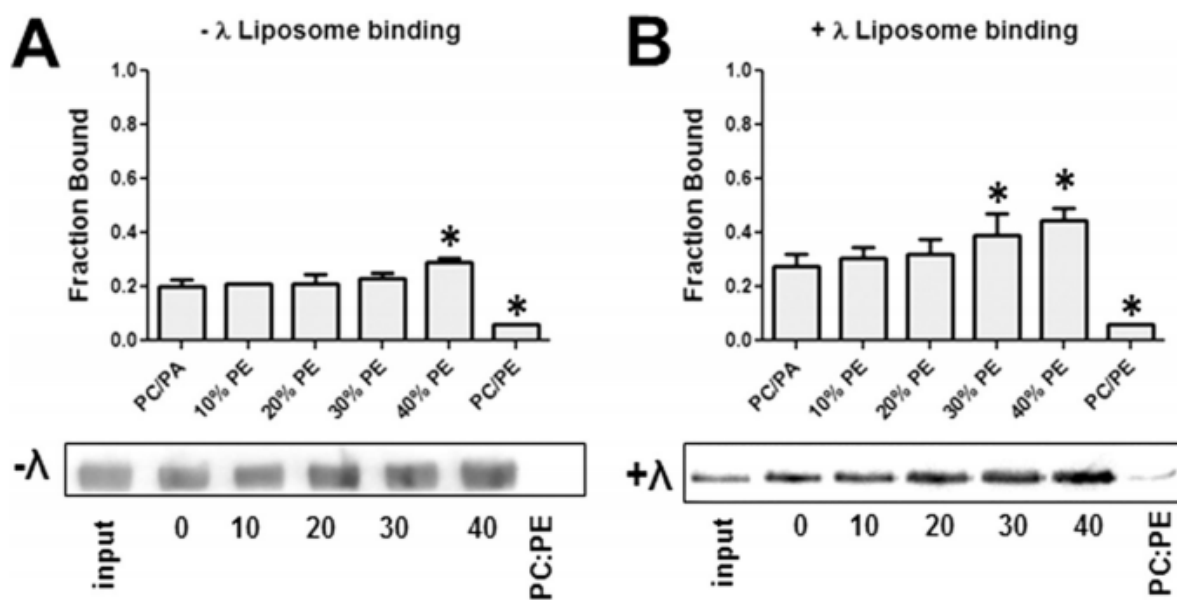


**Figure 3.3 Effect of PC or PE on lipin 1 physical association with liposomes. A,**

Phosphorylated (-λ) lipin 1 was mixed in buffer B with PC liposomes containing PA at 20 mol% and the indicated concentrations of PE replacing PC, or PE:PC liposomes without PA. After 20 min incubation the lipin 1-liposome mixture was subjected to liposome floatation and the amount of lipin 1 recovered after floatation was measured. The graph illustrates the amount of lipin 1 bound to liposomes as a percent of the total amount of lipin 1 in the binding reaction, +/- standard deviation. Each binding assay was performed at least three times and \* indicates  $p < 0.05$  when comparing PC:PA liposomes with 40% PC:PE:PA liposomes and PC:PE liposomes.

Bottom, representative immunoblot of lipin 1 (anti-FLAG) recovered after floatation. Input is 20% of the amount incubated with the liposomes. B, Dephosphorylated (+λ) lipin 1 binding to PC:PE:PA liposomes was measured as described in A. Each binding assay was performed at least three times and \* indicates  $p < 0.05$  when comparing PC:PA liposomes with 30 and 40% PC:PE:PA liposomes and PC:PE liposomes

Figure 3.4 Effect of amphiphilic amines on lipin 1 association with membranes and PAP activity.

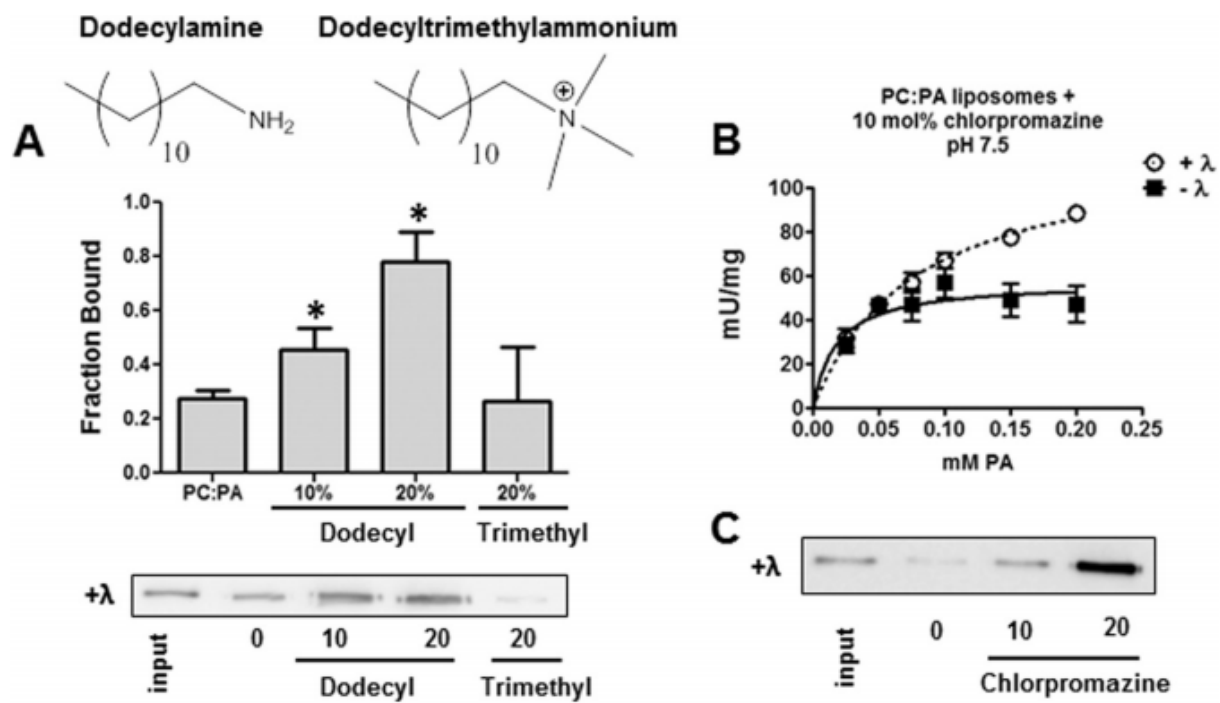


**Figure 3.4 Effect of amphiphilic amines on lipin 1 association with membranes and PAP**

**activity.** A, Dephosphorylated lipin 1 (+ $\lambda$ ) binding to liposomes containing the indicated mol% concentration of dodecylamine and dodecyltrimethylammonium. Binding assay was performed by flotation as described in Fig. 3A. Each binding assay was performed at least three times and \* indicates  $p < 0.05$  when comparing PC:PA liposomes with PC:PA liposomes containing 10 and 20 mol% dodecylamine. Bottom, representative immunoblot of lipin 1 (anti-FLAG) recovered after floatation at the indicated concentrations of chlorpromazine. B, Phosphorylated (- $\lambda$ ) and dephosphorylated (+ $\lambda$ ) lipin 1 PAP activity using 100 nm PC:PA liposomes containing PA at 10 mol% and chlorpromazine at 10 mol%. PAP assays were performed as a function of PA molar concentration at pH 7.5. C, Dephosphorylated lipin 1 (+ $\lambda$ ) binding to liposomes was performed as described in Fig 3A, but with the indicated mol% of chlorpromazine.

Figure 3.5 Effect of pH on lipin 1 PAP activity.

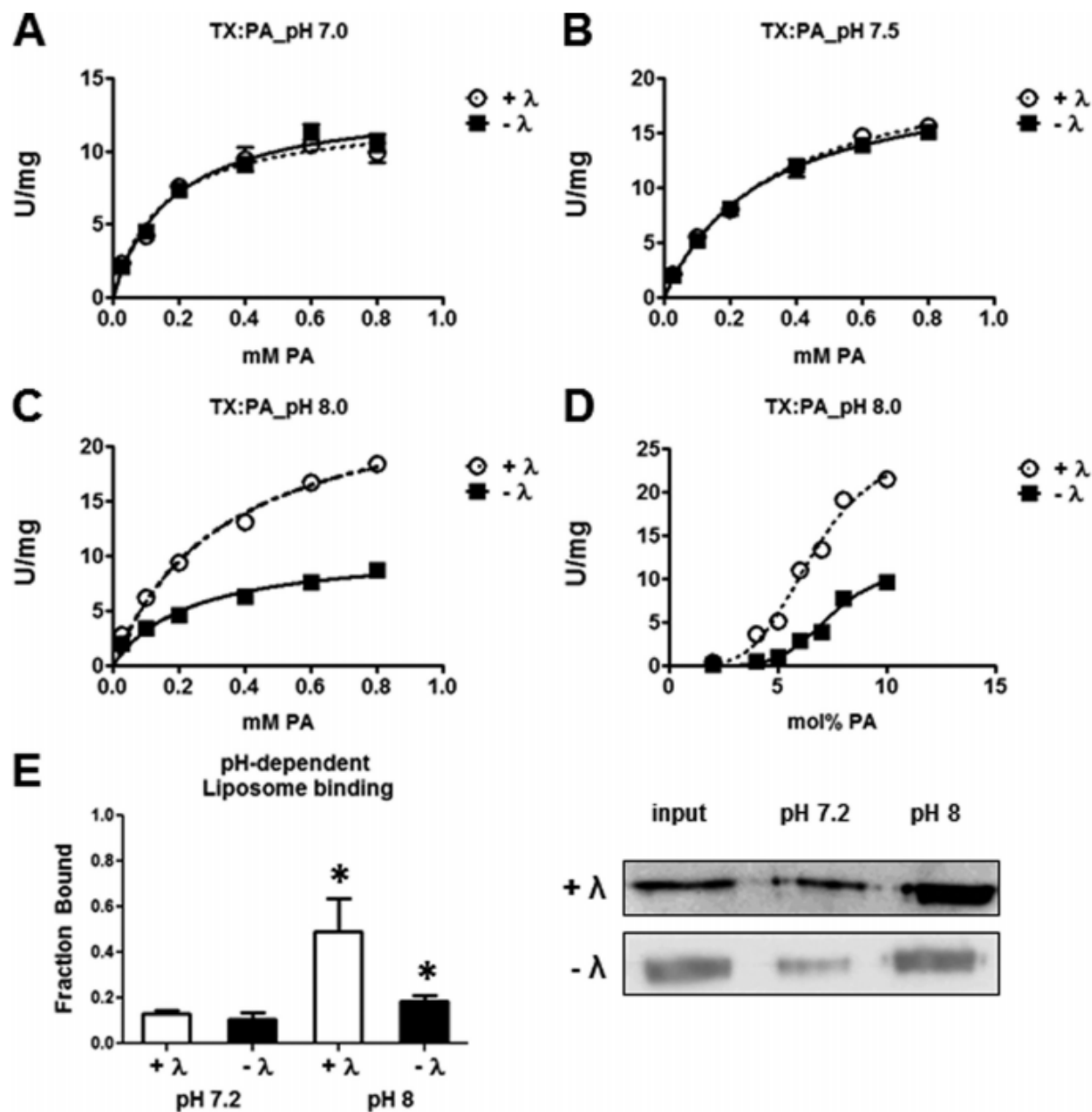


**Figure 3.5 Effect of pH on lipin 1 PAP activity.** A-C, Phosphorylated (- $\lambda$ ) and dephosphorylated (+ $\lambda$ ) lipin 1 PAP activity using Triton X-100 mixed micelles containing 9.1 mol% PA was measured as a function of the molar concentration of PA in at the indicated pH. D, Phosphorylated (- $\lambda$ ) and dephosphorylated (+ $\lambda$ ) lipin 1 PAP activity using Triton X-100 mixed micelles containing 1 mM final concentration of PA was measured as a function of the surface concentration of PA (mol%) at pH 8.0. The surface concentration of PA was 2, 4, 5, 6, 7, 8, and 10 mol%. E, Phosphorylated (- $\lambda$ ) and dephosphorylated lipin 1 (+ $\lambda$ ) binding to 100 nm PC:PA liposomes at pH 7.2 and 8.0 were performed as described in Fig 3A. Input is 20% of the amount incubated with the liposomes. Each binding assay was performed at least three times and \* indicates  $p < 0.05$  when comparing binding between pH 7.2 and pH 8.0 for both + $\lambda$  and - $\lambda$ . Bottom, representative immunoblot of lipin 1 (anti-FLAG) recovered after floatation at the indicated pH.

**Table 3.2**Kinetic data for lipin 1b +/-  $\lambda$  phosphatase using TX:PA micelles at varying pH.

Kinetic constants with respect to molar PA concentration.

		$K_m^{\text{app}}$	$k_{\text{cat}}$	$k_{\text{cat}}/K_m^{\text{app}}$
		$\mu\text{M}$	$\text{s}^{-1}$	$\text{s}^{-1}\mu\text{M}^{-1}$
pH 7	+ $\lambda$	150 $\pm$ 40	41.6 $\pm$ 6.80	0.280
	- $\lambda$	180 $\pm$ 40	45.2 $\pm$ 3.20	0.250
pH 7.5	+ $\lambda$	330 $\pm$ 50	74.9 $\pm$ 4.30	0.230
	- $\lambda$	300 $\pm$ 20	69.2 $\pm$ 2.10	0.231
pH 8	+ $\lambda$	340 $\pm$ 60	86.3 $\pm$ 6.80	0.254
	- $\lambda$	230 $\pm$ 70	35.5 $\pm$ 4.0	0.154

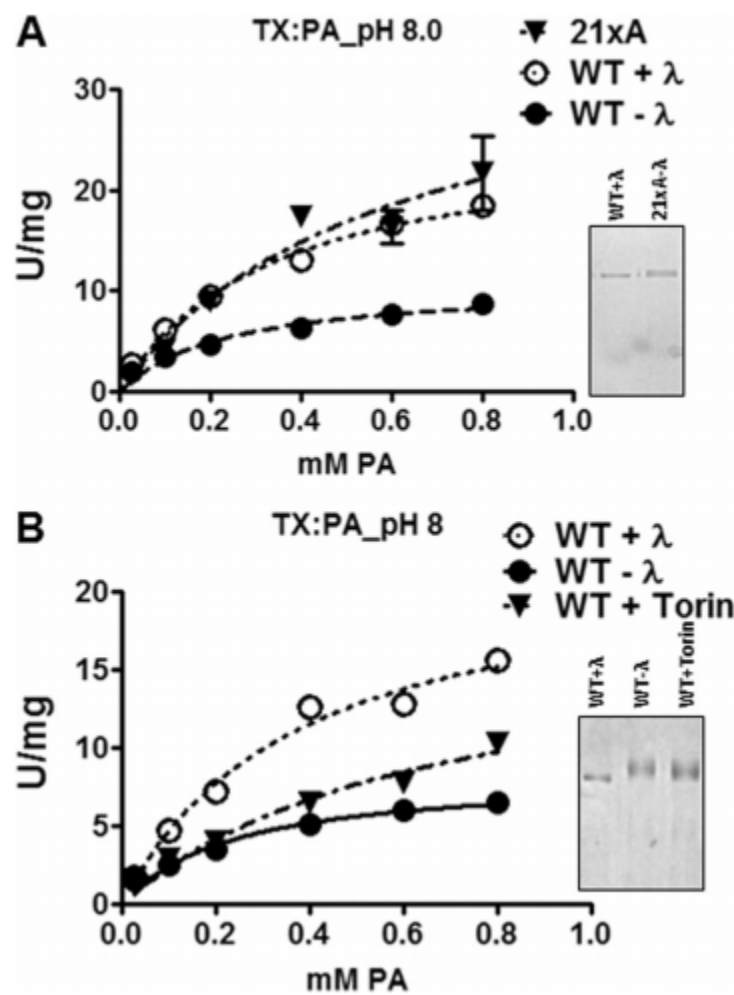
**Table 3.3**

Kinetic data for lipin 1b +/-  $\lambda$  phosphatase using TX:PA micelles at pH 8 with respect to the surface concentration of PA.

Kinetic constants with respect to surface PA concentration.

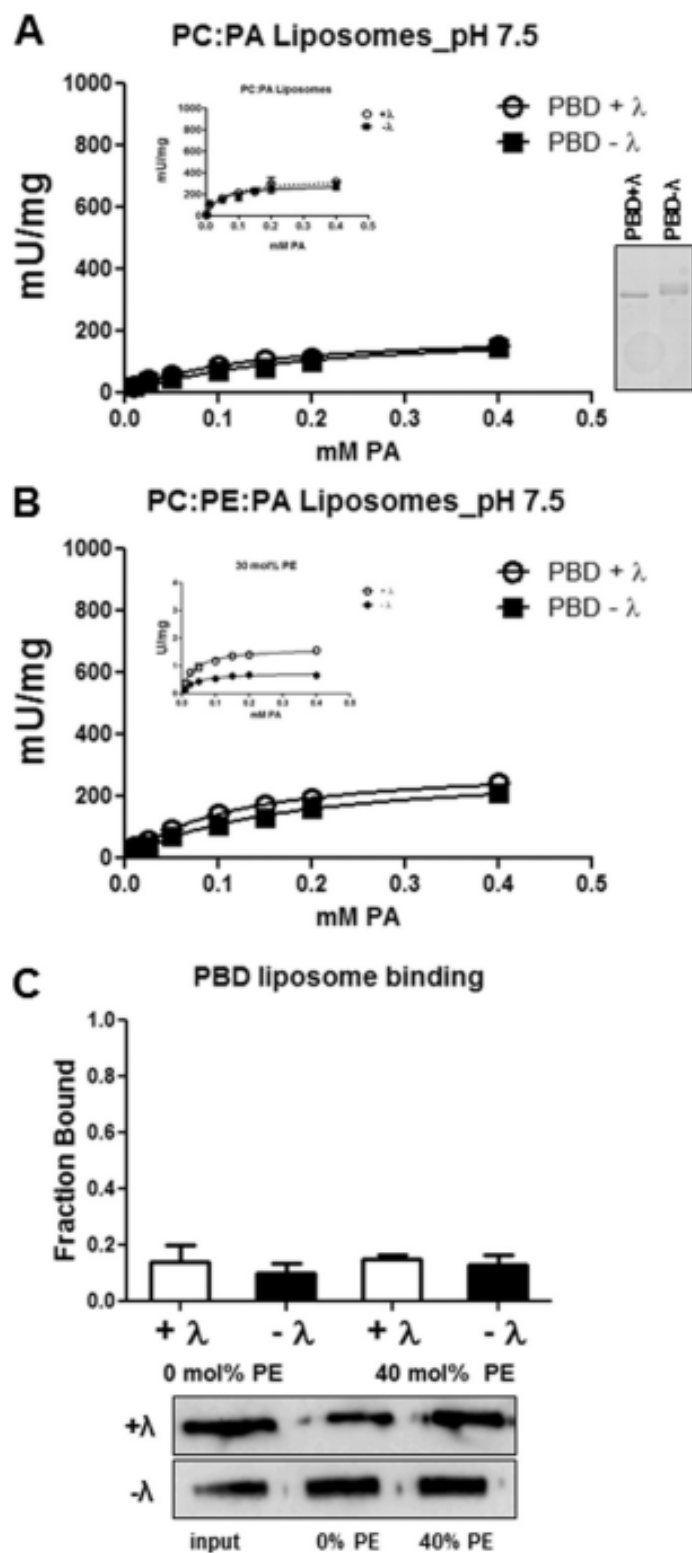
		$K_m^{\text{app}}$	$k_{\text{cat}}$	$k_{\text{cat}}/K_m^{\text{app}}$	Hill no.
		<i>mol%</i>	$s^{-1}$	$s^{-1} \text{ mol}\%^{-1}$	
pH 8	+ $\lambda$	$6.4 \pm 0.16$	$84.9 \pm 10.2$	13.3	$4.31 \pm 0.9$
	- $\lambda$	$7.4 \pm 0.11$	$37.7 \pm 5.7$	5.10	$6.10 \pm 1.5$

Figure 3.6 Effect of mTOR inhibition and S/T mutation to A on lipin 1 PAP activity.



**Figure 3.6 Effect of mTOR inhibition and S/T mutation to A on lipin 1 PAP activity.** A, HEK293T cells were transfected with FLAG-tagged wild type lipin 1 or the 21xA mutant. Two days after transfection the cells were homogenized in buffer A and lipin 1 was purified as described in Fig. 1A. While the protein was still attached to the FLAG beads, the wild type was treated with lambda phosphatase (WT+ $\lambda$ ) while the 21xA mutant was not (21xA- $\lambda$ ). PAP activity was measured in TX:PA micelles (9.1 mol% PA) as a function of PA molar concentration at pH 8.0. The inset to the right is a SDS-PAGE gel of purified lipin 1 treated with phosphatase (WT+ $\lambda$ ) and the lipin 1 21xA mutant untreated (21xA- $\lambda$ ), stained with Coomassie. B, HEK293T cells were transfected for 48 hrs with an expression vector for FLAG-tagged lipin 1b. 250 nM torin1 was added (WT+Torin) or not 16 hrs before the cells were homogenized in buffer A and the lipin 1 contained in the extracts was bound to FLAG beads, purified and treated with or without lambda phosphatase (WT+  $\lambda$ , WT-  $\lambda$ ) as described in Fig 1A. PAP activity was measured in TX:PA micelles (9.1 mol% PA) as a function of PA molar concentration at pH 8.0. The inset to the right is a SDS-PAGE gel of purified lipin 1 +/-  $\lambda$  phosphatase, and lipin 1 treated with torin1, stained with Coomassie.

Figure 3.7 Role of the polybasic domain (PBD) in lipin 1 PAP activity.



**Figure 3.7 Role of the polybasic domain (PBD) in lipin 1 PAP activity.** A, HEK293T cells were transfected with FLAG-tagged PBD mutant of lipin 1. Two days after transfection the cells were homogenized in buffer A and the PBD mutant of lipin 1 (PBD) was purified and treated with lambda phosphatase or not as described in Fig. 1A. PAP activity for dephosphorylated (PBD+  $\lambda$ ) or phosphorylated (PBD-  $\lambda$ ) PBD mutant was measured in PC:PA liposomes (90:10) mol% as a function of PA molar concentration at pH 7.5, as described in Fig. 1D. The inset within the graph is the data from wild type lipin 1 taken from Fig. 1D and shown for convenience. The inset to the right is a SDS-PAGE gel of purified lipin 1-PBD, +/-  $\lambda$  phosphatase, stained with Coomassie. B, The PAP activity for dephosphorylated (PBD+  $\lambda$ ) or phosphorylated (PBD-  $\lambda$ ) PBD mutant was measured in PC:PE:PA liposomes (60:30:10) mol% as a function of PA molar concentration at pH 7.5, as described in Fig 2B. The inset within the graph is the data from WT lipin 1 taken from Fig. 2B and shown for convenience. C, Phosphorylated (- $\lambda$ ) and dephosphorylated (+ $\lambda$ ) PBD mutant binding to 100 nm PC:PE:PA liposomes (40:40:20 mol%) at pH 7.2 was performed as described in Fig 3A. Input is 20% of the amount incubated with the liposomes. Each binding assay was performed at least three times. Bottom, representative immunoblot of the PBD mutant (anti-FLAG) recovered after floatation.

**Table 3.4**

Kinetic data for the PBD mutant of lipin 1b +/-  $\lambda$  phosphatase using liposomes composed of 10 mol% PA and 90 mol% (PC + PE) with PE mol% indicated.

	$K_m^{\text{app}}$	$k_{\text{cat}}$	$k_{\text{cat}}/K_m^{\text{app}}$
	$\mu\text{M}$	$\text{s}^{-1}$	$\text{s}^{-1}\mu\text{M}^{-1}$
<b>PBD + <math>\lambda</math></b>			
0% PE	$120 \pm 20$	$0.64 \pm 0.04$	0.005
30% PE	$110 \pm 10$	$1.00 \pm 0.05$	0.009
<b>PBD - <math>\lambda</math></b>			
0% PE	$190 \pm 50$	$0.69 \pm 0.09$	0.004
30% PE	$170 \pm 30$	$0.98 \pm 0.09$	0.006

Figure 3.8 Model representation of lipin 1 binding to PA.

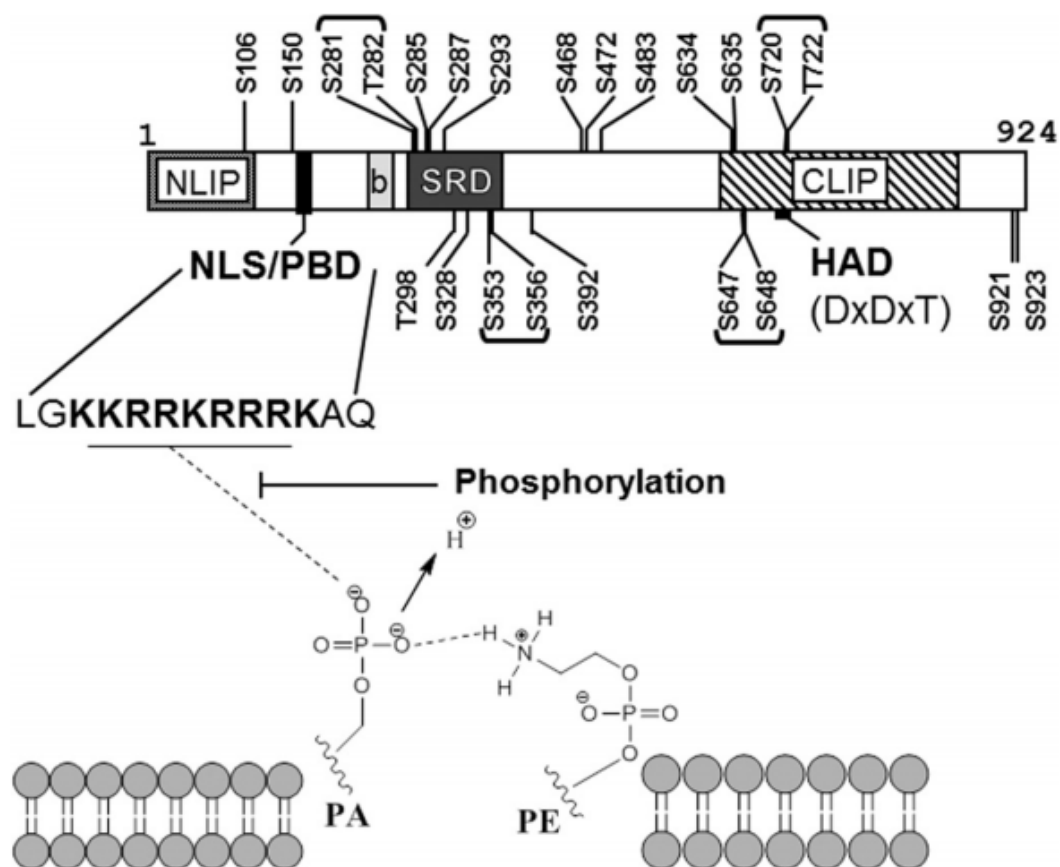


**Figure 3.8 Model representation of lipin 1 binding to PA.** Phosphorylated Ser/Thr residues identified by number where brackets indicate either or both residues may be phosphorylated, NLIP and CLIP are conserved NH<sub>2</sub>- and COOH-LIPin homology domains, HAD is Haloacid Dehalogenase - like domain identified by DxDxT, NLS/PBD is the Nuclear Localization Sequence/polybasic domain with the sequence shown below, SRD is the serine rich domain previously identified to bind to 14-3-3, b is the 33 amino acid alternatively spliced exon.

## CHAPTER 4

### LIPIN 2 BINDS PHOSPHATIDIC ACID BY THE ELECTROSTATIC-HYDROGEN BOND SWITCH MECHANISM INDEPENDENT OF PHOSPHORYLATION

#### ABSTRACT

Lipin 2 is a phosphatidic acid phosphatase (PAP) responsible for the penultimate step of triglyceride synthesis, dephosphorylation of PA to generate DAG. The lipin family of PA phosphatases is composed of lipin 1-3 which are members of the conserved Haloacid Dehalogenase superfamily. Although genetic alteration of LPIN2 in humans is known to cause Majeed's Syndrome, little is known about the biochemical regulation of its PAP activity. Here, in an attempt to gain a better general understanding of the biochemical nature of lipin 2, we have performed kinetic and phosphorylation analyses. We provide evidence that lipin 2, like lipin 1, binds PA via the electrostatic-hydrogen bond switch mechanism but has a lower rate of catalysis. Like lipin 1, lipin 2 is highly phosphorylated and we identify 15 phosphosites. However, unlike lipin 1, the phosphorylation of lipin 2 is not induced by insulin signaling nor is it sensitive to inhibition of mTOR. Importantly, phosphorylation of lipin 2 does not negatively regulate either membrane binding or PAP activity. This suggests that lipin 2 functions as a constitutively active PA phosphatase in stark contrast to the high degree of phosphorylation-mediated regulation of lipin 1. This knowledge of lipin 2 regulation is important for a deeper understanding of how the lipin family functions with respect to lipid synthesis, and more generally, as an example of how the membrane environment around PA can influence its effector proteins.

## INTRODUCTION

Lipin 2 is a  $Mg^{2+}$  dependent phosphatidic acid phosphatase and a member of the lipin family consisting of lipin 1-3 which are members of the Haloacid Dehalogenase (HAD) superfamily (<sup>8</sup>, reviewed in <sup>1</sup>). The lipins translocate between the cytosol and the ER membrane where they bind PA in response to multiple regulatory inputs to form DAG. Being soluble proteins, the lipins reside at a unique regulatory node in TAG synthesis as the other TAG biosynthetic enzymes are integral membrane proteins <sup>74</sup>. Additionally, cellular PAP activity influences production of specific phospholipids. Phosphatidylglycerol, phosphatidylinositol and cardiolipin are formed from PA by the CDP DAG pathway whereas phosphatidylcholine (PC), phosphatidylethanolamine (PE) and phosphatidylserine (PS) are formed from DAG via the Kennedy pathway <sup>75</sup>.

The best studied lipin family member, lipin 1, is highly phosphorylated in response to insulin/PI3K/mTOR signaling with several validated rapamycin and Torin1 sensitive phosphosites <sup>7,9,35</sup>. This signaling is known to control lipin 1 cellular localization. mTOR dependent phosphorylation sequesters lipin 1 to the cytoplasm while inhibition of mTORC1 and 2 with Torin1, an ATP competitive inhibitor, results in lipin 1 translocation to the ER membrane and nucleus. While lipin 1 phosphorylation has been correlated with its cytosolic localization, a mechanistic basis for phosphorylation controlling lipin 1 membrane binding has only recently been elucidated. PA, the lipin family's substrate, is a phosphomonoester. This unique lipid head group yields two dissociable protons, with approximate pKa's of 3 and 7.9 <sup>42</sup>. Considering that pKa<sub>2</sub> falls within the physiological pH range, PA can be either mono or di-anionic. Deprotonation of PA is enhanced in the presence of primary amines, such as the head group of PE, through the formation of a hydrogen bond with the PA phosphate group thereby lowering

pKa<sub>2</sub> to ~6.9<sup>42</sup>. In an *in vitro* phosphatase and membrane binding liposome assay, lipin 1 activity increased correspondingly with increases in the mol% of PE, which increase the ratio di-anionic to mono-anionic PA<sup>29</sup>. This is consistent with the electrostatic-hydrogen bond switch mechanism elegantly demonstrated by Kooijman et al.<sup>46</sup>. This response is mediated through the lipin 1 PA binding domain, known as the polybasic domain, PBD, which consists of a nine amino acid stretch of lysines and arginines. The PBD is conserved within the lipin family and the specific sequence of lysines and arginines is unique to each lipin family member and highly conserved between species. Phosphorylation of lipin 1 has been shown to exert a negative regulation on lipin 1 PA binding, suggestive of an interaction or competition between phospho-S/T within lipin 1 and the phosphomonoester head group of PA competing for PBD binding within lipin 1<sup>29</sup>. This evidence suggests that lipin 1 binds PA by the electrostatic-hydrogen bond switch mechanism and this is negatively regulated by phosphorylation.

The relative PAP activity of human lipin 2 has been previously determined in cell lysates<sup>41, 76</sup>. In this study we examine lipin 2 kinetics, first as a general characterization and then with respect to PA charge and phosphorylation. Our data suggest that lipin 2 preferentially binds di-anionic PA, similar to lipin 1, and is a constitutively active PAP enzyme with respect to phosphorylation. In addition, we have identified novel phosphorylation sites within lipin 2 and have examined the cellular localization in 3T3-L1 adipocytes in response to inhibition of mTOR signaling.

## RESULTS

*Purification and enzymatic characterization of lipin 2* – To obtain purified lipin 2 for detailed kinetic analyses, HeLa cells were infected with adenovirus expressing FLAG-tagged lipin 2. The recombinant protein was purified from cell lysates using anti-FLAG agarose beads, followed by extensive washes, elution by FLAG peptide and dialysis, which yielded a highly purified enzyme preparation (**Figure 4.1A**).

Because lipin 2 is relatively uncharacterized and no studies have been performed with purified lipin 2 we first performed a series of basic biochemical characterizations. The subsequent experimental parameters were measured against 0.5 mM PA solubilized at the indicated amount of Triton-X100. The linear range of phosphatase activity with respect to time was determined (**Figure 4.1B**) under these conditions the specific activity of lipin 2 was 0.14  $\mu\text{mol}/\text{min}/\text{mg}$ . The optimal pH for lipin 2 PAP activity was determined (**Figure 4.1C**) and found to peak at pH 7.2. Lipin 2 PAP activity declined with increasing molar concentrations of Triton X-100, a characteristic of surface dilution kinetics also exhibited by lipin 1 (**Figure 4.1D**)<sup>48</sup>.

Like lipin 1, lipin 2 PAP activity required a divalent cation. Optimal PAP activity for lipin 2 was achieved with 0.5 mM  $\text{Mg}^{2+}$  (**Figure 4.1E**) and approximately half of this maximal activity was achieved with a 50-fold lower concentration of  $\text{Mn}^{2+}$  (**Figure 4.1F**). Alkylating agents such as N-ethylmaleimide are known to inhibit lipin 1 PAP activity and similar effects are observed with lipin 2 (**Figure 4.1G**,  $\text{IC}_{50} = 0.1 \text{ mM}$ ). Maximal PAP activity is achieved with the addition of 10 mM  $\beta$ -mercaptoethanol (**Figure 4.1H**), similar to lipin 1. The results from **Figure 4.1D-H** are quite similar to those reported for human lipin 1, with the primary difference being the magnitude of the optimum activity<sup>37</sup>.

*Lipin 2 membrane binding and PAP activity are stimulated by di-anionic PA, characteristic of the electrostatic-hydrogen bond switch mechanism* – To determine what effect the charge on the PA head group has on lipin 2 PAP activity and membrane binding, Lipin 2 substrate, PA, was presented in a lipid bilayer with and without primary amines to modulate PA charge. Liposomes containing [<sup>32</sup>P]-PA and unlabeled PA and PC (10:90 mol%) and PA, PE, and PC (10:30:60 mol%) were used to measure the rate of phosphate hydrolysis where the majority of PA is mono (**Figure 4.2A**) and di-anionic (**Figure 4.2B**). The mol% composition was held constant while the molar concentration of PA was increased. Analysis of the data according to the Michaelis-Menten equation showed no significant effect on the measured  $K_m^{app}$  for 0 and 30 mol% PE which were  $3.3 \pm 0.4 \times 10^{-5}$  and  $3.6 \pm 0.6 \times 10^{-5}$  (M) respectively. However, both the turnover number and catalytic efficiency increased approximately 4 fold in the presence of PE (**Table 4.1**), indicating that PA charge does indeed influence lipin 2 PAP activity.

To determine if the observed increase in lipin 2 phosphatase activity is a result of increased membrane association or active site efficiency, or both, lipin 2 binding to similarly constructed liposomes was measured (**Figure 4.3A**). FLAG-tagged Venus-lipin 2 was purified and subjected to liposome assays. Total binding increases approximately 0.5-fold with 30 mol% PE. To demonstrate that the modulation of PA charge is responsible for increasing lipin 2 membrane binding, increasing mol% of PE was titrated into the liposomes while holding the molar concentration of PA at saturation. As seen in **Figure 4.3B**, at constant PA levels the increase in PE corresponds with an increase in total lipin 2 binding to membranes. A similar experiment was performed with a Venus-tagged lipin 1 to directly compare the binding affinity of lipin 2 with lipin 1 (**Figure 4.3C**). Under these conditions the dissociation constant ( $K_d$ ) of lipin 1 ( $0.066 \pm 0.003 \times 10^{-5}$  (M)) to PC/PA/PE liposomes is substantially higher than lipin 2 ( $1.5 \pm$

$0.3 \times 10^{-5}$  (M)). The results from **Figure 4.2** and **4.3** clearly demonstrate that, similar to lipin 1, lipin 2 PAP activity and binding to liposomes are both increased with conversion of the charge of PA from mono-anionic to di-anionic.

*Characterization of lipin 2 phosphorylation* – Because of the importance of phosphorylation in negatively regulating lipin 1 we utilized mass spectrometry to identify the phosphorylated residues within lipin 2. Affinity-purified lipin 2 was trypsin digested and subjected to LC-MS/MS. Sequence coverage of lipin 2 was 91%, missing the region between amino acids 428 and 482. The MS/MS spectrum derived from a representative phosphopeptide is shown (**Figure 4.4A**). In this case, fragments of the peptide that contained phosphoserine 106 had the mass predicted from the amino acid composition (LPAYLATS(ph)PIPTEDQFFK) plus 80 atomic mass units. Including S106, 15 phosphorylation sites were identified on lipin 2 (**Figure 4.4B**). The location of the sites with respect to other features of lipin 2 is shown (**Figure 4.4C**). The majority (12/15) of the phosphorylated residues were found in the low homology region (LHR) between the CLIP and NLIP domains (**Figure 4.4C**). Interestingly, S106 and S150, residing at the end of the NLIP domain and immediately before the polybasic domain respectively, are phosphorylated in both lipin 1 and lipin 2. In addition, S243 in lipin 2 is homologous to S285 in lipin 1. Most of the sites identified were phosphorylated at high stoichiometry, as estimated by comparison with lambda-phosphatase treated lipin 2 (**Figure 4.4B**). Due to the complexity of the MS/MS spectra for the peptide from Q335-K379, we were unable to unambiguously assign exact position of two phosphorylated residues. To indicate this ambiguity, the two sites, one at S337/S341/T342 and the other at S365/S367, are reported within brackets. Thus, we demonstrate that lipin 2 contains numerous phosphorylated Ser and Thr residues, with only a few of these in common with lipin 1.

Having both confirmed that lipin 2 is phosphorylated and identified the phosphorylated residues, we next determined if phosphorylation has an intrinsic effect on lipin 2 phosphatase activity. To do so, lipin 2 was purified and treated with lambda phosphatase to remove phosphates to generate a non-phosphorylated lipin 2. As reported for lipin 1, a decrease in mobility on SDS-PAGE is observed for phosphorylated (-λ) compared to phosphatase-treated (+λ) lipin 2 (**Figure 4.5A**). However, even more so than in the case of lipin 1, dephosphorylated lipin 2 still displays an aberrant mobility by SDS-PAGE migrating at 145-150 kDa instead of a predicted 95 kDa. To determine the efficiency of phosphatase treatment, HeLa cells were incubated with 0.02 mCi [<sup>32</sup>P]ATP for two h and lipin 2 was immunoprecipitated and subjected to dephosphorylation by Lambda phosphatase for the indicated amount of time (**Figure 4.5B**). A 30 minute phosphatase treatment removed >90% of the radiolabel.

We next performed a series of kinetic analyses to determine the effect of phosphorylation on lipin 2 PAP activity. For enzymes that follow surface dilution kinetics such as lipin 2, as determined by the results from **Figure 4.1D**, the bulk and surface concentration of the substrate need to be considered. Phosphorylated and non-phosphorylated lipin 2 showed no significant difference in kinetic constants when measured against the bulk concentration of PA (**Figure 4.6A and B**) or the surface concentration of PA (**Figure 4.6C and D**) using PA/Triton X-100 mixed micelles. For phosphorylated and dephosphorylated lipin 2 the apparent  $K_m$  and  $V_{max}$  for PA against the bulk concentration is  $6.5 \pm 0.5 \times 10^{-5}$  and  $8.3 \pm 1.2 \times 10^{-5}$  M, and  $136.9 \pm 3.0$  and  $132.3 \pm 5.3$  nmol/min/mg, respectively. When measured against the surface concentration of PA the  $V_{max}$  and  $h$  values were  $251 \pm 93$  and  $213 \pm 120$  nmol/min/mg and  $1.3 \pm 0.7$  and  $1.4 \pm 0.5$  respectively. These apparent  $h$  values suggest lipin 2 is not cooperative with respect to the

surface concentration of PA, unlike what has been found for lipin 1<sup>29</sup>. Therefore at neutral pH, where the majority of PA is mono-anionic, lipin 2 shows no effect of phosphorylation.

Because lipin 1 PAP activity is influenced by both phosphorylation and PA charge, we determined whether lipin 2 PAP activity is similarly influenced. Liposomes containing PA:PC (10:90 mol%) and PA:PE:PC (10:30:60 mol%) were used to determine if substrate charge altered phosphatase activity in the context of phosphorylation. PAP activity for phosphorylated ( $-\lambda$ ) lipin 2 was performed in **Figure 4.2A** and **B**. Dephosphorylated ( $+\lambda$ ) lipin 2 PAP activity towards liposomes without PE (mono-anionic PA) and with PE (di-anionic PA) is shown in **Figure 4.6E** and **F**. These kinetic constants are summarized in **Table 4.1**. Surprisingly, dephosphorylated lipin 2 displayed similar kinetic parameters as phosphorylated lipin 2 against both PE and non PE containing liposomes. Thus, while the electrostatic charge of PA plays a crucial role in the regulation of both phosphorylated and dephosphorylated lipin 2, lipin 2 PAP activity is independent of phosphorylation, at least as measured under these conditions. These results demonstrate that in contrast to lipin 1, the PAP activity of lipin 2 is not negatively regulated by phosphorylation.

*Phosphorylation and localization of lipin 2 in 3T3-L1 adipocytes* – It has been previously reported that lipin 2 is phosphorylated in 3T3-L1 adipocytes<sup>23b</sup>. Because lipin 1 phosphorylation is highly induced in response to insulin stimulation, we sought to determine if the phosphorylation of lipin 2 is similarly induced. Due to low expression levels of lipin 2 in differentiated adipocytes<sup>23a</sup>, FLAG-tagged lipin 2 was overexpressed in 3T3-L1 adipocytes using adenovirus and after 72 h the cells were radiolabeled with [<sup>32</sup>P] orthophosphate for 120 min under serum free conditions. The labeled adipocytes were then incubated with or without 250 nM Torin1 for 30 min and then with or without 10 mU/ml insulin for 15 min. Radiolabeled

FLAG-tagged lipin 2 and endogenous lipin 1 were then isolated by immunoprecipitation, electrophoresed by SDS-PAGE and transferred to membranes. After phosphoimaging the membranes, the levels of lipin 1 and 2 were determined by immunoblotting and used to normalize the amount of  $^{32}\text{P}$  incorporated. Insulin induces a significant degree of  $^{32}\text{P}$  incorporation into lipin 1 as previously reported, however, despite a high degree of basal phosphorylation insulin, did not increase the amount of radiolabel in lipin 2 (**Figure 4.7A**)<sup>9</sup>. In addition, while numerous publications have described lipin 1 phosphorylation as dependent on the activity of mTOR (<sup>7,9,35</sup> and **Figure 4.7**), complete inhibition of mTORC1 and 2 activities by the dual mTOR inhibitor Torin1 did not affect the phosphorylation of lipin 2. These experiments demonstrate that in 3T3-L1 adipocytes phosphorylation of lipin 2 is neither stimulated by insulin nor sensitive to mTOR inhibition. Finally, S106 in lipin 1 is specifically phosphorylated in response to insulin in an mTOR-dependent manner<sup>77</sup>. While this phosphosite is conserved in lipin 2, and the phosphospecific antibody previously described does recognize this phosphorylation, no change in immunoreactivity for lipin 2 was seen with either insulin or Torin1 (**Figure 4.7A and B**).

Phosphorylation of lipin 1 via the mTOR signaling pathway regulates its intracellular localization<sup>35</sup>. Although we saw no reduction in lipin 2 phosphorylation upon mTOR inhibition, we wanted to determine whether lipin 2 intracellular localization was changed under the same conditions. 3T3-L1 adipocytes were treated with or without the mTORC1 and 2 dual inhibitor, Torin1, and insulin and then subjected to biochemical fractionation (**Figure 4.7C**). As previously reported there is a translocation of lipin 1 from the microsomal fraction to the soluble fraction upon insulin stimulation and 30 min Torin1 pre-treatment completely blocks this translocation, unlike what was reported for rapamycin<sup>9</sup>. While only a small fraction of either

lipin associates with membranes, there was no change in lipin 2 localization with either insulin or Torin1 treatment.

As an additional confirmation for these observations, we fixed differentiated 3T3-L1 adipocytes and visualized endogenous lipin 2 expression by immunofluorescence staining (**Figure 4.8**). As a control we simultaneously visualized lipin 1 under these conditions. Either lipid droplets (BODIPY, **Figure 4.8A** and **B**) or the ER (PDI, **Figure 4.8C** and **D**) were also visualized. As expected lipin 1 showed a cytosolic localization that was altered to ER membrane/nuclear location after overnight Torin1 treatment. It was very clear that lipin 2 showed no such change in location with Torin1 treatment. Punctate staining of lipin 2 was observed throughout the cell and localization was not altered with inhibition of mTOR signaling. Therefore, lipin 2 phosphorylation and localization appears to be insensitive to insulin stimulation or mTOR inhibition.

## DISCUSSION

These studies establish that lipin 2 is a constitutively active PAP enzyme with respect to phosphorylation. Using a combination of enzyme kinetics, mass spectrometry and immunofluorescence we have provided strong convergent evidence. These findings indicate that biochemical regulation of lipin 2 PAP activity is quite different from lipin 1. The implications are important for a better understanding of the distinct and overlapping tissue specific expression of lipin 1 and 2, as well as the resulting phenotype in mice and humans when expression is lost.

The finding that lipin 2 membrane binding and PAP activity are stimulated by di-anionic PA suggests that lipin 2 binds PA by the electrostatic-hydrogen bond switch mechanism. This is similar to previous studies demonstrating that lipin 1 binds PA in a similar way. This suggests that perhaps the charge sensing ability of lipin 1 and 2 is a defining characteristic of the lipin family and possibly other PA binding proteins in general<sup>72, 78</sup>. Therefore, previously unappreciated aspects of cellular physiology might be central to lipin family regulation. Considering that the second pKa for the PA phosphate group falls within the physiological pH range, fluctuations in intracellular pH and changes in the ratios of di-anionic to mono-anionic PA at the ER membrane could potentially influence both lipin 1 and 2 cellular PAP activity. Furthermore, alterations in the relative abundance of PE in the endoplasmic reticular membrane are potential means of accomplishing such changes in this ratio. It is interesting to consider that the lipin family substrate can exert a form of regulation on its catalytic effector simply by the composition the surrounding membrane. Perhaps the differential tissue expression of the lipins has evolved to take advantage of unique cellular membrane environments and thus different biochemical presentations of PA allow for more efficient lipid processing. The kinetic studies performed herein suggest that this may be the case for both lipin 1 and 2.

In stark contrast to lipin 1, phosphorylation of lipin 2 has no effect on PAP activity. This suggests that there is more post-translational control of lipin 1 PAP activity, while lipin 2 might be considered a constitutively active PAP enzyme. This is best illustrated by the differences in the catalytic efficiencies of lipin 1 and 2 with respect to phosphorylation (**Table 4.1**). At 30 mol% PE dephosphorylation of lipin 2 has no effect on catalytic efficiency whereas for lipin 1 dephosphorylation greatly increases catalytic efficiency (100% increase, **Figure 4.9** and <sup>29</sup>). While this study has examined how phosphorylation affects the PAP activity of lipin 2 in an isolated system, if such an effect exists within cells it is likely to be exerted through interactions with other regulatory proteins, such as the 14-3-3s <sup>30</sup>. However, the lack of stimulation of lipin 2 phosphorylation by insulin and in the absence of alterations in lipin 2 localization during stimulation suggests that lipin 2 PAP activity is not acutely regulated. Interestingly, while the PAP activity of lipin 2 was roughly a third of that of lipin 1 using PA/PC liposomes, the PAP activity of lipin 2 against Triton X-100/PA micelles was substantially lower than lipin 1 (~1%). Whether this represents a detergent sensitivity or is simply reflects the ability of the two enzymes to access substrate under differing modes of presentation is unknown.

It is also unclear mechanistically how lipin 1 PAP activity is negatively regulated by phosphorylation and lipin 2 activity is not. Differential phosphorylation between the two isoforms may provide an explanation. Two phosphorylated residues identified in lipin 2 are of significant interest. S106 of lipin 1 has been unambiguously demonstrated to be downstream of mTOR as demonstrated by its sensitivity to rapamycin and Torin1 <sup>9,35</sup>. S106 is found at the very end of the NLIP domain <sup>6</sup>, a region of the lipin family predicted to fold as an immunoglobulin-like beta sandwich <sup>79</sup>. Preventing S106 phosphorylation by mutation to Ala does not affect lipin 1 localization or PAP activity <sup>35</sup>. Despite a high degree of similarity in the surrounding

sequence, S106 of lipin 2, while phosphorylated, shows no sensitivity to mTOR inhibition. Lipin 1 contains a serine-rich domain with up to six phosphorylated Ser and Thr residues from amino acids 291 to 298 (numbering for lipin 1b) that has been implicated in binding to 14-3-3 to regulate nuclear localization and has been termed the serine-rich domain (SRD)<sup>30, 35</sup>. Within lipin 2, only residue S243 was found to be phosphorylated. Interestingly, this residue is found in a conserved micro-homology domain PKSDSEL, one of the few regions of homology within the LHR in all three lipin family proteins. However, outside of this very short domain there is little similarity between the lipin family members in the LHR and this falls within a region of no obvious predicted secondary structure. A more detailed understanding of the higher order structure within the lipin family will be necessary to understand precisely how phosphorylation affects PAP activity.

Studies in cell culture as well as lipin 2 knockout mice show that the expression of lipin 1 and 2 are inversely correlated, most likely via a post-transcriptional mechanism<sup>22a, 23b, 24</sup>. Cells appear to adapt to the loss of lipin 1 PAP activity by increasing PAP activity through the induction of lipin 2. However, our studies have demonstrated that lipin 2 cannot be negatively regulated via acute hormonal stimulation. Thus, in instances where the loss of lipin 1 leads to increased expression of the non-regulatable PAP activity of lipin 2 it should be considered that the phenotypic consequences may be ascribed not to loss of PAP activity but rather to the occurrence of a compensatory but non-regulatable PAP activity. For example, in the fatty liver dystrophy (*fld*) mice the loss of lipin 1 causes only a modest decline in the overall levels of PAP activity in the liver due primarily to the induction of lipin 2<sup>22a, 77</sup>. However, as the name of these animals implies, there is ectopic accumulation of triglycerides found in the liver, rather than a defect as might be supposed from decreased PAP activity. It may be that the dysregulation of the

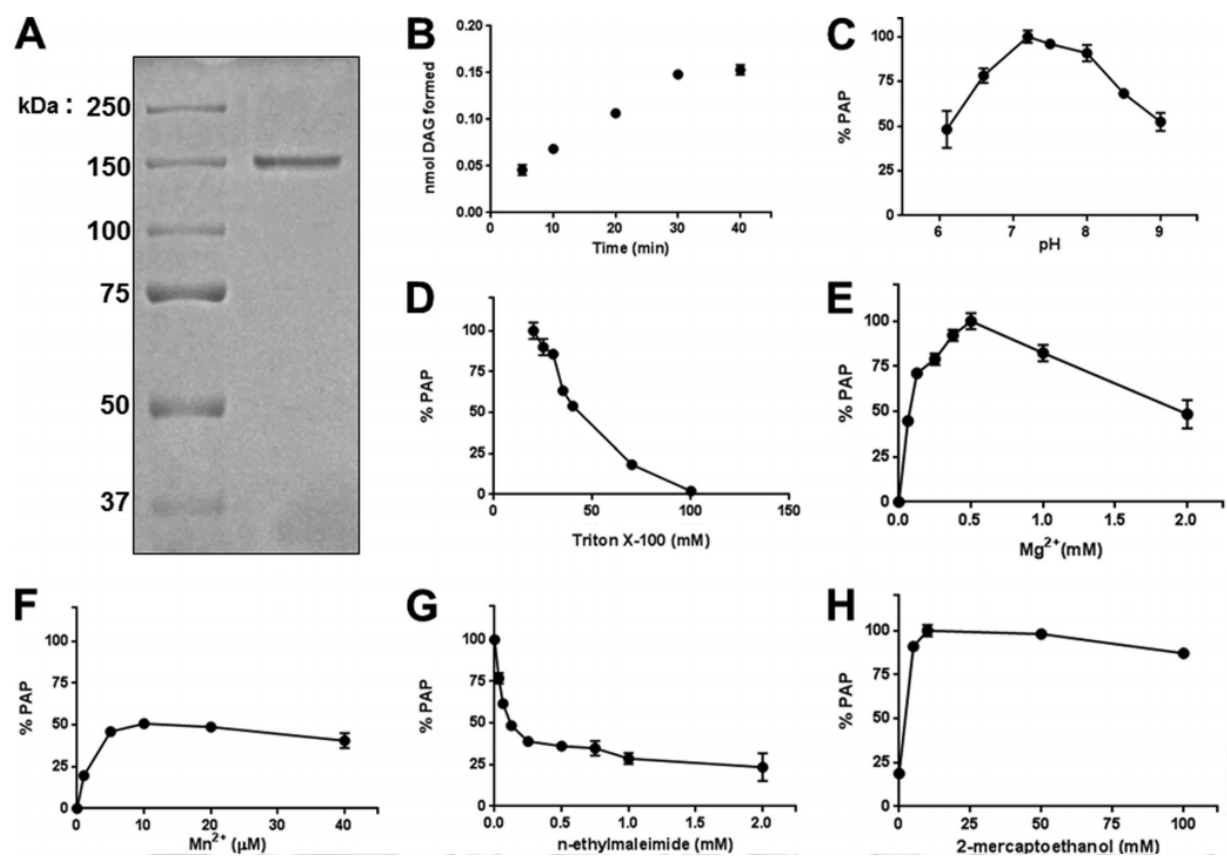
PAP activity in the liver in the form of lipin 2 accounts for the pathological accumulation of lipid. Future work investigating the physiological roles of these paralogs should consider their functional differences, particularly in light of the observed developmental compensation.

It has been demonstrated that a portion of lipin 2 is associated with a detergent-insoluble fraction in HeLa cells that is only completely extractable by the inclusion of high salt concentrations<sup>23b</sup>. We also observed that more rigorous conditions were required for complete isolation of lipin 2 (see methods). However, by directly measuring lipin 2 affinity for membranes containing PA we found that isolated lipin 2 has a far lower affinity than lipin 1, while the latter is easily solubilized by detergent. Because lipin 2 is a peripheral membrane protein it is curious that mild lysis conditions are insufficient for complete solubility. Future directions will need to investigate whether lipin 2 associates with detergent-insoluble lipid domains or with an insoluble integral membrane protein or components of the cytoskeleton.

Cellular fractionation studies suggest that the majority of both lipin species are found in the soluble fraction. Immunofluorescent staining of 3T3-L1 adipocytes shows that endogenous lipin 1 and lipin 2 form punctate structures that co-localize with the ER. The precise nature of these structures is currently unclear. We have previously shown that within cells the lipins form tetramers<sup>32</sup> and by Atomic Force Microscopy (AFM) have found that recombinant lipin 1 can form even higher order structures on lipid bilayers<sup>80</sup>. In addition, lipin 1 has been found to interact with the human lipodystrophy protein seipin<sup>81</sup>, and seipin itself has been found to form large oligomeric structures<sup>82</sup>. While the identification of lipin localization to punctate spots is interesting, further study will be necessary to uncover the nature and/or function of lipin protein cellular localization to these structures.

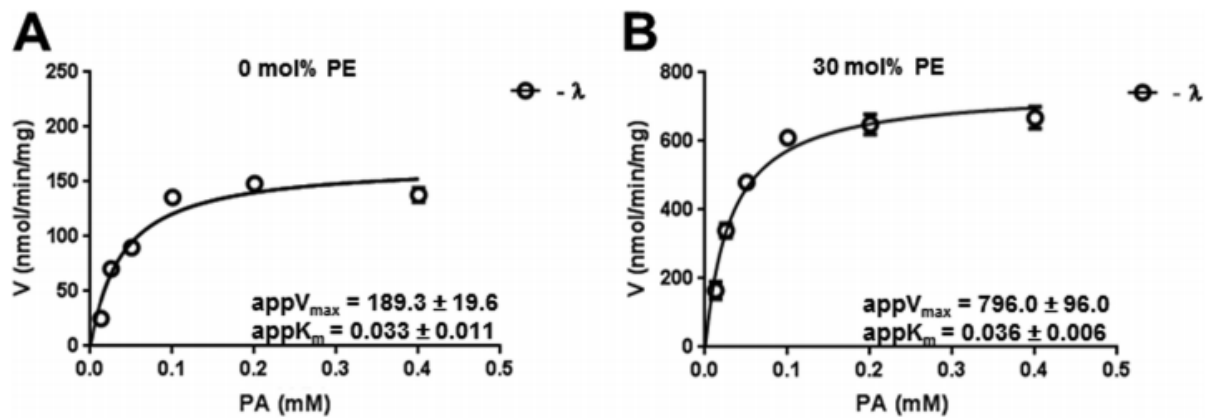
Our conclusions support a role for lipin 2 as a constitutive enzyme that provides relatively low levels of PAP activity that is not under acute negative regulation. This contrasts with lipin 1 functioning as a more active PAP enzyme that is under tight negative regulation by hormonal signaling.

FIGURE 4.1 Purification and initial characterization of lipin 2.



**Figure 4.1 Purification and initial characterization of lipin 2.** A, A FLAG tagged lipin 2 was expressed in HeLa cells using adenovirus for 72 h, after which cells were harvested and lysed in homogenization buffer A and cleared lysates were incubated with anti-FLAG agarose beads for 2-4 h. The slurry was packed onto a screening column, washed extensively and eluted with FLAG peptide and dialyzed. A representative 8.75% acrylamide SDS-PAGE gel stained with Coomassie blue is shown with 500 ng of purified lipin 2. B, the linear range of lipin 2 phosphatase activity (50 ng) is shown towards Triton X-100/PA mixed micelles (9.1 mol%). C, lipin 2 PA phosphatase activity was measured at the indicated pH in 50mM Tris-maleate-glycine. D, the indicated concentrations of Triton X-100 were used to measure PA phosphatase activity against 0.5 mM PA. E, Lipin 2 PA phosphatase activity was measured with the indicated concentrations of MgCl<sub>2</sub>, and F, MnCl<sub>2</sub>. G, lipin 2 PA phosphatase activity was measured with the indicated concentrations of N-ethylmaleimide in the absence of β-mercaptoethanol and H, lipin 2 PA phosphatase activity was measured with the indicated concentrations of β-mercaptoethanol. Maximum PA phosphatase activity is set to 100%. The data shown are the means ± S.D. from triplicate experiments.

FIGURE 4.2 Effects of PA charge on lipin 2 PA phosphatase activity.

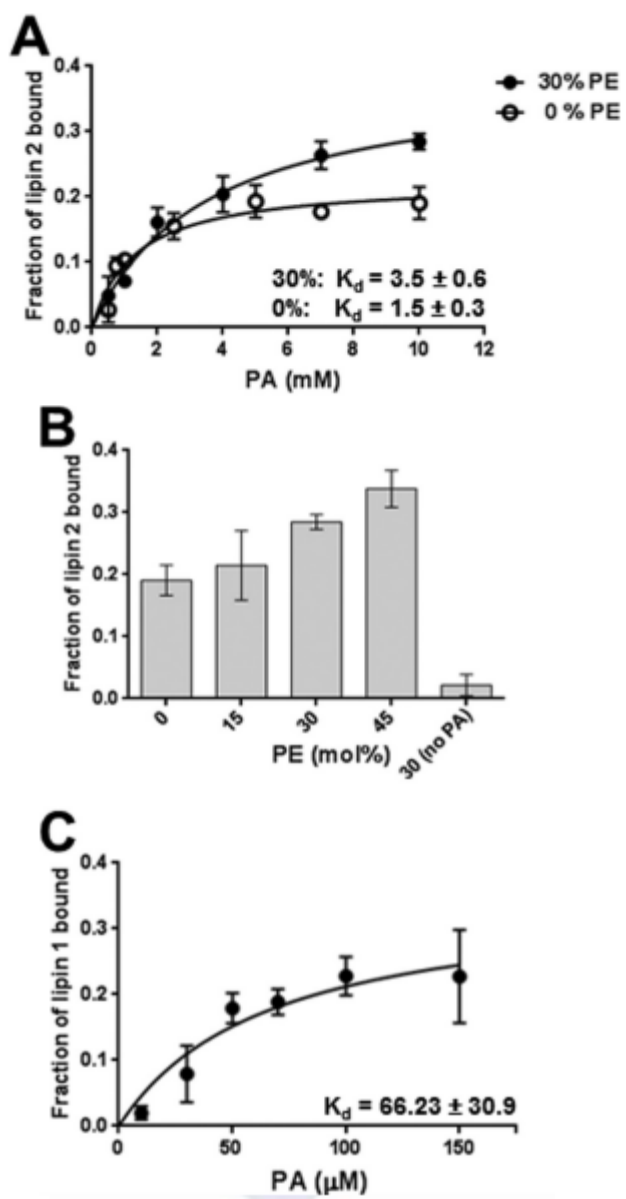


**Figure 4.2 Effects of PA charge on lipin 2 PA phosphatase activity.** A, Lipin 2 PA phosphatase activity was measured using PA:PC (10:90 mol%) liposomes and, B, PA:PE:PC (10:30:60 mol%) liposomes at the indicated molar concentration. The data shown are the means  $\pm$  S.D. from triplicate experiments.

**Table 4.1** Steady-state kinetic data for lipin 2 using liposomes composed of 10 mol % PA and 90 mol% (PE + PC) with PE mol % indicated.

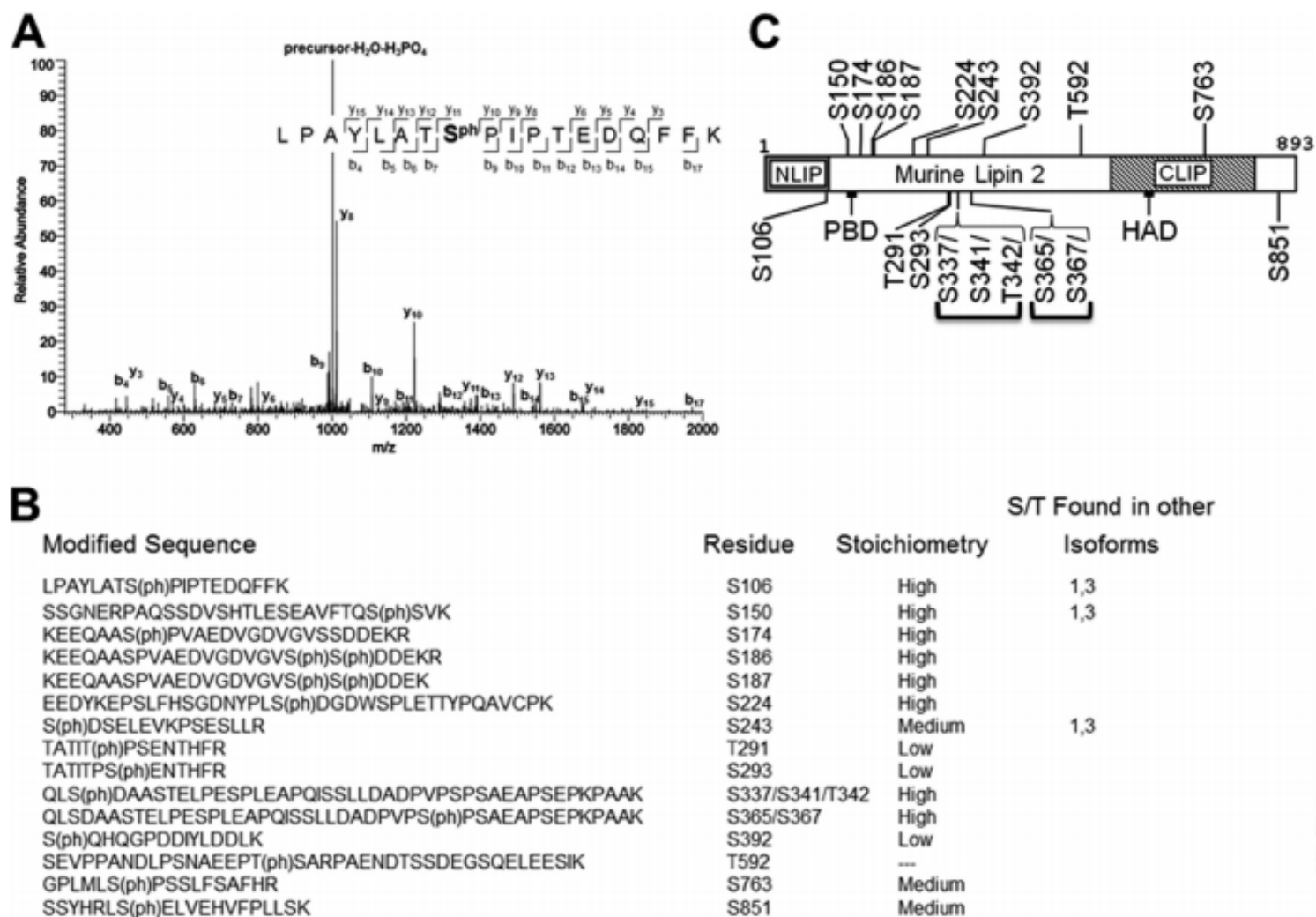
Lipin 2	mol % PE	$k_{\text{cat}}$ $s^{-1}$	$K_m^{\text{app}}$ $M$	$k_{\text{cat}}/K_m^{\text{app}}$ $M^{-1} s^{-1}$
+λ	0	$0.59 \pm 0.02$	$3.8 \pm 0.5 \times 10^{-5}$	$1.5 \times 10^4$
+λ	30	$2.54 \pm 0.32$	$2.7 \pm 1.3 \times 10^{-5}$	$9.4 \times 10^4$
-λ	0	$0.63 \pm 0.03$	$3.3 \pm 0.4 \times 10^{-5}$	$1.9 \times 10^4$
-λ	30	$2.65 \pm 0.39$	$3.6 \pm 0.6 \times 10^{-5}$	$7.3 \times 10^4$

Figure 4.3 Effects of PA charge on lipin 2 membrane binding.



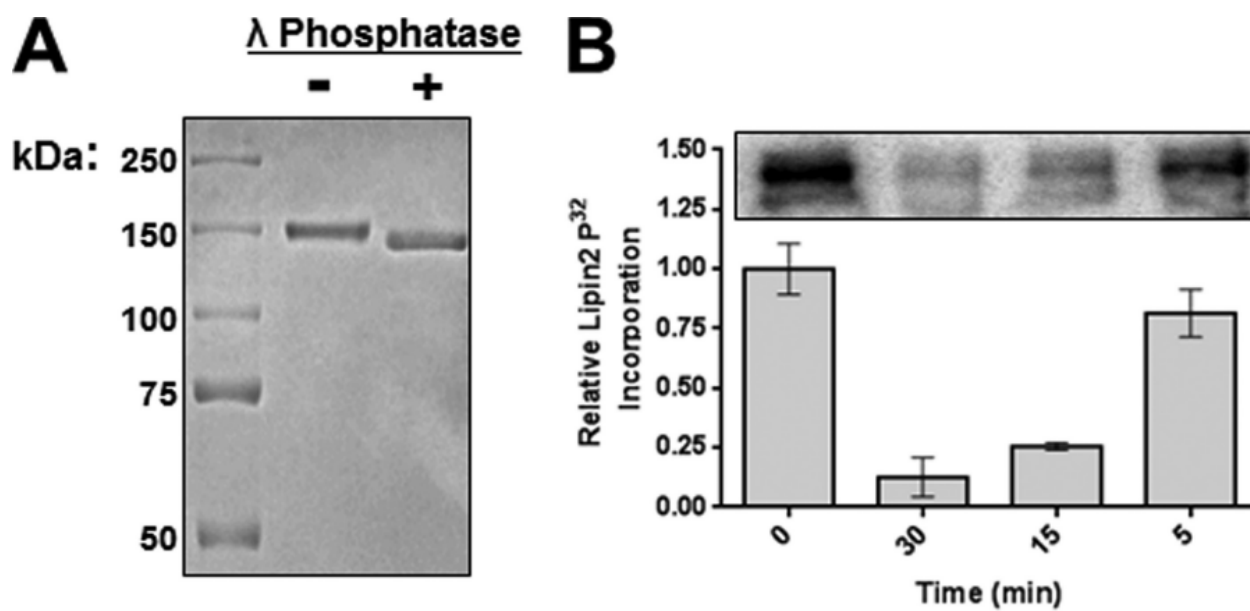
**Figure 4.3 Effects of PA charge on lipin 2 membrane binding.** A, Lipin 2 binding to liposomes composed of PA:PC (20 mol% PA, 0% PE, 79.9 mol% PC, 0.1 mol% pyrene-PC) and PA:PE:PC (20 mol% PA, 30 mol% PE, 49.9 mol% PC, 0.1 mol% pyrene-PC). Venus-tagged lipin 2 and the indicated concentration of liposomes were incubated for 20 min at 30°C then an equal volume of 80% (w/v) sucrose in Buffer B was added. This mixture was placed in 5 x 41 mm Beckman tubes and was carefully overlaid with 150 µl of 20% (w/v), and 50 µl of 0% (w/v) sucrose in Buffer B and centrifuged in a SW 55Ti swinging bucket rotor containing nylon inserts at 240,000 x g for one h. The top 50 µl fraction was collected with a Hamilton syringe and pyrene and Venus absorption were measured to determine the percent liposome recovery after flotation in addition to the fraction of lipin 2 bound to the liposomes. Fraction bound was determined from triplicate experiments. B, FLAG-Venus-lipin 2 binding to PA containing liposomes increases as the mol% PE increases. Binding was performed as previously described with the indicated mol% PE. Binding was performed at saturating PA concentrations, 10 mM. C, FLAG-Venus-lipin 1 binding to PA:PC liposomes (20 mol% PA, 79.9 mol% PC, 0.1 mol% pyrene-PC) was performed as described for lipin 2 in A. The data are shown as means ± S.D. from triplicate experiments.

Figure 4.4 Mass spectrometric analysis of lipin 2 phosphorylation.



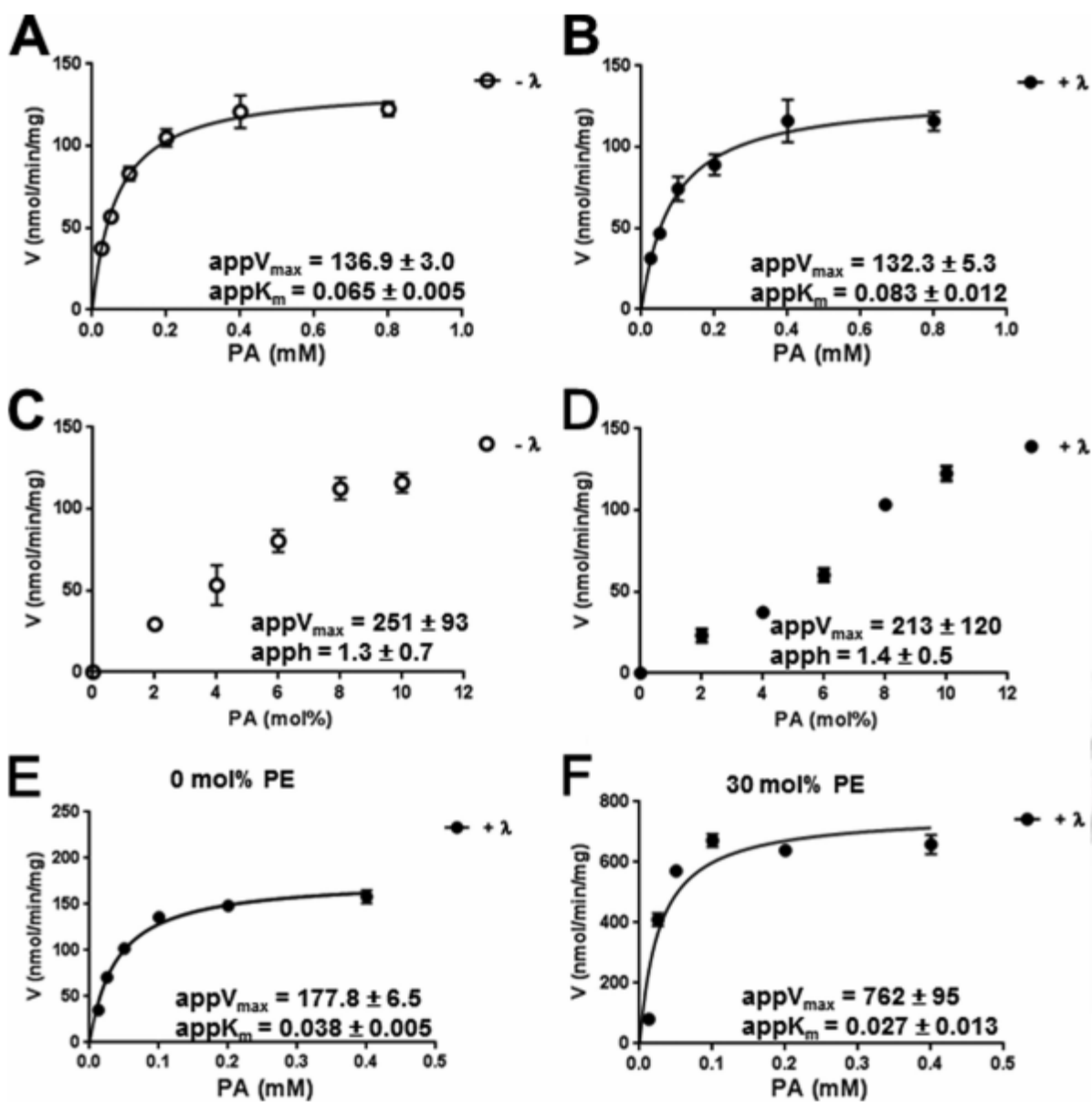
**Figure 4.4 Mass spectrometric analysis of lipin 2 phosphorylation.** A, The MS/MS spectrum of the peptide containing phosphorylated Ser<sup>106</sup> is shown. B, summary of the identified phosphorylation sites in lipin 2. Amino acid sequences and approximate stoichiometries of the phosphopeptides identified by MS/MS analyses are shown. Also shown is whether the residue identified as phosphorylated in lipin 2 is conserved within lipin 1 and 3. Note that this does not necessarily mean that the conserved residue is phosphorylated in lipin 1 and 3. C, cartoon showing identified phosphorylation sites in relation to each other and domains within lipin 2. If the site could not be confidently localized (>95% certainty), a range of possible positions is indicated with brackets.

Figure 4.5 Lambda phosphatase treatment of lipin 2.

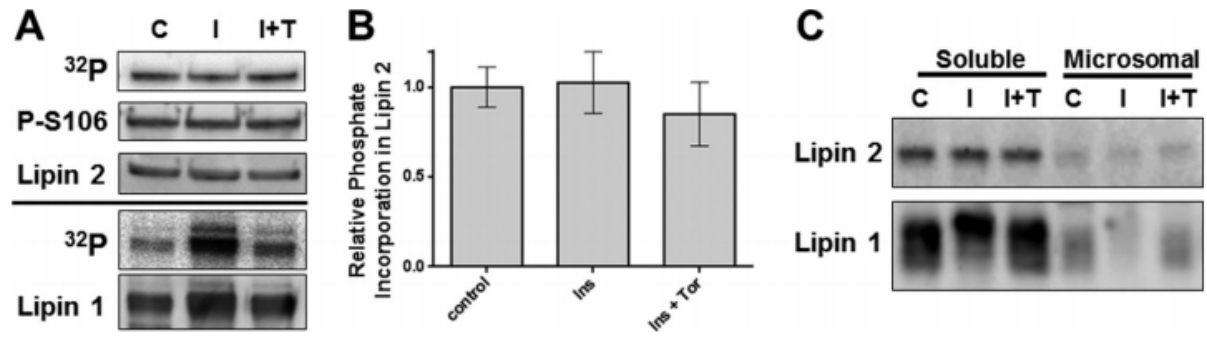


**Figure 4.5 Lambda phosphatase treatment of lipin 2.** A, Lipin 2 was purified as previously described and treated with lambda phosphatase for 30 min. A representative 8.75% acrylamide SDS-PAGE gel stained with Coomassie blue is shown for 500 ng of dephosphorylated (+  $\lambda$ ) and phosphorylated (- $\lambda$ ) lipin 2. B, HeLa cells expressing Lipin 2 were incubated with 0.02 mCi/ml [ $^{32}$ P]ATP for 2 h and Lipin 2 was immunoprecipitated and treated with lambda phosphatase for the indicated amount of time. Quantitation of phosphate removal was determined by autoradiography of lipin 2 after running on an 8.75% acrylamide SDS-PAGE gel and transferred to PVDF. Graph shows means  $\pm$  S.D. of  $^{32}$ P incorporation from triplicate experiments.

Figure 4.6 Effect of lipin 2 phosphorylation on PA phosphatase activity.

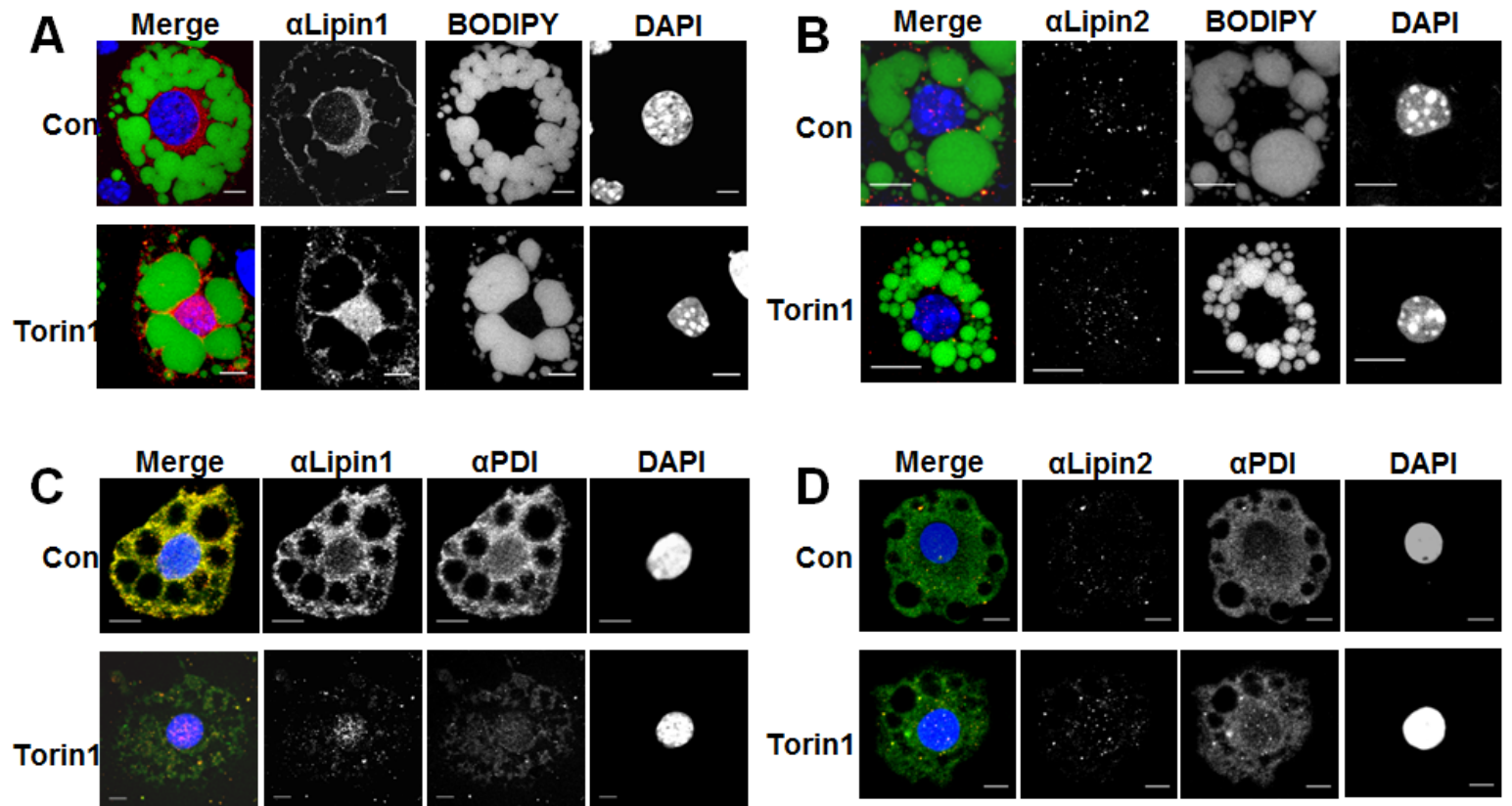


**Figure 4.6 Effect of lipin 2 phosphorylation on PA phosphatase activity.** Phosphorylated (- $\lambda$ ) and dephosphorylated (+ $\lambda$ ) lipin 2 PA phosphatase activity against Triton X-100/PA micelles was measured with respect to the molar, A and B, and surface, C and D, concentrations of PA. With respect to the molar concentration of PA, the molar ratio of Triton X-100: PA was 10:1 (9.1 mol%) and assayed against increasing molar PA concentrations. With respect to the surface concentration, the molar concentration of PA was maintained at 1 mM while decreasing the ratio of Triton X-100: PA. E and F, lipin 2 PA phosphatase activity was measured using liposomes with 0 and 30 mol% PE, 90 and 30 mol% PC, respectively and 10 mol% PA. The data shown are the means  $\pm$  S.D. from triplicate experiments. The best fit curves were derived from kinetic analysis of the data.

**Figure 4.7 Phosphorylation of lipin 1 and 2 in 3T3-L1 adipocytes.**

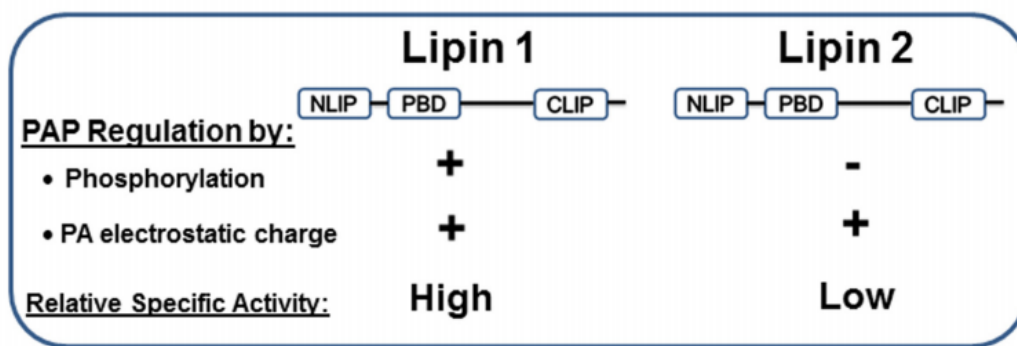
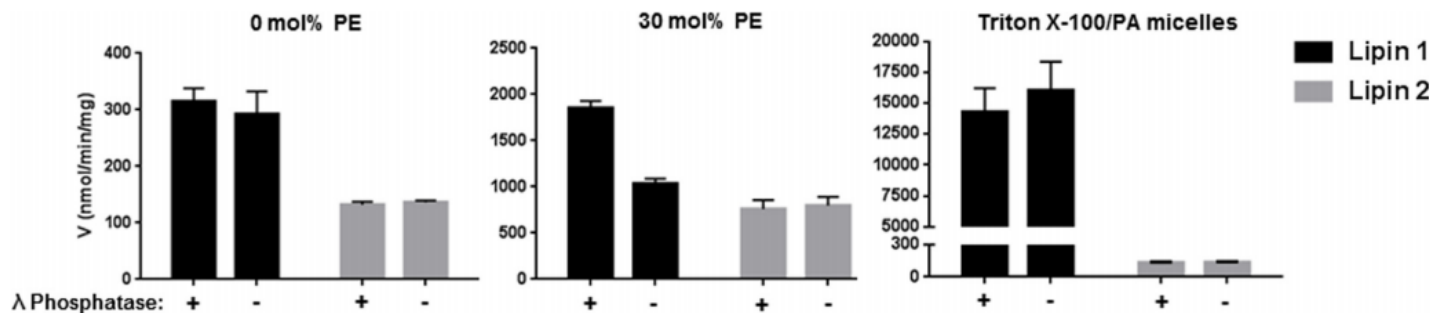
**Figure 4.7 Phosphorylation of lipin 1 and 2 in 3T3-L1 adipocytes.** A, 3T3-L1 adipocytes were cultured with 0.5 mCi/ml [ $^{32}$ P] orthophosphate for 2 h in the absence of serum. Treatments were as follows: with or without 10 mU/ml insulin for the last 15 min (control, **C** or **I**), or Torin1 pretreatment for 30 min prior to insulin stimulation (**I+T**). Endogenous lipin 1 and FLAG-tagged lipin 2 expressed by adenovirus were immunoprecipitated with lipin 1 or FLAG antibodies, subjected to SDS-PAGE, and transferred to PVDF membrane for phosphoimaging and immunoblotting. Representative immunoblot and phosphoimage from triplicate experiments. B, Quantitation of data in A, n=3. C, 3T3-L1 adipocytes were serum starved for 2 h (control, **C**) and then treated with or without insulin (**I**) and insulin plus Torin1(**I+T**) as described in A. After insulin stimulation fractions containing soluble and microsomal proteins were isolated, and lipin 1 and 2 immunoblots were prepared.

Figure 4.8 Lipin 2 subcellular localization in 3T3-L1 adipocytes.



**Figure 4.8 Lipin 2 subcellular localization in 3T3-L1 adipocytes.** 3T3-L1 adipocytes were plated onto coverslips in 6-well plates and incubated in DMEM with 10% FBS. On day 8 adipocytes were treated overnight (16 h) with either 250 nM Torin1 or vehicle (0.025% DMSO). A, Red, endogenous lipin 1, and B, endogenous lipin 2; Green, BODIPY; Blue, DAPI. C, Red, endogenous lipin 1, and D, endogenous lipin 2; Green, PDI; Blue, DAPI.

Figure 4.9 Model of lipin 1 vs lipin 2 enzymatic activity.



**Figure 4.9 Model of lipin 1 vs lipin 2 enzymatic activity.** A, Comparison of specific activity at saturating PA concentrations between lipin 1 and 2 measured with liposomes containing 0 and 30 mol% PE and Triton X-100/PA micelles. Data derived from the data contained herein and Eaton et al. <sup>29</sup>. B, a schematic representing important similarities and differences between lipin 1 and 2. NLIP and CLIP are conserved NH<sub>2</sub>- and COOH- lipin homology domains, PBD is the polybasic domain.

## CHAPTER 5

### ASSEMBLY OF HIGH MOLECULAR WEIGHT COMPLEXES OF LIPIN ON A SUPPORTED LIPID BILAYER OBSERVED BY ATOMIC FORCE MICROSCOPY

#### ABSTRACT

Lipins are phosphatidic acid phosphatases involved in the biosynthesis of triacylglycerols and phospholipids. They are associated with the endoplasmic reticulum but can also travel into the nucleus and alter gene expression. Previous studies indicate lipins in solution form high molecular weight complexes, possibly tetramers. This study was undertaken to determine if lipins form complexes on membranes as well. Murine lipin 1b was applied to a supported bilayer of phosphatidylcholine, phosphatidylserine, and cholesterol and examined by atomic force microscopy (AFM) over time. Lipin on bare mica appeared as a symmetric particle with a volume consistent with the size of a monomer. On the bilayer lipin initially bound as asymmetric, curved particles which sometimes assembled into circular structures with an open center. Subsequently, lipin assemblies grew into large, symmetric particles with an average volume twelve times that of the monomer. Over time some of the lipin assemblies were removed from the bilayer by the AFM probe leaving behind “footprints” composed of complex patterns that may reflect the substructure of the lipin assemblies. The lipin complexes appeared very flat, with a diameter 20 times their height. The footprints had a similar diameter, providing confirmation of the extensive deformation of the protein under the AFM probe. The ability of lipin to form large complexes on membranes may have significant implications for the local concentrations of the product, diacylglycerol, formed during hydrolysis of phosphatidic acid and

for cooperative hormonal regulation of lipin activity through phosphorylation of one or more monomers in the complexes.

## INTRODUCTION

Biophysical studies of soluble lipin indicate that the protein can form homomeric and heteromeric complexes, possibly tetramers, with other lipin isoforms both in solution and in the cytoplasm of cells.<sup>32</sup> However, the nature of the protein-lipid complexes that lipin forms when interacting with membranes is not known. Because of the fundamental importance of the ability of lipin to interact reversibly with membranes, this study was undertaken to visualize the interaction of lipin with membranes *in vitro* by atomic force microscopy (AFM). The results provide novel insights into the interaction of lipin with itself on membranes to form unexpectedly large complexes. The nature of these complexes may significantly influence the mechanism of lipin action on membrane-bound substrates and the cooperative regulation of lipin by phosphorylation of monomers within the complexes.

## RESULTS

*Lipin in air on mica* - Lipin was initially imaged in air on a bare mica support. Single particles and clusters were observed as seen in **Figure 5.1**. Analysis of single particles indicated an average height of  $0.676 \pm 0.078$  nm ( $n=26$ ), diameter at half height of  $17.0 \pm 1.7$  nm and a calculated molecular volume (see Materials and Methods) of  $77.4 \pm 16.2$  nm<sup>3</sup>. The distributions of particle dimensions are shown in the histograms in **Figure 5.2**. At higher magnification (**Figure 5.1 C, D**) the individual particles had a lumpy appearance indicative of some substructure, but because of the different orientations of the particles on the mica a particular molecular shape could not be assigned to the particles.

*Lipin in buffer on mica and on a supported bilayer* - Lipin was visualized after applying to a supported lipid bilayer composed of 50% PC, 25%PS, 25% cholesterol by weight in a buffer of 150 mM NaCl, 50 mM HEPES-NaOH (pH7.4), 2 mM CaCl<sub>2</sub>. Because the bilayer was not complete it was possible to visualize lipin both on the bilayer and on the bare mica (**Figure 5.3**). Initially the lipin did not adhere tightly enough to the bare mica to be imaged and the particles appeared as streaks as they were pushed ahead of the probe during imaging (**Figure 5.3, bottom**). After 90 minutes the lipin adhered more tightly to the mica and could be imaged although the particles were somewhat extended in the direction of probe motion suggesting some movement under the action of the probe (**Figure 5.4**) and the particles did not have the lumpy appearance that was resolved when lipin was imaged in air. Nonetheless, the dimensions of the particles on mica under buffer were similar to those visualized in air: height,  $0.603 \pm 0.082$  nm ( $n=24$ ); diameter  $16.4 \pm 2.3$  nm; and molecular volume  $65.3 \pm 20.2$  nm<sup>3</sup> (see histograms in **Figure 5.6**). This similarity in size of the “dry” lipin versus lipin in buffer suggests the protein

remains hydrated on the mica surface during imaging in air, and has also been reported in comparisons of other proteins observed by AFM in air and in buffer.<sup>59</sup>

In contrast, when lipin bound to the lipid bilayer it assembled into larger particles. After 30 minutes a mixture of particle sizes was visualized (**Figures 5.5**). The smaller particles appeared as oblong, slightly curved structures, sometimes assembled into complete circles (**Figures 5.5**). The heights of these structures above the bilayer ranged from 0.2 to 0.5 nm (e.g. **Figure 5.F**). Also present were larger, essentially globular structures. However, in some cases imaging of the same spot revealed that a larger particle had been apparently partially disrupted, leaving a ring-like structure behind.

After 90 minutes, most of the particles on the bilayer were of the larger class (**Figure 5.6**), suggesting that the smaller structures were intermediates in the pathway to formation of the larger structures. The larger particles which became stabilized on the bilayer had a height of  $1.63 \pm 0.24$  nm ( $n=78$ ), diameter at half-height of  $36.2 \pm 5.9$  nm, and molecular volume of  $884.2 \pm 373.2$  nm<sup>3</sup> (see histograms in **Figure 5.2**).

*“Footprints” left in the bilayer by displacement of lipin particles* - After the lipin particles on the bilayer were fairly stable (after 90 minutes), they were sometimes knocked off the bilayer by the AFM probe (**Figures 5.6 A-F**). At this point in time they did not leave a smaller structure behind as they did when first forming on the bilayer. Instead a distinct “footprint” was left as a partial hole in the bilayer. In several instances the displacement occurred after the probe had made sufficient contact with the particle to generate an image of part of the particle, then, as the probe continued the particle was removed, resulting in an image of part of a particle and part of a footprint (**Figures 5.6 A-F**). These footprints were complex,

consisting of three or four adjacent holes (e.g., **Figure 5.6 G, H**), possibly as a result of removal of parts of the membrane underlying the particle that were tightly bound to the protein multimers. The diameter of the footprints was typically close to but slightly greater than the apparent diameter of the protein before it was displaced (**Table 5.1**). The depth ranged up to 0.3 nm (e.g., **Figure 5.6I**), however, it is not clear whether the probe would have been able to reach the bottom of the holes because of the finite diameter of the probe.

## DISCUSSION

Comparing the images of lipin bound directly to mica, either in air or under buffer, with lipin bound to a supported lipid bilayer it is apparent that lipin undergoes a process of assembly into larger complexes on the bilayer, and does not remain bound to the bilayer as single particles. The sizes of lipin particles on the bare mica and on the bilayer are summarized in Table 2, including the molecular volumes calculated from the AFM measurements by the method described in Materials and Methods. The transition to the larger size particle was monitored by AFM which revealed that the assembly process employed intermediate steps to produce the larger complexes. The smallest particles initially seen bound to the bilayer were not as high as lipin bound to mica (0.2 to 0.5 nm on the bilayer versus 0.6 to 0.7 nm on mica) and had a more elongated shape. These intermediate structures were typically curved and often appeared to assemble to form nearly circular structures. For a period of 30 to 60 minutes these structures increased in size to form globular particles, although sometimes the larger particles were reduced in size and reverted to the circular shapes. The impression given by these images is that the initial assembly process is dynamic and reversible. It is possible that perturbation by the AFM probe was responsible for causing the disassembly of intermediate size particles before they achieved a more stable structural endpoint.

Subsequent to this period of growth the larger particles that formed were stable but had a fairly broad distribution in sizes. The average size corresponded to a volume that was twelve fold greater than the initial size of independent lipin particles on mica (**Table 5.2**). This may be an underestimate if some of the lipin was buried in the bilayer because the height of the particles was measured relative to the surface of the bilayer. This average size would correspond to a dodecamer of lipin monomers. However, the breadth of the histogram of molecular volumes

(**Figure 5.2**) suggests the calculated average size likely includes contributions from complexes of a range of sizes whose exact compositions could not be resolved. For example, in the case of particle number 1 in **Figures 5.6A-F**, a cross section revealed that this particle had a saddle at its peak and was twice as wide in one dimension as the average particle width. Therefore it was likely to have been a poorly resolved multiple particle. Such particles were excluded from the determination of the average size of particles when, as in this case, their morphology clearly indicated they were composed of two or more large particles. However, even after excluding these there remained a significant fraction of particles that were twice the average size (see the histogram in **Figure 5.2**) that were retained in the analysis because no clear resolution onto multiple particles was evident from cross section analysis.

It is possible that the HAD domain in lipin might drive the formation of lipin tetramers. The lipid phosphatase catalytic domain of lipin is a member of the haloacid dehalogenase structural superfamily.<sup>8</sup> A homologous domain in vertebrate cytidine monophosphate-sialic acid synthetase forms a tetramer which in turn drives tetramerization of the complete synthetase molecule.<sup>83</sup> It is possible that the corresponding domain in lipin might drive the formation of a lipin tetramer. Indeed, gel filtration analysis of soluble lipin indicates a molecular size of about 600kDa, possibly representing a tetramer or a higher order complex of the 100 kDa monomer.<sup>32</sup> However, the gel filtration analysis may be misleading if lipin in solution is a highly asymmetric molecule. Our observations of lipin on mica suggest it is not asymmetric, and the molecular volumes we measured for lipin on mica are more consistent with a monomer than a tetramer (see **Table 5.2**). However, the smallest lipin particles seen initially on the bilayer during assembly of the larger complexes were distinctly asymmetric as described above. When interacting with a lipid bilayer the globular monomer may undergo a conformational change to form the extended

molecules that were initially seen on the bilayer. These extended monomers may then assemble to form tetramers, which may also associate with one another on the bilayer to form octamers, dodecamers, or even higher order structures.

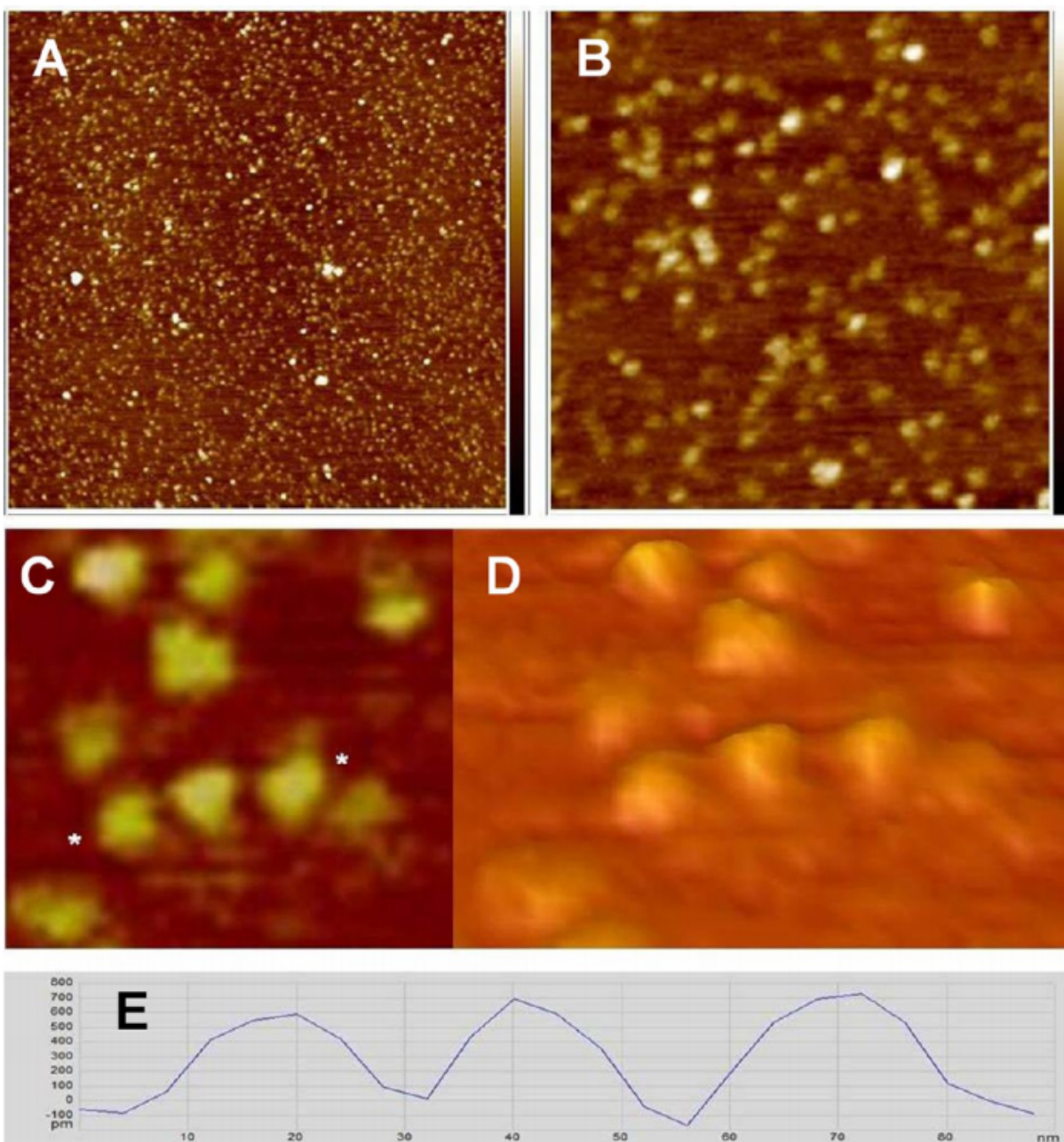
Such a self-assembly process may be important for the function of lipin on membranes. Cooperative interactions between membrane-bound lipin molecules may strengthen the interaction with the bilayer, resulting in a structure that cannot be removed from the membrane without damaging the membrane, as suggested by the appearance of the footprints when mature lipin complexes were displaced by the AFM probe. The assembly of lipin complexes on the membrane may also enable lipin to form high local concentrations of diacylglycerol from hydrolysis of its substrate, phosphatidic acid.

In spite of the uncertainties inherent in determining the exact molecular volumes of lipin complexes by AFM, and the significant deformation of the complexes that occurred during imaging, the conclusion that lipin assembles on membranes to form particles that on average are 12 fold larger than the lipin monomer seems firm. This result is likely to be of considerable importance in understanding the regulation of lipin as well as the nature of the deposition of the product, diacylglycerol, in the membrane during complex lipid synthesis.

Several aspects of the lipin assembly process observed here warrant more detailed investigation. Electron microscopy studies of lipin monomers and higher order complexes will be essential to unequivocally determine their morphology, molecular content, and organization. The effects of lipin phosphorylation, which reduces the affinity of lipin for lipids *in vitro* and its localization in cells<sup>1</sup>, on the lipin assembly process on bilayers could be investigated by AFM. The possible effects of lipid composition, particularly the inclusion of the substrate, phosphatidic

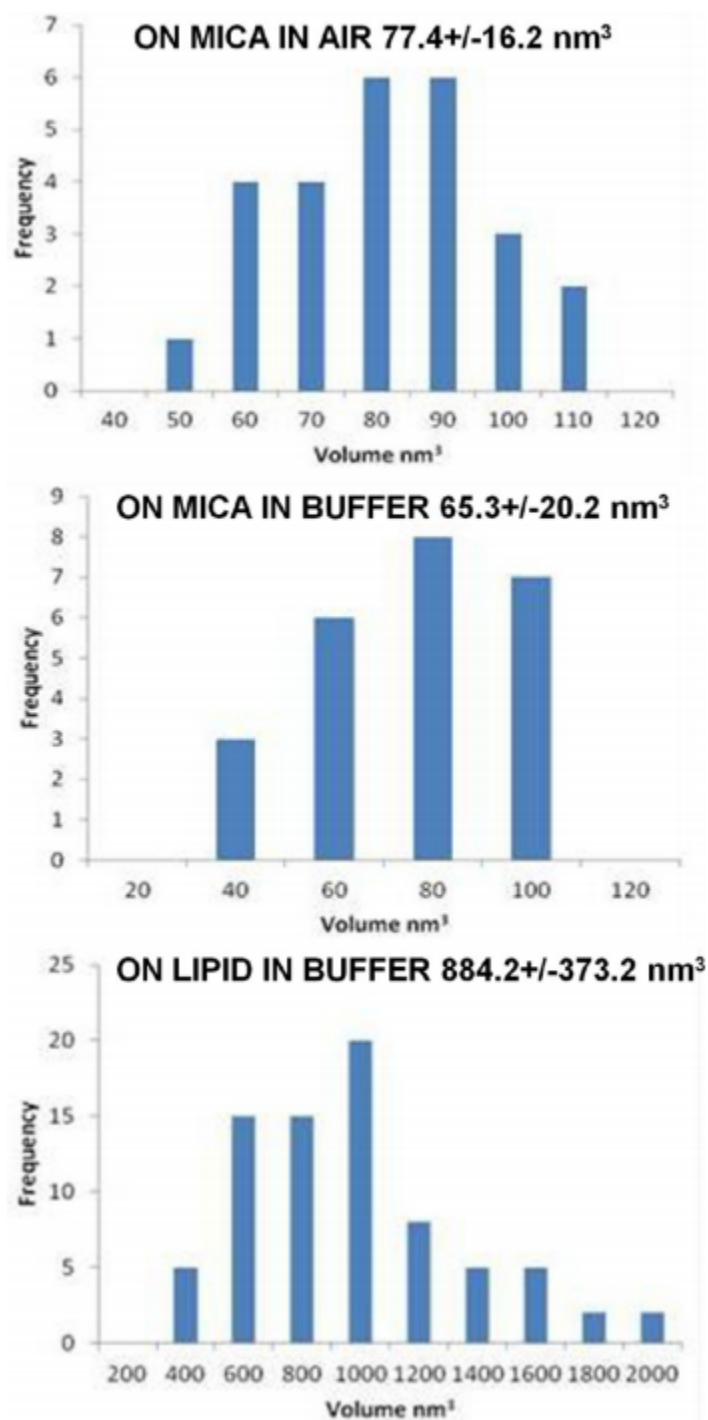
acid, and product, diacylglycerol, in the bilayer could likewise be determined. It would also be of interest to assess whether heterocomplexes of different lipin isoforms might assemble by different pathways or to different final states since multiple lipin isoforms are co-expressed in cells.<sup>19-21</sup> The AFM technology might also be used to address whether lipin may co-assemble with other enzymes in the triacylglycerol or phospholipid synthetic pathways to form efficient lipid-modifying protein assemblies amenable to coordinated regulation by phosphorylation or other modifications.

Figure 5.1 Lipin imaged in air on mica.



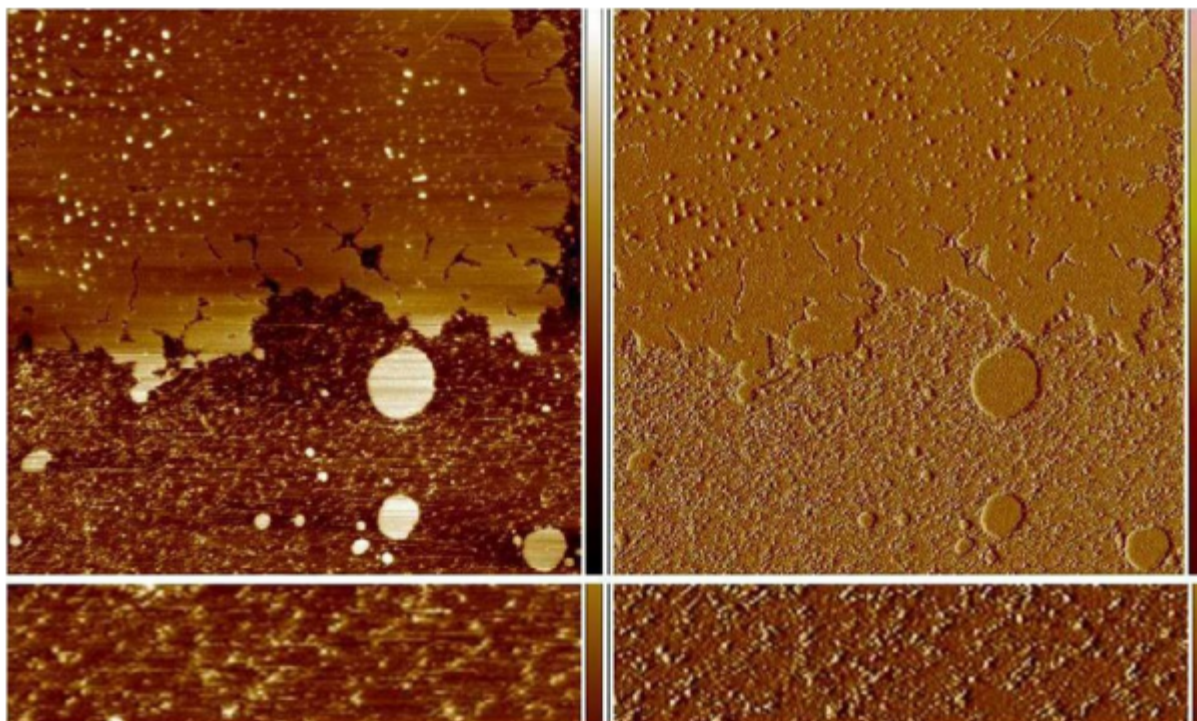
**Figure 5.1 Lipin imaged in air on mica.** (A–C) Height images obtained in peak force tapping mode: (A)  $2\ \mu\text{m} \times 2\ \mu\text{m}$ , (B)  $500\ \text{nm} \times 500\ \text{nm}$ , and (C)  $130\ \text{nm} \times 130\ \text{nm}$ . The height scale on the right in panels A and B is  $-1.5$  to  $1.5\ \text{nm}$ . (D) Three-dimensional representation of the same are seen in panel C, viewed at an oblique angle. (E) Cross section profile of the three particles between the asterisks in panel C. Vertical scale on the cross section of  $-100$  to  $800\ \text{pm}$  and horizontal scale of  $0$ – $90\ \text{nm}$ .

Figure 5.2 Histograms of the molecular volumes of lipin particles calculated as described in Materials and Methods.



**Figure 5.2. Histograms of the molecular volumes of lipin particles calculated as described in Materials and Methods:** (top) lipin visualized on mica in air, (middle) lipin on mica in buffer, and (bottom) lipin on the lipid bilayer in buffer

**Figure 5.3 Lipin imaged in buffer on a supported lipid bilayer and on mica.**



**Figure 5.3 Lipin imaged in buffer on a supported lipid bilayer and on mica.** In the top left panel, the height image is  $5 \times 5 \mu\text{m}$  and the height scale on the right  $-2$  to  $2 \text{ nm}$ . Dark areas represent the mica substrate and lighter areas the lipid bilayer. Lipin appears as a variety of size particles on the lipid bilayer. The bottom left panel is a higher-magnification view ( $0.5 \mu\text{m} \times 2 \mu\text{m}$ ) of a portion of the bare mica seen in the height image above. Lipin on the mica is not stable to imaging and is pushed by the probe creating the streaks at a  $45^\circ$  angle. Panels on the right are the amplitude error images of the same areas seen on the left, with an amplitude error scale of  $-5$  to  $5 \text{ mv}$ .

**Figure 5.4** After extended incubation in buffer, lipin adheres strongly enough to the mica to be visualized.

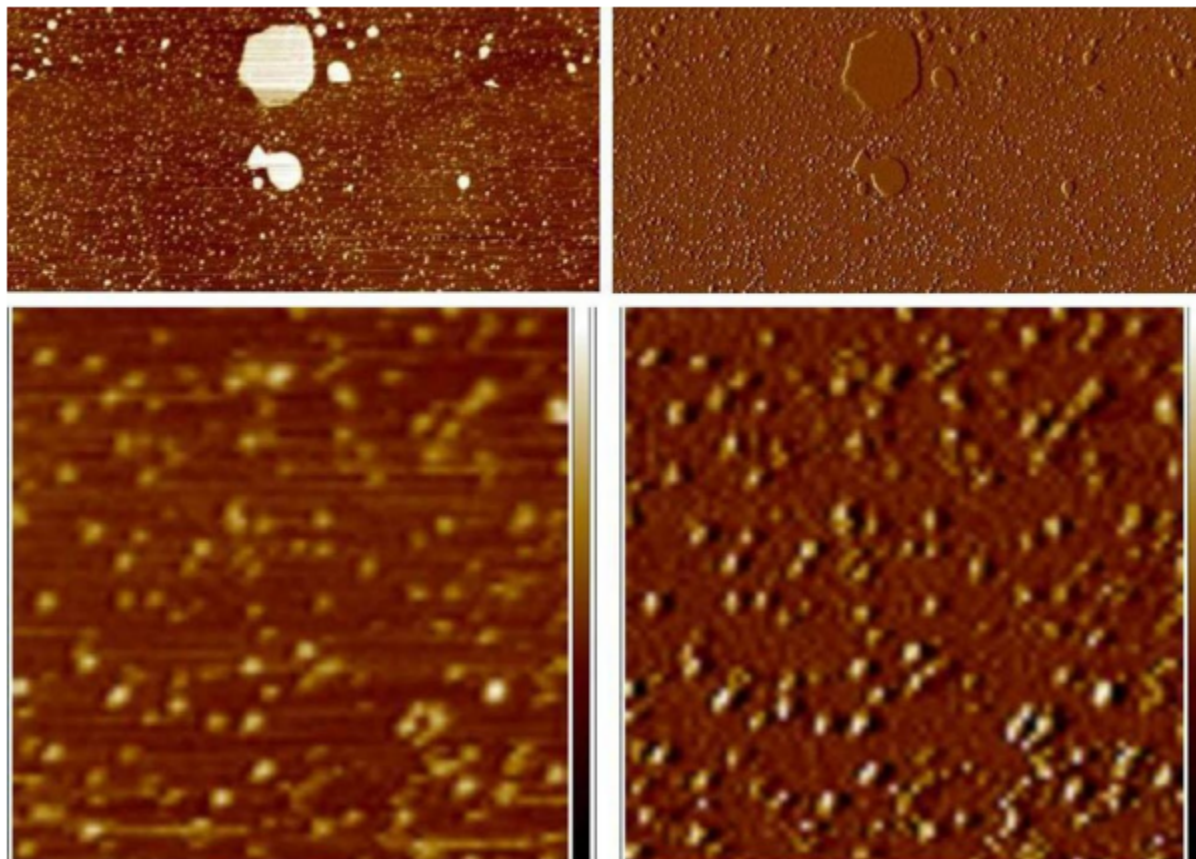


**Figure 5.4 After extended incubation in buffer, lipin adheres strongly enough to the mica to be visualized.** An area of bare mica adjacent to the patch of the bilayer seen in Figure 3 is shown at low magnification in the top panels ( $2.4 \mu\text{m} \times 5 \mu\text{m}$ ): (left) height image and (right) amplitude error image of the same region. The large bright objects in the height image are small patches of lipid bilayer, and the small particles on the mica are lipin. The bottom panels show a portion of the same field at a higher magnification ( $750 \text{ nm} \times 750 \text{ nm}$ ): (left) height image with a height scale of  $-2$  to  $2 \text{ nm}$  and (right) corresponding amplitude error image with an amplitude error scale of  $-10$  to  $10 \text{ mv}$ . The lipin particles move slightly toward the top right under the force of the probe, distorting the appearance of the particles.

**Figure 5.5** Higher-magnification view of lipin bound to the supported lipid bilayer seen in Figure 3.

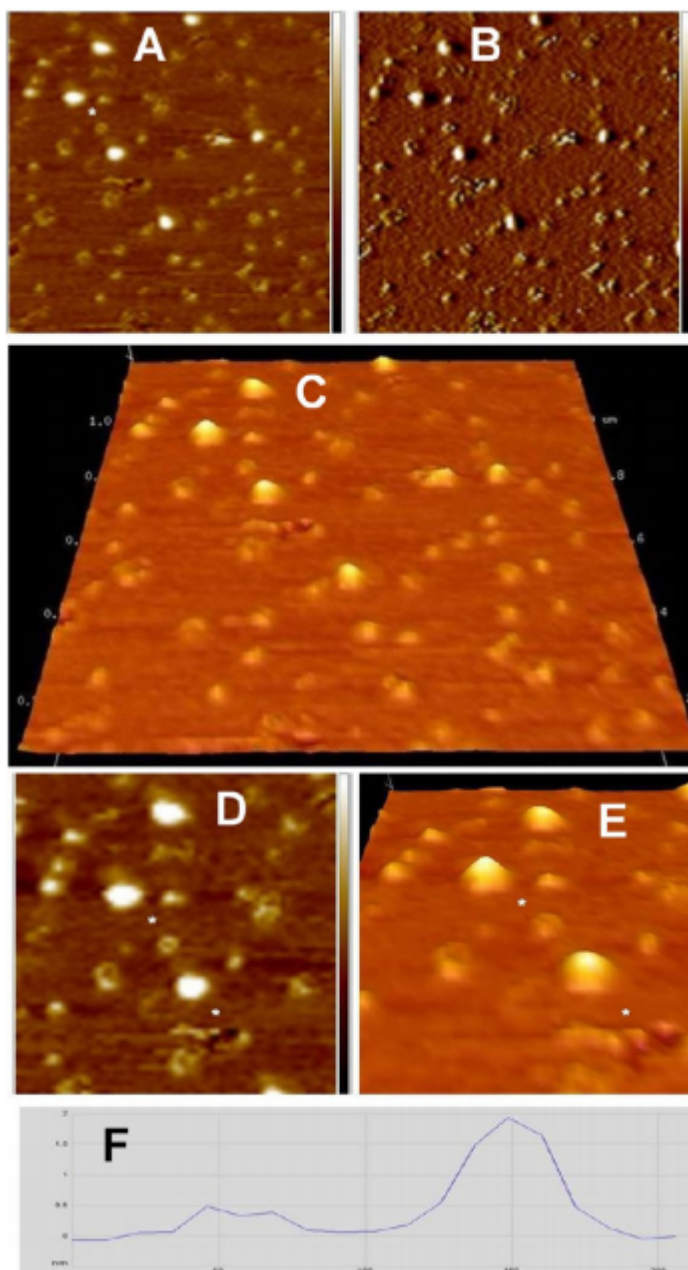


**Figure 5.5 Higher-magnification view of lipin bound to the supported lipid bilayer seen in Figure 3.**

Higher-magnification view of lipin bound to the supported lipid bilayer seen in Figure 3. (A) Height image of  $1\mu\text{m} \times 1\mu\text{m}$  with a height scale of -1.5 to 1.5 nm. (B) Amplitude error image corresponding to the height image in panel A with an amplitude error scale -5 to 5 mv. Note the coexistence of large, round lipin particles (appearing bright in the height image in panel A) and smaller lipin particles that have a linear, curved, or nearly circular morphology. One example of a particle with a circular morphology is seen at higher magnification in panels D and E. (C) Three-dimensional representation of the area seen in panels A and B. The vertical scale has been magnified 10-fold to aid in visualization of the topography. (D and E) Higher-magnification views of variously sized lipin aggregates from a portion of panel A. (D) Height image of  $615\text{ nm} \times 615\text{ nm}$  with a height scale of -1 to 1 nm. A three-dimensional representation of the same area is shown in panel E with the vertical scale magnified 10-fold to aid in visualization of the topography. (F) The cross section profile between the two asterisks in panel D and E goes through the small circular lipin particle and the adjacent large particle. The vertical scale on the cross section was from 0 to 2 nm with a horizontal scale of 0-200 nm.

**Figure 5.6** Large lipin particles leave behind “footprints” when they are displaced by the AFM probe.

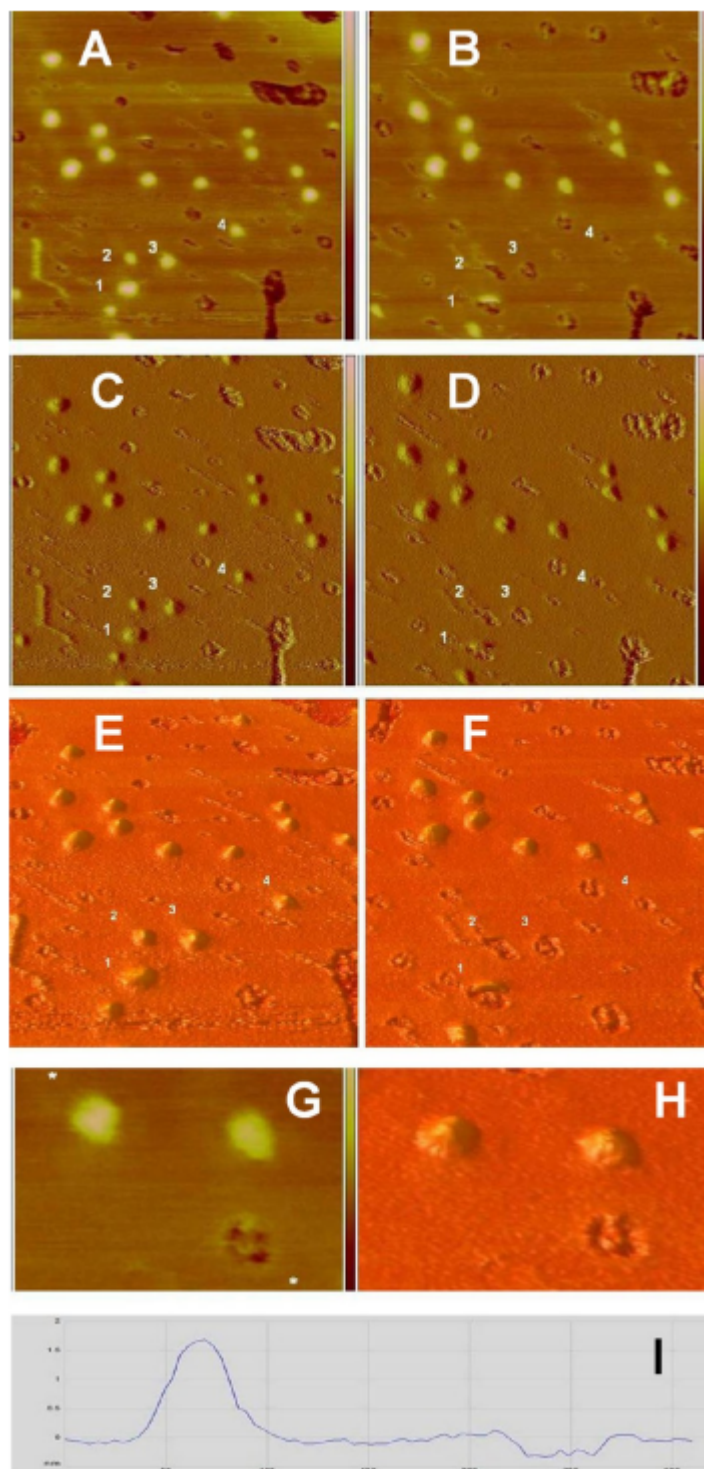


**Figure 5.6 Large lipin particles leave behind “footprints” when they are displaced by the AFM probe.** (A–F) Lipin bound to the supported lipid bilayer is viewed in two scans 512 s apart. Left panels (A, C, and E) are from a scan in the downward direction taking 256 s. The height image is in panel A ( $1\ \mu\text{m} \times 1\ \mu\text{m}$ , with a height scale of  $-2$  to  $2\ \text{nm}$ ); the corresponding amplitude error image is in panel C (amplitude error scale of  $-5$  to  $5\ \text{mV}$ ). Panel E shows a three-dimensional representation of the area seen in panels A and C with the vertical scale magnified 10-fold to aid visualization of the topography. The panels on the right [B (height image), D (amplitude error image), and F (three-dimensional representation)] were captured at the same location during the next downward pass of the probe (after one upward pass). Lipin aggregates appear as bright objects in the height images. Depressions, holes, or footprints in the bilayer appear as dark areas. Note that the lipin particles labeled 1–4 in the left panels (particles are immediately to the bottom right of the numbers) are replaced by corresponding lipin footprints labeled 1–4 in the right panels. Particle 1 appears to have been sliced in half (panels B, D, and F) because the probe displaced the particle when it was passing near the center of the particle. The footprint left by particle 2 appears to be a doublet, possibly indicating the lipin particle rolled ahead of the probe and formed a second footprint before being fully displaced. (G–I) Higher-magnification views of two lipin aggregates and a lipin footprint on the supported bilayer. The height image (G) is close-up of a region near the center of panel B ( $220\ \text{nm} \times 300\ \text{nm}$ , height scale truncated; refer to the full height scale of  $-2$  to  $2\ \text{nm}$  in panel B). The corresponding three-dimensional representation is shown in panel H. Note the complex pattern present in the single footprint in panels G and H. A cross section profile across one of the lipin particles and the lipin footprint (between the asterisks marked on the height image in panel G) is shown in panel I (vertical scale of  $-0.5$  to  $2\ \text{nm}$ , horizontal scale of  $0$ – $300\ \text{nm}$ ).

**Table 5.1 Dimensions (nanometers) of lipin particles and their respective footprints on the supported bilayer**

particle <sup>a</sup>	particle horizontal width <sup>b</sup>	particle vertical width <sup>b</sup>	footprint horizontal width	footprint vertical width
1	71.7 <sup>c</sup>	49.0	78.3	nd <sup>d</sup>
2	42.4	42.6	48.9	nd <sup>e</sup>
3	55.5	45.8	58.7	52.3
4	52.2	42.5	52.2	45.7

<sup>a</sup>Particle numbers correspond to the particles as numbered in Figure 6.

<sup>b</sup>Particle widths were measured at the base (full height), not the half-height. <sup>c</sup>The profile of this particle suggests it is two poorly resolved lipin particles sitting adjacent to one another in the horizontal direction resulting in this large horizontal measurement. <sup>d</sup>Not determined because part of the footprint is occupied by the particle that was removed during imaging. <sup>e</sup>Not determined because this footprint appears as a doublet in the vertical direction possibly because the particle was pushed ahead of the probe during imaging and created two footprints.

**Table 5.2 Average dimensions of lipin particles and comparison with hypothetical volumes based on molecular weight**

imaging conditions	$H^a$ (nm)	$D_{\text{half}}$ (nm)	$V_{\text{half}}$ (nm <sup>3</sup> )	$D_{\text{full}}$ (nm)	$V_{\text{full}}$ (nm <sup>3</sup> )	$V_c$ (nm <sup>3</sup> )
in air on mica	0.676	17.0	77.4	24.02	153.4	193.4 (monomer)
in buffer on mica	0.603	16.4	65.3	23.20	127.3	193.4 (monomer)
in buffer on bilayer	1.63	36.2	884.2	51.14	1676.5	774 (tetramer)

<sup>a</sup> $H$  is the particle height.  $D_{\text{half}}$  is the particle diameter at half-height.  $V_{\text{half}}$  is the calculated volume of the particle when modeled as a spherical cap using the diameter at half-height in the calculation following the method of Schneider and colleagues.<sup>10</sup>  $D_{\text{full}}$  is the diameter at full height of the particle estimated from the relationship  $D_{\text{full}} = \sqrt{2} \times D_{\text{half}}$  (see Discussion).  $V_{\text{full}}$  is the calculated volume of the particle using the diameter at full height in the calculation.  $V_c$  is the calculated volume of a lipin monomer or tetramer based on its molecular weight using the method described in the Discussion and ref 10.

#### Acknowledgment of collaborative study

Author's Contribution: J.M.E. purified lipin 1, C.E.C. performed AFM studies and wrote manuscript

## CHAPTER 6

### RHABDOMYOLYSIS ASSOCIATED MUTATIONS IN HUMAN LIPIN 1 LEAD TO DEFECTIVE PHOSPHATIDIC ACID PHOSPHATASE ACTIVITY

#### ABSTRACT

Rhabdomyolysis is an acute syndrome due to extensive injury of skeletal muscle, with muscle fiber necrosis or permeabilization of the sarcolemma that results in muscle protein release into the blood. Mutations in the human gene encoding lipin 1 are a common cause of recurrent rhabdomyolysis in children. Lipin 1 is a bi-functional intracellular protein that dephosphorylates phosphatidic acid to form diacylglycerol and acts as a transcriptional coregulatory protein. However, it is unknown whether defects in one or both of these molecular activities are involved in the etiology of rhabdomyolysis. Herein, we cloned cDNAs to overexpress and purify recombinant lipin 1 proteins harboring mutations associated with rhabdomyolysis in children. Three mutant alleles were characterized. A predicted exonic deletion in the C-terminus of the protein (E766-S838\_del) was not expressed at the RNA or protein level. Lipin 1 L635P was expressed, but the protein was less stable and targeted for proteosomal degradation. Lipin 1 R725H was well-expressed and retained its transcriptional regulatory function. However, both L635P and R725H proteins were found to be deficient in PAP activity. Altogether, these data suggest that loss of lipin 1-mediated PAP activity may be involved in the pathogenesis of rhabdomyolysis in lipin 1 deficiency.

## INTRODUCTION

Lipin 1 is a lipid phosphatase that converts phosphatidic acid to diacylglycerol<sup>8</sup>. Lipin 1 also traffics to the nucleus to directly interact with DNA-bound transcription factors to regulate expression of genes encoding mitochondrial fatty acid oxidation enzymes<sup>34,35,33</sup>. Whether defects in lipin 1 PAP activity or transcriptional regulatory function, or both, underlie the pathogenesis of rhabdomyolysis in people with lipin 1 mutations is unknown.

Rhabdomyolysis is an acute syndrome due to extensive injury of skeletal muscle resulting in the release of muscle proteins into the blood. Crush injury, treatment with statins, exercise overexertion, and inherited defects are the most common causes of rhabdomyolysis. Mutations in the gene encoding lipin 1 have been identified as a cause of recurrent, early-onset, pediatric rhabdomyolysis.<sup>84,17,15</sup>

## RESULTS

The most common lipin 1 mutation in Caucasians<sup>84</sup> is an exon 17-18 deletion that is predicted to delete amino acids E766-S838 in the C-terminus of the lipin 1 protein. When the analogous deletion was made in a human lipin 1 cDNA in an expression vector, little lipin 1 mRNA or protein were expressed and in a pulse chase experiment, little <sup>35</sup>S-methionine containing protein was synthesized. (data not shown) This indicates that the mutation resulting in the E766-S838\_del is likely a complete loss of function allele.

Two point mutations in lipin 1 were recently identified, L635P and R725H (**Figure 6.1**). Expression analysis demonstrated that lipin 1 L635P protein is expressed but is less stable and targeted for proteasomal degradation. The lipin 1 R725H protein is well expressed and results in a stable protein. (data not shown) The two human lipin 1 mutant proteins and the wild type protein were transiently transfected in HEK293T cells and purified using a similar method previously described for lipin 1. PAP activities were measured using Triton X-100/PA mixed micelles. (**Figure 6.2**) Both mutants show an approximately 6 fold reduction in the turnover compared to wild type human lipin 1. For WT lipin 1  $k_{cat}$  was  $131.5 \pm 15.7 \text{ s}^{-1}$  compared to  $21.8 \pm 1.5$  and  $17.0 \pm 4.1$  for the R725H and L635P mutants, respectively. The  $K_m$  for WT lipin 1 was  $0.51 \pm 0.14 \text{ mM}$  and there was no significant difference for the two mutants. These results indicate that the two lipin 1 mutant proteins are intrinsically-deficient in PAP activity.

Compared to WT lipin 1, the ability of lipin 1 R725H to coactivate MEF2A and PGC-1 $\alpha$ , which are transcriptional regulators relevant to skeletal muscle, was not affected (data not shown). These data suggest that a disease-associated mutation in lipin 1 leads to deficiency in PAP activity, but does not impair transcriptional regulatory function.

## DISCUSSION

Michot and colleagues demonstrated defects in PAP activity in isolated myocytes from 3 patients with lipin 1 mutations<sup>85</sup>. However, the mutations in these patients resulted in complete loss of lipin 1 mRNA expression and a distinction regarding impaired transcriptional regulatory function or PAP activity could not be made. By using purified lipin 1 proteins, we show that single amino acid substitutions in human lipin 1 that are associated with rhabdomyolysis disrupt PAP activity, but do not affect nuclear transcriptional regulatory function. Taken together, these data are consistent with a role for loss of lipin1-mediated PAP activity in the pathogenesis of rhabdomyolysis in humans.

The data presented herein suggest that abnormalities in PAP activity play a role in myopathy and necrosis leading to the rhabdomyolysis, presumably through an altered glycerolipid profile. Cellular accumulation of PA may be toxic through activation of inflammatory MAPK signaling cascades.<sup>13</sup> PA also activates mTORC1 kinase<sup>86</sup> which has been linked to development of muscle injury and myopathy.<sup>87</sup> A number of mitochondrial defects lead to recurrent rhabdomyolysis<sup>88,89</sup> and lipin 1 PAP activity impacts mitochondrial function by regulating fission and fusion.<sup>90</sup> Broad generalizations based on two point mutants regarding this conclusion should be tempered accordingly. However, clear links between the loss of lipin 1-mediated PAP activity and myocyte damage can be drawn.

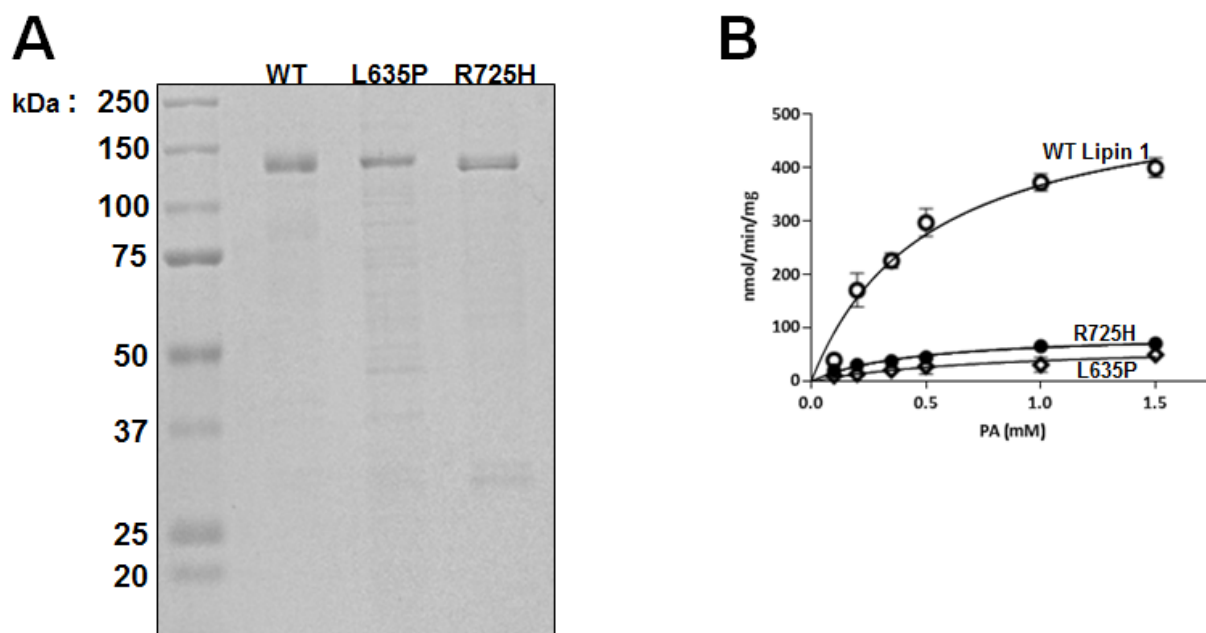
In conclusion, we present evidence that single amino acid substitutions in lipin 1 that are associated with recurrent rhabdomyolysis result in loss of PAP catalytic activity. This may facilitate the identification of the pathogenic mechanisms leading to myocyte cell death and suggest targeted therapies to treat afflicted patients.

**Figure 6.1 Lipin 1 mutations associated with rhabdomyolysis**

**A**

lipin 1,	634	QLKTLKLNKGNPNDVVS	VTTQYQGTCRCEGTIYLWNWDDR	VII	SDIDGT	ITRSDT	LGHIL	PTLGK
lipin 2,	645	QIAKLLHDGPNPNDVVS	ITTQYQGTCTRCAGTIYLWNWDR	III	SDIDGT	ITKSDA	LGQIL	PQLGK
lipin 3,	600	QIRRLNLQEGANDVVS	VTTQYQGTCTRCATIIYLWKWDDR	VVI	SDIDGT	ITKSDA	LGHIL	PQLGK
					<b>HAD I</b>		<b>NRID</b>	
lipin 1,	699	DWTHQGIKLYHKV	QNGYKFLYCSARA	IGM	DMTRGYLHWVNERGT	VLPQG	PLL	LSPSSLFSAL
lipin 2,	710	DWTHQGIKLYHSIN	ENGYKFLYCSARA	IGM	DMTRGYLHWVNDKGT	ILPRG	PLML	LSPSSLFSAL
lipin 3,	665	DWTHQGITSLYHKI	QNGYKFLYCSARA	IGM	DLTKGYLQWVSEGGCS	LPKGP	PILL	LSPSSLFSAL
					<b>HAD II</b>			

**FIGURE 6.1 Lipin 1 mutations associated with rhabdomyolysis.** Alignment of lipin 1, 2, and 3 protein sequences. The catalytic site (DIDGT) for phosphatidic acid phosphohydrolase (PAP) activity and 3 other haloacid dehalogenase (HAD) domains that are important for regulating PAP activity are noted. The nuclear receptor interaction domain (NRID) is important for transcriptional regulatory function. Amino acid substitutions or deletions in lipin 1 mutant alleles are in red font.

**FIGURE 6.2 Lipin 1 proteins with disease-associated mutations lack PAP activity**

**FIGURE 6.2 Lipin 1 proteins with disease-associated mutations lack PAP activity.** A. Coomassie stain of purified human lipin 1 proteins. B. PAP activity of purified human lipin 1 proteins was measured as a function of the bulk concentration of PA.

Acknowledgment of collaborative study

J.M.E. purified WT and mutant lipin proteins and analyzed their kinetics

Finck Lab responsible for the rest of resulting manuscript

## CHAPTER 7

### CONCLUSIONS AND FUTURE DIRECTIONS

#### *Summary and Conclusions*

These studies have conceptually advanced the lipin field with respect to how lipin 1 moves from the cytosol to ER membrane, a process that regulates its enzymatic activity. Using a biochemical approach we demonstrate how lipin 1 binds its substrate and how phosphorylation exerts control over this process. Collectively, we have established that lipin 1 binds its lipid substrate with a previously undefined PA binding motif separate from the catalytic active site. The polybasic domain contains basic residues capable of sensing the cationic charge on the phosphate group of PA and most importantly, favors association with a di-anionic charge. By breaking convention and looking beyond detergent micelles to more physiologic model membranes using liposomes, we have provided experimental evidence that lipin 1 binds PA by the electrostatic-hydrogen bond switch mechanism, a process inhibited by phosphorylation. This novel finding helps to mechanistically explain prior reports from the literature regarding the correlation between mTORC1 dependent phosphorylation and localization while revealing other points of influence in lipin 1 cellular translocation. Intracellular pH and the ratio of phospholipid species at the ER membrane were previously unappreciated stimuli for lipin 1 translocation and these studies suggest both can significantly influence lipin 1 membrane association by altering the charge carried by PA thereby affecting binding affinity. These finding encompass the exciting first evidence of a possible link between intracellular pH and lipid metabolism in mammalian cells.

As far as we know this work is the first to use lipin 1 purified from mammalian cells, harboring multiple phosphorylated residues. Because we had a unique reagent to the lipin field, we pursued other techniques to answer novel questions about the biochemical characteristics of lipin. Previous observations from the lab have strongly suggested that lipin forms large structures, possibly tetramers, in solution and in the cytoplasm. We wanted to know if a similar effect can be observed when lipin binds a lipid bilayer. Through a collaborative effort we were able to image lipin 1 on a supported lipid bilayer by atomic force microscopy. These biophysical studies demonstrated that lipin forms high molecular weight structures when bound to the bilayer as a function of time in what appeared to be a reversible association, a finding that will likely help in understanding lipin structure-function.

Our expertise in lipin purification and kinetic analysis gave us the opportunity for other collaborative studies. We were able to demonstrate that lipin 1 mutations associated with rhabdomyolysis have defects in PAP activity. This finding provides further evidence for the role of lipin 1 PAP activity in the pathogenesis of this acute syndrome.

Because we found a novel mechanism in the relationship between lipin 1 phosphorylation and membrane association, it was a natural progression to ask if lipin 2 binds PA in a similar way. Indeed, experimental evidence suggests that lipin 2 binds PA by the electrostatic-hydrogen bond switch mechanism, however, with a crucial distinction. Phosphorylation had no effect on PA binding or catalytic activity, suggesting that lipin 2 is a constitutively active PAP enzyme with respect to phosphorylation. Additionally, lipin 2 is not down stream of mTOR in adipocytes. These studies provide evidence for differential regulation of phosphatase activity within the lipin family.

### *Future Directions*

This work began with the goal of determining how phosphorylation of lipin 1 controlled membrane binding, which is relevant for defining a mechanism by which phosphorylation controls intracellular trafficking. Future studies should focus on demonstrating that lipin 1 binds PA by the electrostatic hydrogen-bond switch mechanism in adipocytes. Using a protonophore to modulate intracellular pH and knocking down lipid synthesis genes would potentially allow one to control the charge carried by the PA headgroup at internal membranes. Localization studies with respect to phosphorylation under this system could make it possible to demonstrate this mechanism inside cells. These studies could help to separate and define the effects of localized pH, membrane phospholipid content and phosphorylation with respect to lipin translocation, the effects of the two former likely have been solely attributed to the effects phosphorylation. Additionally, preliminary results suggest that lipin 3 binds PA by the electrostatic-hydrogen bond switch mechanism; however, more detailed studies are warranted. (data not shown)

These results should also be considered in the context of some of the limitations of the experimental system. While purifying lipin from mammalian cells affords the lipin protein in its native post translationally modified state, a requisite for studying phosphorylation, detailing the heterogeneity of such a pool of lipin is challenging. Similarly, experimentally defining a functional effect of particular phosphorylated residues requires alternative approaches. For example, to try to functionally assess mTOR dependent phosphorylation, we purified lipin 1 from HEK293T cells pretreated with Torin 1. We observed little change in the electrophoretic

mobility of this lipin, exemplifying that comparison of differentially phosphorylated lipin in this manner can be misleading. An alternative approach to stoichiometrically study one specific phosphorylation site could involve the use of protein semi-synthesis.<sup>91</sup> For instance, studying a specific phosphorylation site with known stoichiometry is possible if this phosphorylated residue is close to either the amino or carboxy terminus. Synthetic peptides containing a phosphorylated residue can be ligated into purified recombinant protein yielding a site specific, stoichiometric modification. Such an approach would aid in the interpretation of *in vitro* kinetic analysis. Furthermore, this approach can be used to study a specific phosphorylation site *in vivo* by ligating a synthetic peptide containing a nonhydrolyzable phosphonate, thus resistant to phosphatases, into recombinant protein and microinjection into cells. This chemical biology approach has helped to define how casein kinase II is regulated by post translational modification at specific residues and could be a viable option for future studies with lipin.<sup>92</sup>

Considering the narrow focus of this project, future studies can bring our findings into finer resolution. A kinetic analysis of PAP activity with the lipins' polybasic domains could potentially explain the relative ranking in specific activity among the lipin family. Preliminary studies examining the contributions of isoform specific PBDs on PAP activity by exchanging the lipin 1 PBD into a lipin 2 protein suggests that each isoforms' unique PBD gives differential affinity for PA (data not shown). It would be worthwhile to determine if replacing the lipin 2 PBD with the lipin 1 PBD is sufficient to increase PAP activity to levels that resemble wild type lipin 1. This analysis could be further carried out by examining all pairwise combinations.

Future physical studies examining lipin structure-function could help to define how phosphorylation regulates lipin 1. If the effect of phosphorylation is through a conformational change, using small angle X-ray scattering on phosphorylated and dephosphorylated lipin 1

would be an appropriate technique to answer this question. Furthermore, to follow up on our findings that lipin 1 forms high molecular weight complexes, electron microscopy could be used to confirm these results. Additional use of AFM could be used to determine if lipin forms complexes with other enzymes involved in lipid synthesis, forming a lipid synthesis complex.

## CHAPTER 8

### Publications Resulting from this Work

Eaton, J. M., Mullins, G. R., Brindley, D. N.; Harris, T. E., Phosphorylation of lipin 1 and charge on the phosphatidic Acid head group control its phosphatidic Acid phosphatase activity and membrane association. *The Journal of Biological Chemistry* 2013, 288 (14), 9933-45.

Creutz, C. E., Eaton, J.M., Harris, T.E. Assembly of High Molecular Weight Complexes of Lipin on a Supported Lipid Bilayer Observed by Atomic Force Microscopy. *Biochemistry* 2013, 52 (30), 5092-102

Eaton, J.M., Takkellapati, S., Lawrence, R.T., McQueeney, K.E., Boroda, S., Mullins, G.R., Sherwood, S.G., Fink, B.N., Villen, J., Harris, T.E. Lipin 2 binds phosphatidic acid by the electrostatic-hydrogen bond switch mechanism independent of phosphorylation. *The Journal of Biological Chemistry* 2014, 289 (26) 18055-66.

*In Preparation:*

Schweitzer, G.C., Collier, S.L., Chen, Z., Eaton, J.M., Pestronk, A., Harris, T.E., Finck, B.N., Rhabdomyolysis-Associated Mutations in Human Lipin 1 Lead to Defective Phosphatidic Acid Phosphohydrolase Activity.

## REFERENCES

1. Harris, T. E.; Finck, B. N., Dual function lipin proteins and glycerolipid metabolism. *Trends in endocrinology and metabolism: TEM* **2011**, *22* (6), 226-33.
2. Walther, T. C.; Farese, R. V., Jr., Lipid droplets and cellular lipid metabolism. *Annual review of biochemistry* **2012**, *81*, 687-714.
3. Kennedy, E. P.; Smith, S. W.; Weiss, S. B., New synthesis of lecithin in an isolated enzyme system. *Nature* **1956**, *178* (4533), 594-5.
4. Hubscher, G.; Brindley, D. N.; Smith, M. E.; Sedgwick, B., Stimulation of biosynthesis of glyceride. *Nature* **1967**, *216* (5114), 449-53.
5. Brindley, D. N., Intracellular translocation of phosphatidate phosphohydrolase and its possible role in the control of glycerolipid synthesis. *Progress in lipid research* **1984**, *23* (3), 115-33.
6. Peterfy, M.; Phan, J.; Xu, P.; Reue, K., Lipodystrophy in the fld mouse results from mutation of a new gene encoding a nuclear protein, lipin. *Nature genetics* **2001**, *27* (1), 121-4.
7. Huffman, T. A.; Mothe-Satney, I.; Lawrence, J. C., Jr., Insulin-stimulated phosphorylation of lipin mediated by the mammalian target of rapamycin. *Proceedings of the National Academy of Sciences of the United States of America* **2002**, *99* (2), 1047-52.
8. Han, G. S.; Wu, W. I.; Carman, G. M., The *Saccharomyces cerevisiae* Lipin homolog is a Mg<sup>2+</sup>-dependent phosphatidate phosphatase enzyme. *The Journal of biological chemistry* **2006**, *281* (14), 9210-8.
9. Harris, T. E.; Huffman, T. A.; Chi, A.; Shabanowitz, J.; Hunt, D. F.; Kumar, A.; Lawrence, J. C., Jr., Insulin controls subcellular localization and multisite phosphorylation of the phosphatidic acid phosphatase, lipin 1. *The Journal of biological chemistry* **2007**, *282* (1), 277-86.
10. Langner, C. A.; Birkenmeier, E. H.; Ben-Zeev, O.; Schotz, M. C.; Sweet, H. O.; Davisson, M. T.; Gordon, J. I., The fatty liver dystrophy (fld) mutation. A new mutant mouse with a developmental abnormality in triglyceride metabolism and associated tissue-specific defects in lipoprotein lipase and hepatic lipase activities. *The Journal of biological chemistry* **1989**, *264* (14), 7994-8003.
11. Reue, K.; Xu, P.; Wang, X. P.; Slavin, B. G., Adipose tissue deficiency, glucose intolerance, and increased atherosclerosis result from mutation in the mouse fatty liver dystrophy (fld) gene. *Journal of lipid research* **2000**, *41* (7), 1067-76.
12. Langner, C. A.; Birkenmeier, E. H.; Roth, K. A.; Bronson, R. T.; Gordon, J. I., Characterization of the peripheral neuropathy in neonatal and adult mice that are homozygous

for the fatty liver dystrophy (fld) mutation. *The Journal of biological chemistry* **1991**, 266 (18), 11955-64.

13. Nadra, K.; de Preux Charles, A. S.; Medard, J. J.; Hendriks, W. T.; Han, G. S.; Gres, S.; Carman, G. M.; Saulnier-Blache, J. S.; Verheijen, M. H.; Chrast, R., Phosphatidic acid mediates demyelination in *Lpin1* mutant mice. *Genes & development* **2008**, 22 (12), 1647-61.

14. Zhang, P.; Takeuchi, K.; Csaki, L. S.; Reue, K., Lipin-1 phosphatidic phosphatase activity modulates phosphatidate levels to promote peroxisome proliferator-activated receptor gamma (PPARgamma) gene expression during adipogenesis. *The Journal of biological chemistry* **2012**, 287 (5), 3485-94.

15. Zeharia, A.; Shaag, A.; Houtkooper, R. H.; Hindi, T.; de Lonlay, P.; Erez, G.; Hubert, L.; Saada, A.; de Keyzer, Y.; Eshel, G.; Vaz, F. M.; Pines, O.; Elpeleg, O., Mutations in LPIN1 cause recurrent acute myoglobinuria in childhood. *American journal of human genetics* **2008**, 83 (4), 489-94.

16. Bosch, X.; Poch, E.; Grau, J. M., Rhabdomyolysis and acute kidney injury. *The New England journal of medicine* **2009**, 361 (1), 62-72.

17. Michot, C.; Hubert, L.; Brivet, M.; De Meirleir, L.; Valayannopoulos, V.; Muller-Felber, W.; Venkateswaran, R.; Ogier, H.; Desguerre, I.; Altuzarra, C.; Thompson, E.; Smitka, M.; Huebner, A.; Husson, M.; Horvath, R.; Chinnery, P.; Vaz, F. M.; Munnich, A.; Elpeleg, O.; Delahodde, A.; de Keyzer, Y.; de Lonlay, P., LPIN1 gene mutations: a major cause of severe rhabdomyolysis in early childhood. *Human mutation* **2010**, 31 (7), E1564-73.

18. He, C.; Bassik, M. C.; Moresi, V.; Sun, K.; Wei, Y.; Zou, Z.; An, Z.; Loh, J.; Fisher, J.; Sun, Q.; Korsmeyer, S.; Packer, M.; May, H. I.; Hill, J. A.; Virgin, H. W.; Gilpin, C.; Xiao, G.; Bassel-Duby, R.; Scherer, P. E.; Levine, B., Exercise-induced BCL2-regulated autophagy is required for muscle glucose homeostasis. *Nature* **2012**, 481 (7382), 511-5.

19. Bergounioux, J.; Brassier, A.; Rambaud, C.; Bustarret, O.; Michot, C.; Hubert, L.; Arnoux, J. B.; Laquerriere, A.; Bekri, S.; Galene-Gomez, S.; Bonnet, D.; Hubert, P.; de Lonlay, P., Fatal rhabdomyolysis in 2 children with LPIN1 mutations. *The Journal of pediatrics* **2012**, 160 (6), 1052-4.

20. Zhang, P.; Verity, M. A.; Reue, K., Lipin-1 Regulates Autophagy Clearance and Intersects with Statin Drug Effects in Skeletal Muscle. *Cell metabolism* **2014**.

21. Csaki, L. S.; Dwyer, J. R.; Fong, L. G.; Tontonoz, P.; Young, S. G.; Reue, K., Lipins, lipinopathies, and the modulation of cellular lipid storage and signaling. *Progress in lipid research* **2013**, 52 (3), 305-16.

22. (a) Gropler, M. C.; Harris, T. E.; Hall, A. M.; Wolins, N. E.; Gross, R. W.; Han, X.; Chen, Z.; Finck, B. N., Lipin 2 is a liver-enriched phosphatidate phosphohydrolase enzyme that is dynamically regulated by fasting and obesity in mice. *The Journal of biological chemistry*

- 2009**, 284 (11), 6763-72; (b) Ryu, D.; Seo, W. Y.; Yoon, Y. S.; Kim, Y. N.; Kim, S. S.; Kim, H. J.; Park, T. S.; Choi, C. S.; Koo, S. H., Endoplasmic reticulum stress promotes LIPIN2-dependent hepatic insulin resistance. *Diabetes* **2011**, 60 (4), 1072-81.
23. (a) Sembongi, H.; Miranda, M.; Han, G. S.; Fakas, S.; Grimsey, N.; Vendrell, J.; Carman, G. M.; Siniossoglou, S., Distinct Roles of the Phosphatidate Phosphatases Lipin 1 and 2 during Adipogenesis and Lipid Droplet Biogenesis in 3T3-L1 Cells. *The Journal of biological chemistry* **2013**, 288 (48), 34502-13; (b) Grimsey, N.; Han, G. S.; O'Hara, L.; Rochford, J. J.; Carman, G. M.; Siniossoglou, S., Temporal and spatial regulation of the phosphatidate phosphatases lipin 1 and 2. *The Journal of biological chemistry* **2008**, 283 (43), 29166-74.
24. Dwyer, J. R.; Donkor, J.; Zhang, P.; Csaki, L. S.; Vergnes, L.; Lee, J. M.; Dewald, J.; Brindley, D. N.; Atti, E.; Tetradis, S.; Yoshinaga, Y.; De Jong, P. J.; Fong, L. G.; Young, S. G.; Reue, K., Mouse lipin-1 and lipin-2 cooperate to maintain glycerolipid homeostasis in liver and aging cerebellum. *Proceedings of the National Academy of Sciences of the United States of America* **2012**, 109 (37), E2486-95.
25. Ferguson, P. J.; Chen, S.; Tayeh, M. K.; Ochoa, L.; Leal, S. M.; Pelet, A.; Munnich, A.; Lyonnet, S.; Majeed, H. A.; El-Shanti, H., Homozygous mutations in LPIN2 are responsible for the syndrome of chronic recurrent multifocal osteomyelitis and congenital dyserythropoietic anaemia (Majeed syndrome). *Journal of medical genetics* **2005**, 42 (7), 551-7.
26. Al-Mosawi, Z. S.; Al-Saad, K. K.; Ijadi-Maghsoodi, R.; El-Shanti, H. I.; Ferguson, P. J., A splice site mutation confirms the role of LPIN2 in Majeed syndrome. *Arthritis and rheumatism* **2007**, 56 (3), 960-4.
27. Csaki, L. S.; Dwyer, J. R.; Li, X.; Nguyen, M. H.; Dewald, J.; Brindley, D. N.; Lusic, A. J.; Yoshinaga, Y.; de Jong, P.; Fong, L.; Young, S. G.; Reue, K., Lipin-1 and lipin-3 together determine adiposity in vivo. *Molecular metabolism* **2014**, 3 (2), 145-54.
28. Ren, H.; Federico, L.; Huang, H.; Sunkara, M.; Drennan, T.; Frohman, M. A.; Smyth, S. S.; Morris, A. J., A phosphatidic acid binding/nuclear localization motif determines lipin1 function in lipid metabolism and adipogenesis. *Molecular biology of the cell* **2010**, 21 (18), 3171-81.
29. Eaton, J. M.; Mullins, G. R.; Brindley, D. N.; Harris, T. E., Phosphorylation of lipin 1 and charge on the phosphatidic acid head group control its phosphatidic acid phosphatase activity and membrane association. *The Journal of biological chemistry* **2013**, 288 (14), 9933-45.
30. Peterfy, M.; Harris, T. E.; Fujita, N.; Reue, K., Insulin-stimulated interaction with 14-3-3 promotes cytoplasmic localization of lipin-1 in adipocytes. *The Journal of biological chemistry* **2010**, 285 (6), 3857-64.
31. Burroughs, A. M.; Allen, K. N.; Dunaway-Mariano, D.; Aravind, L., Evolutionary genomics of the HAD superfamily: understanding the structural adaptations and catalytic

diversity in a superfamily of phosphoesterases and allied enzymes. *Journal of molecular biology* **2006**, *361* (5), 1003-34.

32. Liu, G. H.; Qu, J.; Carmack, A. E.; Kim, H. B.; Chen, C.; Ren, H.; Morris, A. J.; Finck, B. N.; Harris, T. E., Lipin proteins form homo- and hetero-oligomers. *The Biochemical journal* **2010**, *432* (1), 65-76.

33. Kim, H. B.; Kumar, A.; Wang, L.; Liu, G. H.; Keller, S. R.; Lawrence, J. C., Jr.; Finck, B. N.; Harris, T. E., Lipin 1 represses NFATc4 transcriptional activity in adipocytes to inhibit secretion of inflammatory factors. *Molecular and cellular biology* **2010**, *30* (12), 3126-39.

34. Finck, B. N.; Gropler, M. C.; Chen, Z.; Leone, T. C.; Croce, M. A.; Harris, T. E.; Lawrence, J. C., Jr.; Kelly, D. P., Lipin 1 is an inducible amplifier of the hepatic PGC-1alpha/PPARalpha regulatory pathway. *Cell metabolism* **2006**, *4* (3), 199-210.

35. Peterson, T. R.; Sengupta, S. S.; Harris, T. E.; Carmack, A. E.; Kang, S. A.; Balderas, E.; Guertin, D. A.; Madden, K. L.; Carpenter, A. E.; Finck, B. N.; Sabatini, D. M., mTOR complex 1 regulates lipin 1 localization to control the SREBP pathway. *Cell* **2011**, *146* (3), 408-20.

36. Coleman, R. A.; Mashek, D. G., Mammalian triacylglycerol metabolism: synthesis, lipolysis, and signaling. *Chemical reviews* **2011**, *111* (10), 6359-86.

37. Han, G. S.; Carman, G. M., Characterization of the human LPIN1-encoded phosphatidate phosphatase isoforms. *The Journal of biological chemistry* **2010**, *285* (19), 14628-38.

38. (a) Choi, H. S.; Su, W. M.; Han, G. S.; Plote, D.; Xu, Z.; Carman, G. M., Pho85p-Pho80p phosphorylation of yeast Pah1p phosphatidate phosphatase regulates its activity, location, abundance, and function in lipid metabolism. *The Journal of biological chemistry* **2012**, *287* (14), 11290-301; (b) Choi, H. S.; Su, W. M.; Morgan, J. M.; Han, G. S.; Xu, Z.; Karanasios, E.; Siniossoglou, S.; Carman, G. M., Phosphorylation of phosphatidate phosphatase regulates its membrane association and physiological functions in *Saccharomyces cerevisiae*: identification of SER(602), THR(723), AND SER(744) as the sites phosphorylated by CDC28 (CDK1)-encoded cyclin-dependent kinase. *The Journal of biological chemistry* **2011**, *286* (2), 1486-98; (c) Xu, Z.; Su, W. M.; Carman, G. M., Fluorescence spectroscopy measures yeast PAH1-encoded phosphatidate phosphatase interaction with liposome membranes. *Journal of lipid research* **2012**, *53* (3), 522-8; (d) Su, W. M.; Han, G. S.; Casciano, J.; Carman, G. M., Protein kinase A-mediated phosphorylation of Pah1p phosphatidate phosphatase functions in conjunction with the Pho85p-Pho80p and Cdc28p-cyclin B kinases to regulate lipid synthesis in yeast. *The Journal of biological chemistry* **2012**, *287* (40), 33364-76; (e) Karanasios, E.; Han, G. S.; Xu, Z.; Carman, G. M.; Siniossoglou, S., A phosphorylation-regulated amphipathic helix controls the membrane translocation and function of the yeast phosphatidate phosphatase. *Proceedings of the National Academy of Sciences of the United States of America* **2010**, *107* (41), 17539-44; (f) O'Hara, L.; Han, G. S.; Peak-Chew, S.; Grimsey, N.; Carman, G. M.; Siniossoglou, S., Control of phospholipid synthesis by phosphorylation of the yeast lipin Pah1p/Smp2p Mg<sup>2+</sup>-dependent phosphatidate phosphatase. *The Journal of biological chemistry* **2006**, *281* (45), 34537-48.

39. Santos-Rosa, H.; Leung, J.; Grimsey, N.; Peak-Chew, S.; Siniosoglou, S., The yeast lipin Smp2 couples phospholipid biosynthesis to nuclear membrane growth. *The EMBO journal* **2005**, *24* (11), 1931-41.
40. (a) Kim, Y.; Gentry, M. S.; Harris, T. E.; Wiley, S. E.; Lawrence, J. C., Jr.; Dixon, J. E., A conserved phosphatase cascade that regulates nuclear membrane biogenesis. *Proceedings of the National Academy of Sciences of the United States of America* **2007**, *104* (16), 6596-601; (b) Wu, R.; Garland, M.; Dunaway-Mariano, D.; Allen, K. N., Homo sapiens dullard protein phosphatase shows a preference for the insulin-dependent phosphorylation site of lipin1. *Biochemistry* **2011**, *50* (15), 3045-7; (c) Han, S.; Bahmanyar, S.; Zhang, P.; Grishin, N.; Oegema, K.; Crooke, R.; Graham, M.; Reue, K.; Dixon, J. E.; Goodman, J. M., Nuclear envelope phosphatase 1-regulatory subunit 1 (formerly TMEM188) is the metazoan Spo7p ortholog and functions in the lipin activation pathway. *The Journal of biological chemistry* **2012**, *287* (5), 3123-37.
41. Donkor, J.; Sariahmetoglu, M.; Dewald, J.; Brindley, D. N.; Reue, K., Three mammalian lipins act as phosphatidate phosphatases with distinct tissue expression patterns. *The Journal of biological chemistry* **2007**, *282* (6), 3450-7.
42. Kooijman, E. E.; Carter, K. M.; van Laar, E. G.; Chupin, V.; Burger, K. N.; de Kruijff, B., What makes the bioactive lipids phosphatidic acid and lysophosphatidic acid so special? *Biochemistry* **2005**, *44* (51), 17007-15.
43. Mengistu, D. H.; Kooijman, E. E.; May, S., Ionization properties of mixed lipid membranes: a Gouy-Chapman model of the electrostatic-hydrogen bond switch. *Biochimica et biophysica acta* **2011**, *1808* (8), 1985-92.
44. Lemmon, M. A., Membrane recognition by phospholipid-binding domains. *Nature reviews. Molecular cell biology* **2008**, *9* (2), 99-111.
45. Stace, C. L.; Ktistakis, N. T., Phosphatidic acid- and phosphatidylserine-binding proteins. *Biochimica et biophysica acta* **2006**, *1761* (8), 913-26.
46. Kooijman, E. E.; Tieleman, D. P.; Testerink, C.; Munnik, T.; Rijkers, D. T.; Burger, K. N.; de Kruijff, B., An electrostatic/hydrogen bond switch as the basis for the specific interaction of phosphatidic acid with proteins. *The Journal of biological chemistry* **2007**, *282* (15), 11356-64.
47. Kooijman, E. E.; Sot, J.; Montes, L. R.; Alonso, A.; Gericke, A.; de Kruijff, B.; Kumar, S.; Goni, F. M., Membrane organization and ionization behavior of the minor but crucial lipid ceramide-1-phosphate. *Biophysical journal* **2008**, *94* (11), 4320-30.
48. Carman, G. M.; Deems, R. A.; Dennis, E. A., Lipid signaling enzymes and surface dilution kinetics. *The Journal of biological chemistry* **1995**, *270* (32), 18711-4.

49. Luo, J.; Deng, Z. L.; Luo, X.; Tang, N.; Song, W. X.; Chen, J.; Sharff, K. A.; Luu, H. H.; Haydon, R. C.; Kinzler, K. W.; Vogelstein, B.; He, T. C., A protocol for rapid generation of recombinant adenoviruses using the AdEasy system. *Nature protocols* **2007**, *2* (5), 1236-47.
50. Han, G. S.; Carman, G. M., Assaying lipid phosphate phosphatase activities. *Methods in molecular biology* **2004**, *284*, 209-16.
51. MacDonald, R. C.; MacDonald, R. I.; Menco, B. P.; Takeshita, K.; Subbarao, N. K.; Hu, L. R., Small-volume extrusion apparatus for preparation of large, unilamellar vesicles. *Biochimica et biophysica acta* **1991**, *1061* (2), 297-303.
52. Hofer, C. T.; Herrmann, A.; Muller, P., Use of liposomes for studying interactions of soluble proteins with cellular membranes. *Methods in molecular biology* **2010**, *606*, 69-82.
53. Ficarro, S. B.; McClelland, M. L.; Stukenberg, P. T.; Burke, D. J.; Ross, M. M.; Shabanowitz, J.; Hunt, D. F.; White, F. M., Phosphoproteome analysis by mass spectrometry and its application to *Saccharomyces cerevisiae*. *Nature biotechnology* **2002**, *20* (3), 301-5.
54. Beausoleil, S. A.; Villen, J.; Gerber, S. A.; Rush, J.; Gygi, S. P., A probability-based approach for high-throughput protein phosphorylation analysis and site localization. *Nature biotechnology* **2006**, *24* (10), 1285-92.
55. Mou, J.; Yang, J.; Shao, Z., Tris(hydroxymethyl)aminomethane (C<sub>4</sub>H<sub>11</sub>NO<sub>3</sub>) induced a ripple phase in supported unilamellar phospholipid bilayers. *Biochemistry* **1994**, *33* (15), 4439-43.
56. Brian, A. A.; McConnell, H. M., Allogeneic stimulation of cytotoxic T cells by supported planar membranes. *Proceedings of the National Academy of Sciences of the United States of America* **1984**, *81* (19), 6159-63.
57. Shahin, V.; Datta, D.; Hui, E.; Henderson, R. M.; Chapman, E. R.; Edwardson, J. M., Synaptotagmin perturbs the structure of phospholipid bilayers. *Biochemistry* **2008**, *47* (7), 2143-52.
58. Alsteens, D.; Dupres, V.; Yunus, S.; Latge, J. P.; Heinisch, J. J.; Dufrene, Y. F., High-resolution imaging of chemical and biological sites on living cells using peak force tapping atomic force microscopy. *Langmuir : the ACS journal of surfaces and colloids* **2012**, *28* (49), 16738-44.
59. Schneider, S. W.; Larmer, J.; Henderson, R. M.; Oberleithner, H., Molecular weights of individual proteins correlate with molecular volumes measured by atomic force microscopy. *Pflugers Archiv : European journal of physiology* **1998**, *435* (3), 362-7.
60. Kooijman, E. E.; Burger, K. N., Biophysics and function of phosphatidic acid: a molecular perspective. *Biochimica et biophysica acta* **2009**, *1791* (9), 881-8.

61. Liu, G. H.; Gerace, L., Sumoylation regulates nuclear localization of lipin-1alpha in neuronal cells. *PloS one* **2009**, *4* (9), e7031.
62. Jamal, Z.; Martin, A.; Gomez-Munoz, A.; Brindley, D. N., Plasma membrane fractions from rat liver contain a phosphatidate phosphohydrolase distinct from that in the endoplasmic reticulum and cytosol. *The Journal of biological chemistry* **1991**, *266* (5), 2988-96.
63. Bowley, M.; Cooling, J.; Burditt, S. L.; Brindley, D. N., The effects of amphiphilic cationic drugs and inorganic cations on the activity of phosphatidate phosphohydrolase. *The Biochemical journal* **1977**, *165* (3), 447-54.
64. (a) Martin-Sanz, P.; Hopewell, R.; Brindley, D. N., Long-chain fatty acids and their acyl-CoA esters cause the translocation of phosphatidate phosphohydrolase from the cytosolic to the microsomal fraction of rat liver. *FEBS letters* **1984**, *175* (2), 284-8; (b) Hopewell, R.; Martin-Sanz, P.; Martin, A.; Saxton, J.; Brindley, D. N., Regulation of the translocation of phosphatidate phosphohydrolase between the cytosol and the endoplasmic reticulum of rat liver. Effects of unsaturated fatty acids, spermine, nucleotides, albumin and chlorpromazine. *The Biochemical journal* **1985**, *232* (2), 485-91.
65. Martin, A.; Hopewell, R.; Martin-Sanz, P.; Morgan, J. E.; Brindley, D. N., Relationship between the displacement of phosphatidate phosphohydrolase from the membrane-associated compartment by chlorpromazine and the inhibition of the synthesis of triacylglycerol and phosphatidylcholine in rat hepatocytes. *Biochimica et biophysica acta* **1986**, *876* (3), 581-91.
66. Eastmond, P. J.; Quettier, A. L.; Kroon, J. T.; Craddock, C.; Adams, N.; Slabas, A. R., Phosphatidic acid phosphohydrolase 1 and 2 regulate phospholipid synthesis at the endoplasmic reticulum in Arabidopsis. *The Plant cell* **2010**, *22* (8), 2796-811.
67. Coleman, R. A.; Lewin, T. M.; Muoio, D. M., Physiological and nutritional regulation of enzymes of triacylglycerol synthesis. *Annual review of nutrition* **2000**, *20*, 77-103.
68. (a) Taylor, S. J.; Saggerson, E. D., Adipose-tissue Mg<sup>2+</sup>-dependent phosphatidate phosphohydrolase. Control of activity and subcellular distribution in vitro and in vivo. *The Biochemical journal* **1986**, *239* (2), 275-84; (b) Moller, F.; Wong, K. H.; Green, P., Control of fat cell phosphohydrolase by lipolytic agents. *Canadian journal of biochemistry* **1981**, *59* (1), 9-15.
69. Civelek, V. N.; Hamilton, J. A.; Tornheim, K.; Kelly, K. L.; Corkey, B. E., Intracellular pH in adipocytes: effects of free fatty acid diffusion across the plasma membrane, lipolytic agonists, and insulin. *Proceedings of the National Academy of Sciences of the United States of America* **1996**, *93* (19), 10139-44.
70. Scott, P. H.; Lawrence, J. C., Jr., Attenuation of mammalian target of rapamycin activity by increased cAMP in 3T3-L1 adipocytes. *The Journal of biological chemistry* **1998**, *273* (51), 34496-501.

71. (a) Vicogne, J.; Vollenweider, D.; Smith, J. R.; Huang, P.; Frohman, M. A.; Pessin, J. E., Asymmetric phospholipid distribution drives in vitro reconstituted SNARE-dependent membrane fusion. *Proceedings of the National Academy of Sciences of the United States of America* **2006**, *103* (40), 14761-6; (b) Huang, P.; Altshuller, Y. M.; Hou, J. C.; Pessin, J. E.; Frohman, M. A., Insulin-stimulated plasma membrane fusion of Glut4 glucose transporter-containing vesicles is regulated by phospholipase D1. *Molecular biology of the cell* **2005**, *16* (6), 2614-23.
72. Shin, J. J.; Loewen, C. J., Putting the pH into phosphatidic acid signaling. *BMC biology* **2011**, *9*, 85.
73. Fu, S.; Yang, L.; Li, P.; Hofmann, O.; Dicker, L.; Hide, W.; Lin, X.; Watkins, S. M.; Ivanov, A. R.; Hotamisligil, G. S., Aberrant lipid metabolism disrupts calcium homeostasis causing liver endoplasmic reticulum stress in obesity. *Nature* **2011**, *473* (7348), 528-31.
74. Coleman, R. A.; Lee, D. P., Enzymes of triacylglycerol synthesis and their regulation. *Progress in lipid research* **2004**, *43* (2), 134-76.
75. Kennedy, E. P., The biological synthesis of phospholipids. *Canadian journal of biochemistry and physiology* **1956**, *34* (2), 334-48.
76. Brindley, D. N.; Pilquil, C.; Sariahmetoglu, M.; Reue, K., Phosphatidate degradation: phosphatidate phosphatases (lipins) and lipid phosphate phosphatases. *Biochimica et biophysica acta* **2009**, *1791* (9), 956-61.
77. Harris, T. E.; Chi, A.; Shabanowitz, J.; Hunt, D. F.; Rhoads, R. E.; Lawrence, J. C., Jr., mTOR-dependent stimulation of the association of eIF4G and eIF3 by insulin. *The EMBO journal* **2006**, *25* (8), 1659-68.
78. Young, B. P.; Shin, J. J.; Oriji, R.; Chao, J. T.; Li, S. C.; Guan, X. L.; Khong, A.; Jan, E.; Wenk, M. R.; Prinz, W. A.; Smits, G. J.; Loewen, C. J., Phosphatidic acid is a pH biosensor that links membrane biogenesis to metabolism. *Science* **2010**, *329* (5995), 1085-8.
79. Kelley, L. A.; Sternberg, M. J., Protein structure prediction on the Web: a case study using the Phyre server. *Nature protocols* **2009**, *4* (3), 363-71.
80. Creutz, C. E.; Eaton, J. M.; Harris, T. E., Assembly of high molecular weight complexes of lipin on a supported lipid bilayer observed by atomic force microscopy. *Biochemistry* **2013**, *52* (30), 5092-102.
81. Sim, M. F.; Dennis, R. J.; Aubry, E. M.; Ramanathan, N.; Sembongi, H.; Saudek, V.; Ito, D.; O'Rahilly, S.; Siniossoglou, S.; Rochford, J. J., The human lipodystrophy protein seipin is an ER membrane adaptor for the adipogenic PA phosphatase lipin 1. *Molecular metabolism* **2012**, *2* (1), 38-46.
82. (a) Fei, W.; Li, H.; Shui, G.; Kapterian, T. S.; Bielby, C.; Du, X.; Brown, A. J.; Li, P.; Wenk, M. R.; Liu, P.; Yang, H., Molecular characterization of seipin and its mutants:

implications for seipin in triacylglycerol synthesis. *Journal of lipid research* **2011**, *52* (12), 2136-47; (b) Binns, D.; Lee, S.; Hilton, C. L.; Jiang, Q. X.; Goodman, J. M., Seipin is a discrete homooligomer. *Biochemistry* **2010**, *49* (50), 10747-55; (c) Sim, M. F.; Talukder, M. M.; Dennis, R. J.; O'Rahilly, S.; Edwardson, J. M.; Rochford, J. J., Analysis of naturally occurring mutations in the human lipodystrophy protein seipin reveals multiple potential pathogenic mechanisms. *Diabetologia* **2013**, *56* (11), 2498-506.

83. Oschlies, M.; Dickmanns, A.; Haselhorst, T.; Schaper, W.; Stummeyer, K.; Tiralongo, J.; Weinhold, B.; Gerardy-Schahn, R.; von Itzstein, M.; Ficner, R.; Munster-Kuhnel, A. K., A C-terminal phosphatase module conserved in vertebrate CMP-sialic acid synthetases provides a tetramerization interface for the physiologically active enzyme. *Journal of molecular biology* **2009**, *393* (1), 83-97.

84. Michot, C.; Hubert, L.; Romero, N. B.; Gouda, A.; Mamoune, A.; Mathew, S.; Kirk, E.; Viollet, L.; Rahman, S.; Bekri, S.; Peters, H.; McGill, J.; Glamuzina, E.; Farrar, M.; von der Hagen, M.; Alexander, I. E.; Kirmse, B.; Barth, M.; Laforet, P.; Benlian, P.; Munnich, A.; JeanPierre, M.; Elpeleg, O.; Pines, O.; Delahodde, A.; de Keyzer, Y.; de Lonlay, P., Study of LPIN1, LPIN2 and LPIN3 in rhabdomyolysis and exercise-induced myalgia. *Journal of inherited metabolic disease* **2012**, *35* (6), 1119-28.

85. Michot, C.; Mamoune, A.; Vamecq, J.; Viou, M. T.; Hsieh, L. S.; Testet, E.; Laine, J.; Hubert, L.; Dessein, A. F.; Fontaine, M.; Ottolenghi, C.; Fouillen, L.; Nadra, K.; Blanc, E.; Bastin, J.; Candon, S.; Pende, M.; Munnich, A.; Smahi, A.; Djouadi, F.; Carman, G. M.; Romero, N.; de Keyzer, Y.; de Lonlay, P., Combination of lipid metabolism alterations and their sensitivity to inflammatory cytokines in human lipin-1-deficient myoblasts. *Biochimica et biophysica acta* **2013**, *1832* (12), 2103-14.

86. Mitra, M. S.; Chen, Z.; Ren, H.; Harris, T. E.; Chambers, K. T.; Hall, A. M.; Nadra, K.; Klein, S.; Chrast, R.; Su, X.; Morris, A. J.; Finck, B. N., Mice with an adipocyte-specific lipin 1 separation-of-function allele reveal unexpected roles for phosphatidic acid in metabolic regulation. *Proceedings of the National Academy of Sciences of the United States of America* **2013**, *110* (2), 642-7.

87. Castets, P.; Lin, S.; Rion, N.; Di Fulvio, S.; Romanino, K.; Guridi, M.; Frank, S.; Tintignac, L. A.; Sinnreich, M.; Ruegg, M. A., Sustained activation of mTORC1 in skeletal muscle inhibits constitutive and starvation-induced autophagy and causes a severe, late-onset myopathy. *Cell metabolism* **2013**, *17* (5), 731-44.

88. Bennett, M. J., Pathophysiology of fatty acid oxidation disorders. *Journal of inherited metabolic disease* **2010**, *33* (5), 533-7.

89. Laforet, P.; Vianey-Saban, C., Disorders of muscle lipid metabolism: diagnostic and therapeutic challenges. *Neuromuscular disorders : NMD* **2010**, *20* (11), 693-700.

90. Huang, H.; Gao, Q.; Peng, X.; Choi, S. Y.; Sarma, K.; Ren, H.; Morris, A. J.; Frohman, M. A., piRNA-associated germline nuage formation and spermatogenesis require MitoPLD profusogenic mitochondrial-surface lipid signaling. *Developmental cell* **2011**, *20* (3), 376-87.
91. Szewczuk, L. M.; Tarrant, M. K.; Cole, P. A., Protein phosphorylation by semisynthesis: from paper to practice. *Methods in enzymology* **2009**, *462*, 1-24.
92. Tarrant, M. K.; Rho, H. S.; Xie, Z.; Jiang, Y. L.; Gross, C.; Culhane, J. C.; Yan, G.; Qian, J.; Ichikawa, Y.; Matsuoka, T.; Zachara, N.; Etzkorn, F. A.; Hart, G. W.; Jeong, J. S.; Blackshaw, S.; Zhu, H.; Cole, P. A., Regulation of CK2 by phosphorylation and O-GlcNAcylation revealed by semisynthesis. *Nature chemical biology* **2012**, *8* (3), 262-9.